Laplace-Domain Analysis of Fluid Line Networks with Applications to Time-Domain Simulation and System Parameter Identification

by

Aaron C. Zecchin

B.E. (Civil) (Hons), B.Sc.

Thesis submitted to The University of Adelaide
School of Civil, Environmental & Mining
Engineering in fulfilment of the requirements for
the degree of
Doctor of Philosophy

References

Abate, J., and P. P. Valko, Multi-precision Laplace transform inversion, *International Journal for Numerical Methods in Engineering*, *60*(5), 979–993, 2004.

Abate, J., and W. Whitt, The fourier-series method for inverting transforms of probability distributions, *Queueing Systems Theory and Applications*, *vol. 10, no. 1-2*, 5–88, 1992.

Abate, J., and W. Whitt, Numerical inversion of Laplace transforms of probability distributions, *ORSA Journal on Computing*, *vol. 7, no. 1*, 36–43, 1995.

Abate, J., and W. Whitt, Computing Laplace transforms for numerical inversion via continued fractions, *Informs Journal on Computing*, *11*(4), 394–405, 1999.

Abate, J., and W. Whitt, A unified framework for numerically inverting Laplace transforms, *Informs Journal on Computing*, *18*(4), 408–421, 2006.

Abate, J., G. L. Choudhury, and W. Whitt, On the Laguerre method for numerically inverting Laplace transforms, *INFORMS Journal on Computing*, *8*(4), 413–27, 1996.

Abramowitz, M., and I. A. Stegun, *Handbook of mathematical functions*, Dover Publications, 1964.

Almondo, A., and M. Sorli, Time domain transmission line modelling using a passivity preserving rational approximation of the frequency dependent transfer matrix, *International Journal of Fluid Power*, *1*(7), 41–50, 2006.

Andersen, J. H., and R. S. Powell, Implicit state-estimation technique for water network monitoring, *Urban Water*, *2*, 123–130, 2000.

Anderson, B. D. O., and S. Vongpanitlerd, *Network analysis and synthesis: a modern systems theory approach*, Prentice-Hall electrical engineering series, Prentice-Hall, Englewood Cliffs, N. J., 1973.

Ansari, J. S., and R. Oldenburger, Propagation of disturbance in fluid lines, *Journal of Basic Engineering, ASME*, *88*(2), 415–422, 1967.

Arfaie, M., K. Suwan, and A. Anderson, Stability and accuracy of pipe friction approximations in method of characteristics solutions for waterhammer, *Mathematical Engineering in Industry*, *4*(1), 265–281, 1993.

Ashton, S. A., and D. N. Shields, Fault detection observer for a class of nonlinear systems, *New Directions in Nonlinear and Observer Design*, *244*, 353–373, 1999.

Auslander, D. M., Distributed system simulation with bilateral delay-line models, *Transactions of the ASME, Journal of Basic Engineering*, pp. 195–200, 1968.

Axworthy, D. H., Water distribution network modelling from steady state to waterhammer, PhD thesis, University of Toronto, 1997.

Ayalew, B., and B. T. Kulakowski, Modal approximation of distributed dynamics for a hydraulic transmission line with pressure input-flow rate output causality, *Journal of Dynamic Systems Measurement and Control-Transactions of the ASME*, *127*(3), 503–507, 2005.

Baghdadi, A. H. A., and H. A. Mansy, A mathematical model for leak location in pipelines, *Applied Mathematical Modelling*, *12*(February), 25–30, 1988.

Barber, A., *Pneumatic handbook*, 7th ed., Trade and Technical Press, Morden, England, 1989.

Beasley, J. D., and S. G. Springer, Algorithm as 111, *Applied Statistics*, *26*, 118–121, 1977.

Benkherouf, A., and A. Y. Allidina, Leak detection and location in gas pipelines, *Institution of Electrical Engineerg, Proceedings D, Control Theory and Applications*, *135*(2, March), 142–148, 1988.

Billmann, L., and R. Isermann, Leak detection method for pipelines, *Automatica*, *23*(3), 381–385, 1987.

Black, P., A review of pipeline leak detection technology, in *Pipeline Systems*, edited by B. Coulbeck and E. Evans, Fluids Mechanics and Its Application, pp. 287–297, Kluwer Academic Publishers, 1992.

Boucher, R. F., and E. E. Kitsios, Simulation of fluid network dynamics by transmission-line modeling, *Proceedings of the Institution of Mechanical Engineers Part C-Journal of Mechanical Engineering Science*, *200*(1), 21–29, 1986.

Brillinger, D. R., *Time series: data analysis and theory*, International series in decision processes, Holt Rinehart and Winston, New York, 1974.

Brown, F. T., The transient response of fluid lines, *Journal of Basic Engineering, ASME*, *84*(3), 547–553, 1962.

Brown, F. T., A unified approach to the analysis of uniform one-dimensional distributed systems, *Trans. ASME J. Eng.*, *89*, 423–432, 1967.

Brown, F. T., and S. E. Nelson, Step responses of liquid lines with frequency-dependent effects of viscosity, *Journal of Basic Engineering, ASME*, *87*(June), 504–510, 1965.

Brown, F. T., and S. C. Tentarelli, Dynamic behavior of complex fluid-filled tubing systems - part 1: Tubing analysis, *Journal of Dynamic Systems Measurement and Control-Transactions of the ASME*, *123*(1), 71–77, 2001.

Brunone, B., Transient test-based technique for leak detection in outfall pipes, *Journal of Water Resources Planning and Management, ASCE*, *125*(5, September/October), 302–306, 1999.

Brunone, B., and M. Ferrante, Detecting leaks in pressurised pipes by means of transients, *Journal of Hydraulic Research, IAHR*, *39*(5), 539–547, 2001.

Brunone, B., U. Golia, and M. Greco, Some remarks on the momentum equations for fast transients, in *Hydraulic Transients with Column Separation (9th and Last Round Table of the IAHR Group), IAHR*, edited by E. Cabrera and M. Fanelli, Valencia, Spain, 1991.

Candy, J. V., and R. B. Rosza, Safeguards design for a plutonium concentrator - an applied estimation approach, *Automatica*, *16*, 615–627, 1980.

Chadwick, R. S., Pulse-wave propagation in an artery with leakage into small side branches, *Applied Mathematical Sciences*, *82*, 5237–5241, 1985.

Chaudhry, M. H., Resonance in pressurized piping systems, *Journal of the Hydraulics Division, ASCE*, *96*(HY9, September), 1819–1839, 1970.

Chaudhry, M. H., *Applied Hydraulic Transients*, 2nd ed., Van Nostrand Reinhold Co., New York, USA, 1987.

Chaudhry, M. H., and M. Y. Husssini, Second-order accurate explicit finite-difference schemes for waterhammer analysis, *Journal of Fluids Engineering*, *107*(December), 523–529, 1985.

Chen, H. X., P. S. K. Chua, and H. L. Lim, Feature extraction, optimization and classification by second generation wavelet and support vector machine for fault diagnosis of water power hydraulic systems, *International Journal of Fluid Power*, *7*(7), 39–52, 2006.

Chen, W.-K., *Linear Networks and Systems*, Brooks/Cole Engineering Division, Monterey, Calif, 1983.

Cole, S. E., Methods of leak detection: An overview, *Journal of the American Water Works Association*, *71*(2), 73–75, 1979.

Collins, M., L. Cooper, R. Helgason, J. Kennington, and L. LeBlanc, Solving the pipe network analysis problem using optimization techniques, *Management Science*, *24*(7), 747–760, 1978.

Contractor, D. N., The reflection of waterhammer pressure waves from minor losses, *Journal of Basic Engineering, ASME*, *87*(June), 445–452, 1965.

Covas, D., and H. Ramos, Leakage detection in single pipelines using pressure wave behaviour, in *Water Industry Systems: Modelling and Optimisation Applications*, edited by D. A. Savic and G. A. Walters, Research Studies Press Ltd., Baldock, Hertfordshire, England, 1999.

Covas, D., and H. Ramos, Hydraulic transients used for leakage detection in water distribution systems, in *4th International Conference on Water Pipeline Systems: Managing Pipeline Assets in an Evolving Market*, pp. 227–241, BHR Group, York, UK, 2001.

Covas, D., H. Ramos, and A. B. de Almeida, Leakage monitoring control and management of water distribution systems: A challenge for the 21st century, in *28th Biennial Congress, IAHR*, Graz, Austria, 1999.

Covas, D., H. Ramos, and A. Betmio de Almeida, Leak location in pipe systems using pressure surges, in *Safe Design and Operation of Industrial Pipe Systems: 8th International Conference on Pressure Surges*, pp. 169–179, BHR Group, The Hague, The Netherlands, 2000.

Covas, D., I. Stoianov, D. Butler, C. Maksimovic, N. Graham, and H. Ramos, Leak detection in pipeline systems by inverse transient analysis - from theory to practice, in *Water Software Systems: Theory and Applications*, vol. 1, edited by B. Ulanicki, B. Coulback, and J. P. Rance, pp. 3–16, Research Studies Press Ltd., Baldock, Hertfordshire, England, 2001.

Covas, D., I. Stoianov, N. Graham, C. Maksimovic, H. Ramos, and D. Butler, Hydraulic transients in polyethylene pipes, in *1st Annual Environmental & Water Resources Systems Analysis Symposium in conjunction with ASCE Environmental & Water Resources Institute Annual Conference*, Roanoke, Virginia, USA, 2002.

Covas, D., H. Ramos, N. Graham, and C. Maksimovic, The interaction between viscoelastic behaviour of the pipe wall, unsteady friction and transient pressures, in *9th International Conference on Pressure Surges*, pp. 63–78, BHR Group, Chester, UK, 2004a.

Covas, D., I. Stoianov, J. F. Mano, H. Ramos, N. Graham, and C. Maksimovic, The dynamic effect of pipe-wall viscoelasticity in hydraulic transients. part i - experimental analysis and creep characterization, *Journal of Hydraulic Research*, *42*(5), 516–530, 2004b.

Covas, D., H. Ramos, and A. B. de Almeida, Standing wave difference method for leak detection in pipeline systems, *Journal of Hydraulic Engineering, ASCE*, *131*(12), 1106–1116, 2005a.

Covas, D., I. Stoianov, J. F. Mano, H. Ramos, N. Graham, and C. Maksimovic, The dynamic effect of pipe-wall viscoelasticity in hydraulic transients. part ii - model development, calibration and verification, *Journal of Hydraulic Research*, *43*(1), 56–70, 2005b.

Crump, K. S., Numerical inversion of Laplace transforms using a Fourier-series approximation, *J. ACM*, *23*, 89–96, 1976.

Datta, R. S. N., and K. Sridharan, Parameter estimation in water-distribution systems by least squares, *Journal of Water Resources Planning and Management, ASCE*, *120*(4), 405–422, 1994.

De Salis, M. H. F., and D. J. Oldham, Determination of the blockage area function of a finite duct from a single pressure response measurement, *Journal of Sound and Vibration*, *221*(1), 180–186, 1999.

de Salis, M. H. F., and D. J. Oldham, The development of a rapid single spectrum method for determining the blockage characteristics of a finite length duct, *Journal of Sound and Vibration*, *243*(4), 625–640, 2001.

de Salis, M. H. F., N. V. Movchan, and D. J. Oldham, Characterizing holes in duct walls using resonance frequencies, *Journla of the Acoustical Society of America*, *111*(6, June), 2583–2593, 2002.

del Valle, Y., G. K. Venayagamoorthy, S. Mohagheghi, J. C. Hernandez, and R. G. Harley, Particle swarm optimization: Basic concepts, variants and applications in power systems, *IEEE Transactions on Evolutionary Computation*, *12*(2), 171–195, 2008.

Dempster, A. P., N. M. Larid, and D. B. Rubin, Maximum likelihood from incomplete data set via the em algorithm, *Journal of the Royal Statistical Society.*, *B 39*(1), 1–38, 1977.

Desoer, C. A., and E. S. Kuh, *Basic Circuit Theory*, McGraw-Hill, New York, 1969.

Desoer, C. A., and M. Vidyasagar, *Feedback Systems: Input-Output Properties*, Academic Press, New York, 1975.

Diestel, R., *Graph Theory*, electronic edition ed., Springer-Verlag, New York, USA, 2000.

Digernes, T., Real-time pipeline detection and identification applied to supervision of oil transport in pipelines, *Modeling, Identification and Control*, *1*(1), 39–49, 1980.

Dinis, J. M., A. K. Wojtanowicz, and S. L. Scott, Leak detection in liquid subsea flowlines with no recorded feed rate, *Journal of Energy Resources Technology, ASME*, *121*, 161–166, 1999.

Elfadel, I. M., H. M. Huang, A. E. Ruehli, A. Dounavis, and M. S. Nakhla, A comparative study of two transient analysis algorithms for lossy transmission lines with frequency-dependent data, *IEEE Transactions on Advanced Packaging*, *25*(2), 143–153, 2002.

Emara-Shabaik, H. E., Y. A. Khulief, and I. Hussaini, A non-linear multiple-model state estimation scheme for pipeline leak detection and isolation, *Proceedings of the Institution of Mechanical Engineers, Part I: Journal of Systems and Control Engineering*, *216*(6), 497–512, 2002.

Ferrante, M., and B. Brunone, Leak detection in pressurised pipes by means of wavelet analysis, in *4th International Conference on Water Pipeline Systems: Managing Pipeline Assets in an Evolving Market*, pp. 243–255, BHR Group, York, UK, 2001.

Ferrante, M., and B. Brunone, Pipe system diagnosis and leak detection by unsteady-state tests 1. Harmonic Analysis, *Advances in Water Resources*, *26*, 95–105, 2003a.

Ferrante, M., and B. Brunone, Pipe system diagnosis and leak detection by unsteady-state tests. 2. wavelet analysis, *Advances in Water Resources*, *26*, 107–116, 2003b.

Ferrante, M., B. Brunone, and A. G. Rossetti, Harmonic analysis of pressure signal during transients for leak detection in pressurized pipes, in *4th International Conference on Water Pipeline Systems: Managing Pipeline Assets in an Evolving Market*, pp. 259–275, BHR Group, York, UK, 2001.

Ferrante, M., B. Brunone, S. Meniconi, and C. Almadori, Wavelet analysis of numerical pressure signals for leak monitoring, in *CCWI 2005, Water Management for the 21-st Century*, vol. 1, edited by D. Savic, G. Walters, R. King, and S.-T. Khu, pp. 329–334, Exeter, UK, 2005.

Fijavz, M. K., D. Mugnolo, and E. Sikolya, Variational and semigroup methods for waves and diffusion in networks, pp. 219–240, Springer, 2007.

Fox, J. A., *Hydraulic Analysis of Unsteady Flow in Pipe Networks*, The Macmillan Press Ltd., London, UK, 1977.

Frank, P. M., and X. C. Ding, Frequency-domain approach to optimally robust residual generation and evaluation for model-based fault-diagnosis, *Automatica*, *30*(5), 789–804, 1994.

Franke, P. G., and F. Seyler, Computation of unsteady pipe flow with respect to viscoelastic material properties, *Journal of Hydraulic Research, IAHR*, *21*(5), 345–353, 1983.

Franklin, G. F., J. D. Powell, and M. L. Workman, *Digital control of dynamic systems*, 3rd ed., Addison-Wesley, Menlo Park, Calif., 1998.

Franklin, G. F., J. D. Powell, and A. Emami-Naeini, *Feedback control of dynamic systems*, 4th ed., Prentice Hall PTR, Upper Saddle River, N. J. London, 2001.

Fuchs, H. V., and R. Riehle, Ten years of experience with leak detection by acoustic signal analysis, *Applied Acoustics*, *33*(1), 1–19, 1991.

Funk, J. E., and D. J. Wood, Frequency response of fluid lines with turbulent flow, *Journal of Fluids Engineering, ASME*, (December), 365–369, 1974.

Furness, R. A., and J. D. Reet, Pipe line leak detection techniques, in *Pipe Line Rules of Thumb Handbook*, edited by E. W. McAllister, 4 ed., pp. 476–484, Gulf Publishing Company, Houston, Texas, 1998.

Gally, M., M. Gney, and E. Rieuford, An investigation of pressure transients in viscoelastic pipes, *Journal of Fluids Engineering, Transactions of the ASME*, *101*(December), 495–499, 1979.

Ghidaoui, M. S., Analysis of discretization strategies in fixed grid method of characteristics solution in closed conduits, Ph. d. thesis, University of Toronto, 1993.

Ghidaoui, M. S., and B. W. Karney, Equivalent differential equations in fixed-grid characteristics method, *Journal of Hydraulic Engineering, ASCE*, *120*(10), 1159–1175, 1994.

Ghidaoui, M. S., B. W. Karney, and D. A. McInnis, Energy estimates for discretization errors in water hammer problems, *Journal of Hydraulic Engineering, ASCE*, *124*(4), 384–393, 1998.

Ghilardi, P., and A. Paoletti, Additional viscoelastic pipes as pressure surges suppressors, in *5th International Conference on Pressure Surges*, pp. 113–121, BHRA, Hannover, Germany, 1986.

Goldberg, D. E., and E. B. Wylie, Characteristics method using time-line interpolations, *Journal of Hydraulic Engineering, ASCE*, *109*(5), 670–683, 1983.

Golub, G. H., and C. Van Loan, *Matrix Computations*, North Oxford Academic, Oxford, 1983.

Goodson, R. E., Distributed system simulation using infinite product expansions, *Simulation*, *15*(6), 255–263, 1970.

Goodson, R. E., and R. G. Leonard, A survey of modeling techniques for fluid line transient, *Journal of Basic Engineering, ASME*, *94*, 474–482, 1972.

Goodson, R. E., and M. P. Polis, Identification of parameters in distributed systems: A synthesising overview, in *Joint Automatic Control Conference*, Identification of parameters in distributed systems, pp. 1–30, ASME, Austin, Texas, US, 1974.

Greco, M., and G. Del Giudice, New approach to water distribution network calibration, *Journal of Hydraulic Engineering, ASCE*, *125*(8, August), 849–854, 1999.

Güney, M. S., Waterhammer in viscoelastic pipes where cross-section parameters are time dependent, in *4th International Conference on Pressure Surges*, pp. 189–204, BHRA Fluid Engineering, Bath, UK, 1983.

Han, Z. G., W. H. Li, and S. L. Shah, Fault detection and isolation in the presence of process uncertainties, *Control Engineering Practice*, *13*(5), 587–599, 2005.

Hansen, P. C., Oblique projections, pseudoinverses, and standard-form transformations, *Tech. Rep. IMM-2004-13*, The Technical University of Denmark, 2004.

Herrera, F., M. Lozano, and J. L. Verdegay, Tackling real-coded genetic algorithms: Operators and tools for behavioural analysis, *Artificial Intelligence Review*, *12*(4), 265–319, 1998.

Hill, D. J., and P. J. Moylan, Dissipative dynamical-systems - basic input-output and state properties, *Journal of the Franklin Institute-Engineering and Applied Mathematics*, *309*(5), 327–357, 1980.

Holman, J. P., *Thermodynamics*, third ed., McGraw-Hill, New York, 1980.

Holmboe, E. L., and W. T. Rouleau, The effect of viscous shear on transients in liquid lines, *Journal of Basic Engineering, ASME*, *89*(March), 174–180, 1967.

Horn, R. A., and C. R. Johnson, *Topics in Matrix Analysis*, Cambridge University Press, Cambridge, New York, 1991.

Horn, R. A., and F. Zhang, Basic properties of the schur complement, in *The Schur Complement and its Applications*, edited by F. Zhang, Springer, New York, 2005.

Hou, M., and P. C. Muller, Fault-detection and isolation observers, *International Journal of Control*, *60*(5), 827–846, 1994.

Hsue, C. Y. Y., and D. A. Hullender, Modal approximations for the fluid dynamics of hydraulic and pneumatic transmission lines, in *Fluid transmission line dynamics: ASME Winter Annual Meeting*, edited by M. E. Franke and T. M. Drzewiecki, Boston, Massachusetts, 1983.

Hullender, D. A., and A. J. Healey, Rational polynomial approximations for fluid transmission line models, in *Fluid transmission line dynamics: ASME Winter Annual Meeting*, edited by M. E. Franke and T. M. Drzewiecki, pp. 33–55, Washington, Columbia, 1981.

Hullender, D. A., R. L. Woods, and C. H. Hsu, Time domain simulation of fluid transmission lines using minimum order state variable models, in *Fluid transmission line dynamics: ASME Winter Annual Meeting*, edited by M. E. Franke and T. M. Drzewiecki, Boston, Massachusetts, 1983.

Iberall, A. S., Attenuation of oscillatory pressures in instrument lines, *Journal of Research, National Bureau of Standards, USA*, *45*, 85–108, 1950.

Ingeduld, P., E. Zerman, and A. Verwey, Object-oriented hydroinformatics tools for transient flow analysis, in *Water Supply Systems - New Technologies, NATO-ASI*, vol. 15, edited by C. Maksimovic, F. Calomino, and J. Snoxell, pp. 451–462, Springer-Verlag, Berlin, 1996.

Isermann, R., Process fault-detection based on modeling and estimation methods - a survey, *Automatica*, *20*(4), 387–404, 1984.

Ivetic, M., and D. A. Savic, Practical implications of using induced transients for leak detection, in *3rd World Water Forum*, Kyoto, Japan, 2002.

Izquierdo, J., and P. L. Iglesias, Mathematical modelling of hydraulic transients in complex systems, *Mathematical and Computer Modelling*, *39*(4-5), 529–540, 2004.

John, L. R., Forward electrical transmission line model of the human arterial system, *Medical and Biological Engineering and Computing*, *42*(3), 312–321, 2004.

Johnson, B. L., and D. E. Wandling, Transfer functions and input impedances of pressurized piping systems, *Journal of Basic Engineering, ASME*, pp. 440–443, 1967.

Johnson, C. R., Inequalities for a complex matrix whose real part is positive definite, *Transactions of the American Mathematical Society*, *212*, 149–154, 1975.

Jönsson, L., and M. Larson, Leak detection through hydraulic transient analysis, in *Pipeline Systems*, edited by B. Coulbeck and E. P. Evans, pp. 273–286, Kluwer Academic Publishers, 1992.

Jung, B. S., and B. W. Karney, Systematic exploration of pipeline network calibration using transients, *Journal of Hydraulic Research*, *46*, 129–137, 2008.

Kapelan, Z. S., D. A. Savic, and G. A. Walters, A hybrid inverse transient model for leakage detection and roughness calibration in pipe networks, *Journal of Hydraulic Research*, *41*(5), 481–492, 2003.

Kapelan, Z. S., D. A. Savic, and G. A. Walters, Calibration of water distribution hydraulic models using a bayesian-type procedure, *Journal of Hydraulic Engineering, ASCE*, *133*(8), 927–936, 2007.

Karam Jr., J. T., and R. G. Leonard, A simple yet theoretically based time domain model for fluid transmission line systems, *Journal of Fluids Engineering, Transactions of the ASME, Series I*, *95*(4, December), 498–504, 1973.

Karney, B. W., Analysis of fluid transients in large distribution networks, PhD thesis, The University of British Columbia, 1984.

Karney, B. W., Energy relations in transient closed-conduit flow, *Journal of Hydraulic Engineering, ASCE*, *116*(10), 1180–1196, 1990.

Karney, B. W., and M. S. Ghidaoui, Flexible discretization algorithm for fixed-grid moc in pipelines, *Journal of Hydraulic Engineering, ASCE*, *123*(11), 1004–1011, 1997.

Kennedy, J., and R. Eberhart, Particle swarm optimization, in *IEEE Int. Conf. Neural Netw.*, vol. 4, p. 19421948, 1995.

Khulief, Y. A., and H. E. Emara-Shabaik, Laboratory investigation of a multiple-model state estimation scheme for detection and isolation of leaks in pipelines, *Proceedings of the Institution of Mechanical Engineers Part I-Journal of Systems and Control Engineering*, *220*(I1), 1–13, 2006.

Kim, S. H., Address oriented impedance matrix method for generic calibration of heterogeneous pipe network systems, *Journal of Hydraulic Engineering, ASCE, Accepted for Publication*, 2007.

Kim, S. H., Address-oriented impedance matrix method for generic calibration of heterogeneous pipe network systems, *Journal of Hydraulic Engineering, ASCE*, *134*(1), 66–75, 2008.

Kiuchi, T., A leak localization method of pipeline by means of fluid transient model, *Journal of Energy Resources Technology, ASME*, *115*, 162–167, 1993.

Kralik, J., P. Stiegler, Z. Vostry, and J. Zavorka, Modeling the dynamics of flow in gas-pipelines, *IEEE Transactions on Systems Man and Cybernetics*, *14*(4), 586–596, 1984a.

Kralik, J., P. Stiegler, Z. Vostry, and J. Zavorka, A universal dynamic simulation-model of gas-pipeline networks, *IEEE Transactions on Systems Man and Cybernetics*, *14*(4), 597–606, 1984b.

Kramar, M., and E. Sikolya, Spectral properties and asymptotic periodicity of flows in networks, *Mathematische Zeitschrift*, *249*(1), 139–162, 2005.

Kreyszig, E., *Advanced Engineering Mathematics*, 8th ed., John Wiley, New York, 1999.

Krus, P., K. Weddfelt, and J. O. Palmberg, Fast pipeline models for simulation of hydraulic systems, *Journal of Dynamic Systems Measurement and Control-Transactions of the ASME*, *116*(1), 132–136, 1994.

Lee, P. J., Detection of leaks in pipelines using coded pressure signals, *PhD upgrade report*, Department of Civil and Environmental Engineering, University of Adelaide, 2001.

Lee, P. J., J. P. Vítkovský, M. F. Lambert, A. R. Simpson, and J. A. Liggett, Leak detection in pipelines using and inverse resonance method, in *1st Annual Environmental & Water Resources Systems Analysis Symposium in conjunction with ASCE Environmental & Water Resources Institute Annual Conference*, Roanoke, Virginia, USA, 2002.

Lee, P. J., J. P. Vítkovský, M. F. Lambert, A. R. Simpson, and J. A. Liggett, Frequency response coding for the location of leaks in single pipeline systems, in *Pumps, Electromechanical Devices and Systems Applied to Urban Water Management*, vol. 1, edited by E. Cabrera and E. Cabrera Jr., pp. 371–378, Valencia, Spain, 2003a.

Lee, P. J., J. P. Vítkovský, A. R. Simpson, M. F. Lambert, and J. A. Liggett, Discussion to leak detection in pipes by frequency response method using a step excitation, 2002, 40(1), 55-62, *Journal of Hydraulic Research, IAHR*, *41*(2), 221–223, 2003b.

Lee, P. J., J. P. Vítkovský, M. F. Lambert, A. R. Simpson, and J. A. Liggett, Frequency response leak detection using inline valve closures, in *9th International Conference on Pressure Surges*, vol. 2, pp. 239–253, BHR Group Ltd, Chester, UK, 2004.

Lee, P. J., J. P. Vítkovský, M. F. Lambert, A. R. Simpson, and J. A. Liggett, Frequency domain analysis for detecting pipeline leaks, *Journal of Hydraulic Engineering, ASCE*, *131*(7), 596–604, 2005a.

Lee, P. J., J. P. Vítkovský, M. F. Lambert, A. R. Simpson, and J. A. Liggett, Leak location using the pattern of the frequency response diagram in pipelines: a numerical study, *Journal of Sound and Vibration*, *284*(3-5), 1051–1073, 2005b.

Liggett, J. A., and L. C. Chen, Inverse transient analysis in pipe networks, *Journal of Hydraulic Engineering, ASCE*, *120*(8), 934–955, 1994.

Liou, C. P., Pipeline leak detection by impulse response extraction, *Journal of Fluids Engineering, ASME*, *120*(December), 833–838, 1998.

Liou, J. C. P., and J. Tian, Leak detection - transient flow simulation approaches, *Journal of Energy Resources Technology*, *117*(September), 243–248, 1995.

Ljung, L., *System Identification: Theory for the User*, 2 ed., Prentice Hall PTR, Upper Saddle River, New Jersey, 1999.

Loparo, K. A., M. R. Buchner, and K. S. Vasudeva, Leak detection in an experimental heat-exchanger process - a multiple model approach, *IEEE Transactions on Automatic Control*, *36*(2), 167–177, 1991.

Lynn, P. A., *An Introduction to the Analysis and Processing of Signals*, 2nd ed., The Macmillan Press Ltd., Hong Kong, 1982.

Maffucci, A., and G. Miano, On the dynamic equations of linear multiconductor transmission lines with terminal nonlinear multiport resistors, *IEEE Transactions on Circuits and Systems I-Fundamental Theory and Applications*, *45*(8), 812–829, 1998.

Magnus, J. R., and H. Neudecker, *Matrix differential calculus with applications in statistics and econometrics*, Wiley series in probability and statistics, John Wiley, New York, 1999.

Makinen, J., R. Piche, and A. Ellman, Fluid transmission line modeling using a variational method, *Journal of Dynamic Systems Measurement and Control-Transactions of the ASME*, *122*(1), 153–162, 2000.

Margolis, D. L., and W. C. Yang, Bond graph models for fluid networks using modal approximation, *Journal of Dynamic Systems Measurement and Control-Transactions of the ASME*, *107*(3), 169–175, 1985.

Mathai, A. M., and S. B. Provost, *Quadratic forms in random variables : theory and applications*, *Statistics, textbooks and monographs*, vol. 126, M. Dekker, New York, 1992.

Mohapatra, P. K., M. H. Chaudhry, A. Kassem, and J. Moloo, Detection of partial blockages in a branched piping system by the frequency response method, *Journal of Fluids Engineering-Transactions of the ASME*, *128*(5), 1106–1114, 2006a.

Mohapatra, P. K., M. H. Chaudhry, A. A. Kassem, and J. Moloo, Detection of partial blockage in single pipelines, *Journal of Hydraulic Engineering-ASCE*, *132*(2), 200–206, 2006b.

Monticelli, A., *State Estimation in Electric Power Systems : a Generalized Approach*, The Kluwer international series in engineering and computer science ; SECS 507. Power electronics and power systems, Kluwer Academic Publishers, Boston, 1999.

Mpesha, W., S. L. Gassman, and M. H. Chaudhry, Leak detection in pipes by frequency response method, *Journal of Hydraulic Engineering, ASCE*, *127*(2, February), 134–147, 2001.

Mpesha, W., M. H. Chaudhry, and S. L. Gassman, Leak detection in pipes by frequency response method using a step excitation, *Journal of Hydraulic Research, IAHR*, *40*(1), 55–62, 2002.

Muggleton, J. M., M. J. Brennan, and R. J. Pinnington, Wavenumber prediction of waves in buried pipes for water leak detection, *Journal of Sound and Vibration*, *249*(5), 939–954, 2002.

Mukherjee, J., and S. Narasimhan, Leak detection in networks of pipelines by the generalized likelihood ratio method, *Industrial & Engineering Chemistry Research, ASC*, *35*, 1886–1893, 1996.

Munson, B. R., D. F. Young, and T. H. Okiishi, *Fundamentals of Fluid Mechanics*, 4th ed., Wiley, New York, 2002.

Murli, A., and M. Rizzardi, Talbot method for the Laplace inversion problem, *ACM Transactions on Mathematical Software*, *16*(2), 158–168, times Cited: 26, 1990.

Muto, T., and T. Kanei, Resonance and transient-response of pressurized complex pipe systems, *Bulletin of the JSME*, *23*(184), 1610–1617, 1980.

Muto, T., and H. Kayukawa, Transient-response . 2. dynamic-response of tapered fluid lines, *Bulletin of the JSME*, *29*(257), 3725–3730, 1986.

Muto, T., and K. Takahashi, Step responses of single pipeline and series pipelines - transient responses of fluid lines, *Bulletin of the JSME*, *28*(244), 2325–2331, 1985.

Muto, T., Y. Kinoshita, and R. Yoneda, Dynamic-response of tapered fluid lines . 1. transfer-matrix and frequency-response, *Bulletin of the JSME*, *24*(191), 809–815, 1981.

Nash, G. A., and B. W. Karney, Efficient inverse transient analysis in series pipe systems, *Journal of Hydraulic Engineering, ASCE*, *125*(7, July), 761–764, 1999.

Nikolova, N. K., R. Safian, E. A. Soliman, M. H. Bakr, and J. W. Bandler, Accelerated gradient based optimization using adjoint sensitivities, *IEEE Transactions on Antennas and Propagation*, *52*(8), 2147–2157, 2004.

Nixon, W., M. S. Ghidaoui, and A. A. Kolyshkin, Range of validity of the transient damping leakage detection method, *Journal of Hydraulic Engineering, ASCE*, *132*(9), 944–957, 2006.

Ogawa, N., A study on dynamic water pressure in underground pipelines of water supply system during earthquakes, in *Recent Advances in Lifeline Earthquake*

Engineering in Japan, vol. 43, edited by H. Shibata, T. Katayma, and T. Ariman, pp. 55–60, ASME, 1980.

Ogawa, N., T. Mikoshiba, and C. Minowa, Hydraulic effects on a large piping system during strong earthquakes, *Journal of Pressure Vessel Technology, ASME*, *116*(May), 161–168, 1994.

Oldenburger, R., and R. E. Goodson, Simplification of hydraulic line dynamics by use of infinite products, *Journal of Basic Engineering, Transactions of the ASME, Series D*, *86*(1, March), 1–10, 1964.

Piche, R., and A. Ellman, A fluid transmission line model for use with ODE simulators, in *Eighth Bath International Fluid Power Workshop*, Bath, UK, 1995.

Pintelon, R., P. Guillaume, Y. Rolain, J. Schoukens, and H. Vanhamme, Parametric identification of transfer-functions in the frequency-domain - a survey, *IEEE Transactions on Automatic Control*, *39*(11), 2245–2260, 1994.

Pudar, R. S., and J. A. Liggett, Leaks in pipe networks, *Journal of Hydraulic Engineering, ASCE*, *118*(7), 1031–1046, 1992.

Rao, C. R., Statistical proofs of some matrix theorems, *International Statistical Review*, *74*(2), 169–185, 2006.

Reddy, H. P., S. Narasimhan, and S. M. Bhallamudi, Simulation and state estimation of transient flow in gas pipeline networks using a transfer function model, *Industrial and Engineering Chemistry Research*, *45*(11), 3853–3863, 2006.

Reddy, P. V. N., K. Sridharan, and P. V. Rao, Wls method for parameter estimation in water distribution networks, *Journal of Water Resources Planning and Management, ASCE*, *122*(3, May/June), 157–164, 1996.

Rice, J. A., *Mathematical statistics and data analysis*, 2nd ed., Wadsworth, Belmont, CA, 1995.

Rieutord, E., and A. Blanchard, Pulsating viscoelastic pipe flow - water-hammer, *Journal of Hydraulic Research, IAHR*, *17*(3), 217–229, in French, 1979.

Rodriguez-Fernandez, M., E. Balsa-Canto, J. A. Egea, and J. R. Banga, Identifiability and robust parameter estimation in food process modeling: Application to a drying model, *Journal of Food Engineering*, *83*(3), 374–383, 2007.

Romeo, E., C. Royo, and A. Monzon, Improved explicit equations for estimation of the friction factor in rough and smooth pipes, *Chemical Engineering Journal*, *86*(3), 369–374, 2002.

Rouleau, W. T., and F. J. Young, The calculation of surge pressures in pipelines carrying vicous liquids in laminar flow, *Journal of Basic Engineering, ASME*, *87*(March), 266–268, 1965a.

Rouleau, W. T., and F. J. Young, Distortion of short pulses in tapered tube pulse transformers. part i - inviscid liquid, *Journal of Basic Engineering, ASME*, *87*(June), 465–470, 1965b.

Rouleau, W. T., and F. J. Young, Distortion of short pulses in tapered tube pulse transformers. part ii - viscous liquid, *Journal of Basic Engineering, ASME*, *87*(June), 471–477, 1965c.

Rugh, W. J., *Nonlinear Systems Theory*, The Johns Hopkins University Press, Baltimore, 1981.

Sattar, A. M., and M. H. Chaudhry, Leak detection in pipelines by frequency response method, *Journal of Hydraulic Research*, *46*, 138–151, 2008.

Schohl, G. A., Improved approximate method for simulating frequency-dependent friction in transient laminar-flow, *Journal of Fluids Engineering-Transactions of the ASME*, *115*(3), 420–424, 1993.

Schoukens, J., and R. Pintelon, *Identification of linear systems : a practical guideline to accurate modeling*, 1st ed., Pergamon Press, Oxford ; New York, 1991.

Schroeder, M., Synthesis of low-peak-factor signals and binary sequences with low autocorrelation, *Information Theory, IEEE Transactions on*, *16*(1), 85–89, 1970.

Sharp, D. B., Acoustic pulse reflectometry for the measurement of musical wind instruments, PhD, University of Edinburgh, 1996.

Sharp, D. B., Increasing the length of tubular object that can be measured using acoustic pulse reflectometry, *Measurement Science and Technology*, *9*(9), 1469–1479, 1998.

Sharp, D. B., and D. M. Campbell, Leak detection in pipes using acoustic pulse reflectometry, *Acoustica*, *83*(3), 560–566, 1997.

Shields, D. N., S. A. Ashton, and S. Daley, Robust fault detection observers for nonlinear polynomial systems, *International Journal of Systems Science*, *32*(6), 723–737, 2001.

Sibetheros, I. A., E. R. Holley, and J. M. Branski, Spline interpolations for water hammer analysis, *Journal of Hydraulic Engineering, ASCE*, *117*(10), 1332–1352, 1991.

Sikolya, E., Flows in networks with dynamic ramification nodes, *Journal of Evolution Equations*, *5*(3), 441–463, 2005.

Silva, R. A., C. M. Buiatti, S. L. Cruz, and J. A. F. R. Pereira, Pressure wave behaviour and leak detection in pipelines, *Computers & Chemical Engineering*, *20*(Suppliment 6. Part A), S491–S496, 1996.

Sorensen, H. V., D. L. Jones, M. T. Heideman, and C. S. Burrus, Real-valued fast fourier transform algorithms, *IEEE Trans. Acoust. Speech Sig. Processing*, *35*, 849–863, 1987.

Stecki, J. S., and D. C. Davis, Fluid transmission-lines - distributed parameter models . 1. A review of the state-of-the-art, *Proceedings of the Institution of Mechanical Engineers Part A-Journal of Power and Energy*, *200*(4), 215–228, 1986.

Stehfest, F., Algorithm 368. numerical inversion of Laplace transforms, *Commun. ACM*, *13*(1), 47–54, 1970.

Stephens, M. L., Transient response analysis for fault detection and pipeline wall condition assessment in field water transmission and distribution pipelines and networks, PhD, The University of Adelaide, 2008.

Stoianov, I., B. Karney, D. Covas, C. Maksimovic, and N. Graham, Wavelet processing of transient signals for pipeline leak location and quantification, in *Water Software Systems: Theory and Applications*, vol. 1, edited by B. Ulanicki, B. Coulback, and J. P. Rance, pp. 65–76, Research Studies Press Ltd., Baldock, Hertfordshire, England, 2001.

Stoianov, I., D. Covas, B. Karney, C. Maksimovic, and N. Graham, Wavelet analysis of synchronised transient signals for leak location in pipelines, *Submitted to Journal of Hydraulic Engineering, ASCE*, 2002a.

Stoianov, I., B. Karney, D. Covas, C. Maksimovic, and N. Graham, Wavelet processing of transient signals for pipeline leak location and quantification, in *1st Annual Environmental & Water Resources Systems Analysis Symposium in conjunction with ASCE Environmental & Water Resources Institute Annual Conference*, Roanoke, Virginia, USA, 2002b.

Streeter, V. L., E. B. Wylie, and K. W. Bedford, *Fluid Mechanics*, 9th ed., WCB/McGraw Hill, Boston, Mass., 1997.

Suo, L., and E. B. Wylie, Impulse response method for frequency-dependent pipeline transients, *Journal of Fluids Engineering, ASME*, *111*(December), 478–483, 1989.

Suo, L., and E. B. Wylie, Hydraulic transients in rock-bored tunnels, *Journal of Hydraulic Engineering, ASCE*, *116*(2), 196–210, 1990.

Tafuri, A. N., Locating leaks with acoustic technology, *Journal of the American Water Works Association*, *92*(7, July), 57–66, 2000.

Tahmeen, M., T. Muto, and H. Yamada, Simulation of dynamic responses of tapered fluid lines, *JSME International Journal Series B-Fluids and Thermal Engineering*, *44*(2), 247–254, 2001.

Tanji, Y., and A. Ushida, Closed-form expression of RLCG transmission line and its application, *Electronics and Communications in Japan Part Iii-Fundamental Electronic Science*, *87*(4), 1–11, 2004.

Tarantine, F. J., and W. T. Rouleau, Fluid pressure transients in a tapered transmission line, *Journal of Basic Engineering, ASME*, *89*(1), 1967.

Taylor, S. E. M., D. N. Johnston, and D. K. Longmore, Modelling of transient flow in hydraulic pipelines, *Proceedings of the Institution of Mechanical Engineers Part I-Journal of Systems and Control Engineering*, *211*(6), 447–456, 1997.

Tentarelli, S. C., and F. T. Brown, Dynamic behavior of complex fluid-filled tubing systems - part 2: System analysis, *Journal of Dynamic Systems Measurement and Control-Transactions of the ASME*, *123*(1), 78–84, 2001.

Thompson, W. C., and K. D. Skogman, The application of real time flow modeling to pipeline leak detection, *Journal of Energy Resources Technology, ASME*, *105*, 536–541, 1983.

Tijsseling, A. S., Fluid-structure interaction in liquid-filled pipe systems: A review, *Journal of Fluids and Structures, Academic Press Limited*, *10*, 109–146, 1996.

Todini, E., Using a kalman filter approach for looped water distribution networks calibration, in *Water Industry Systems: Modelling and Optimisation Applications*, edited by D. A. Savic and G. A. Walters, Research Studies Press Ltd., Baldock, Hertfordshire, England, 1999.

Todini, E., and S. Pilati, A gradient algorithm for the analysis of pipe networks, in *Computer Applications in Water Supply*, edited by B. Coulbeck and C. H. Orr, pp. 1–20, Research Studies Press, Letchworth, Hertfordshire, UK, 1988.

Tong, J., A generalization of the mean value theorem for integrals, *The College Mathematics Journal*, *33*(5), 408409, 2002.

Trikha, A. K., An efficient method for simulating frequency-dependent friction in transient liquid flow, *Journal of Fluids Engineering, Transactions of the ASME, Series I*, *97*(1, March), 97–105, 1975.

Triverio, P., S. Grivet-Talocia, M. S. Nakhla, F. G. Canavero, and R. Achar, Stability, causality, and passivity in electrical interconnect models, *IEEE Transactions on Advanced Packaging*, *30*(4), 795–808, 2007.

Tschoegl, N. W., *Phenomenological Theory of Linear Viscoelastic Behaviour: An introduction*, Springer-Verlag, Berlin, New York, 1989.

Valko, P. P., and J. Abate, Comparison of sequence accelerators for the Gaver method of numerical Laplace transform inversion, *Computers and Mathematics with Applications*, *48*(3-4), 629–636, times Cited: 22, 2004.

Vanecek, S., A. Verwey, and M. B. Abbott, Hypress: An exercise in object-orientation for waterhammer and water distribution simulation in pipe networks, in *Hydroinformatics '94*, vol. 1, edited by A. Verwey, A. W. Minns, V. Babovic, and C. Maksimovic, pp. 267–274, Rotterdam, Netherlands, 1994.

Vardy, A., J. Brown, and S. He, Signs of unsteady skin friction, in *9th International Conference on Pressure Surges*, pp. 493–507, BHR Group, Chester, UK, 2004.

Vardy, A. E., and J. M. B. Brown, Transient turbulent friction in smooth pipe flows, *Journal of Sound and Vibration*, *259*(5, January), 1011–1036, 2003.

Vardy, A. E., and J. M. B. Brown, Transient turbulent friction in fully-rough pipe flows, *Journal of Sound and Vibration*, *270*, 233–257, 2004.

Vardy, A. E., and J. M. B. Brown, Approximation of turbulent wall shear stresses in highly transient pipe flows, *Journal of Hydraulic Engineering-ASCE*, *133*(11), 1219–1228, 2007.

Vardy, A. E., K. L. Hwang, and J. M. Brown, A weighting function model of transient turbulent pipe friction, *Journal of Hydraulic Research, IAHR*, *31*(4), 533–548, 1993.

Venkatasubramanian, V., R. Rengaswamy, K. Yin, and S. N. Kavuri, A review of process fault detection and diagnosis: Part i: Quantitative model-based methods, *Computers & Chemical Engineering*, *27*(3), 293–311, 2003.

Verde, C., Multi-leak detection and isolation in fluid pipelines, *Control Engineering Practice*, *9*(6), 673–682, 2001.

Verde, C., Minimal order nonlinear observer for leak detection, *Journal of Dynamic Systems Measurement and Control-Transactions of the ASME*, *126*(3), 467–472, 2004.

Verde, C., Accommodation of multi-leak location in a pipeline, *Control Engineering Practice*, *13*(8), 1071–1078, 2005.

Verwey, A., and J. H. Yu, A space-compact high-order implicit scheme for water hammer simulations, in *25th IAHR Congress*, vol. 5, Tokyo, Japan, 1993.

Vítkovský, J. P., Inverse analysis and modelling of unsteady pipe flow: Theory, applications and experimental verification, PhD thesis, Adelaide University, 2001.

Vítkovský, J. P., M. F. Lambert, A. R. Simpson, and A. Bergant, Advances in unsteady friction modelling in transient pipe flow, in *Safe Design and Operation of Industrial Pipe Systems: 8th International Conference on Pressure Surges*, pp. 471–482, BHR Group, The Hague, The Netherlands, 2000.

Vítkovský, J. P., A. R. Simpson, and M. F. Lambert, Optimal measurement site placement for inverse transient leak detection using genetic algorithms, in *3rd IWA World Water Congress*, Melbourne, Australia, 2002.

Vítkovský, J. P., P. J. Lee, M. L. Stephens, M. F. Lambert, A. R. Simpson, and J. A. Liggett, Leak and blockage detection in pipelines via an impulse response method, in *Pumps, Electromechanical Devices and Systems Applied to Urban Water Management*, vol. 1, edited by E. Cabrera and E. Cabrera Jr., pp. 423–430, Valencia, Spain, 2003a.

Vítkovský, J. P., J. A. Liggett, A. R. Simpson, and M. F. Lambert, Optimal measurement site locations for inverse transient analysis in pipe networks, *Journal of Water Resources Planning and Management, ASCE*, *129*(6, November/December), 480–492, 2003b.

Vítkovský, J. P., M. L. Stephens, A. Bergant, M. F. Lambert, and A. R. Simpson, Efficient and accurate calculation of zielke and vardy-brown unsteady friction in pipe transients, in *9th International Conference on Pressure Surges*, vol. 2, pp. 405–419, BHR Group Ltd, Chester, UK, 2004.

Vítkovský, J. P., M. F. Lambert, A. R. Simpson, and J. A. Liggett, Experimental observation and analysis of inverse transients for pipeline leak detection, *Journal of Water Resources Planning and Management-ASCE*, *133*(6), 519–530, 2007.

Wang, G. Z., D. Dong, and C. Z. Fang, Leak detection for transport pipelines based on autoregressive modeling, *IEEE Transactions on Instrumentation and Measurement*, *42*(1), 68–71, 1993.

Wang, H., G. H. Priestman, S. B. M. Beck, and R. F. Boucher, Pressure wave attenuation in an air pipe flow, *Proceedings of the Institution of Mechanical Engineers Part C-Journal of Mechanical Engineering Science*, *214*(4), 619–632, 2000.

Wang, X. J., M. F. Lambert, A. R. Simpson, and J. P. Vítkovský, Leak detection in pipeline systems and networks: A review, in *6th Conference on Hydraulics in Civil Engineering*, pp. 391–400, I. E. Aust., Hobart, Australia, 2001.

Wang, X. J., M. F. Lambert, A. R. Simpson, J. A. Liggett, and J. P. Vitkovsky, Leak detection in pipelines using the damping of fluid transients, *Journal of Hydraulic Engineering, ASCE*, *128*(7), 697–711, 2002a.

Wang, X. J., M. F. Lambert, A. R. Simpson, J. A. Liggett, and J. P. Vítkovský, Leak detection in pipeline systems using the damping of fluid transients, *Journal of Hydraulic Engineering, ASCE*, *128*(7, July), 697–711, 2002b.

Wang, X. J., M. F. Lambert, and A. R. Simpson, Behavior of short lateral dead ends on pipeline transients: A lumped parameter model and an analytical solution, *Journal of Fluids Engineering-Transactions of the ASME*, *127*(3), 529–535, 2005a.

Wang, X. J., M. F. Lambert, and A. R. Simpson, Detection and location of a partial blockage in a pipeline using damping of fluid transients, *Journal of Water Resources Planning and Management, ASCE*, *131*(3), 244–249, 2005b.

Washio, S., T. Konishi, and K. Okamura, Research on wave phenomena in hydraulic lines (1st report, unsteady flow in a uniform pipe), *Bulletin of the Japan Society of Mechanical Engineers*, *17*(111), 1157–1964, 1974a.

Washio, S., T. Konishi, and K. Okamura, Research on wave phenomena in hydraulic lines (2nd report, unsteady liquid flow in a tapered pipe), *Bulletin of the Japan Society of Mechanical Engineers*, *17*(111), 1165–1971, 1974b.

Washio, S., T. Konishi, and Y. Miyazawa, Research on wave phenomena in hydraulic lines (6th report, transient properties of nonlinear elements), *Bulletin of the Japan Society of Mechanical Engineers*, *22*(172), 1399–1406, 1979.

Watanabe, M., and K. Yamaguchi (Eds.), *The EM algorithm and related statistical models*, *Statistics, textbooks and monographs*, vol. 170, Marcel Dekker, New York, 2004.

Watton, J., Modeling of electrohydraulic systems with transmission-lines using modal approximations, *Proceedings of the Institution of Mechanical Engineers Part B-Journal of Engineering Manufacture*, *202*(3), 153–163, 1988.

Wiggert, D. C., and M. J. Sundquist, Fixed-grid characteristics for pipeline transients, *Journal of Hydraulic Engineering, ASCE*, *103*(HY12), 1403–1416, 1977.

Willsky, A. S., A survey of design methods for failure detection in dynamic systems, *Automatica*, *12*, 601–611, 1976.

Wohlers, M. R., *Lumped and Distributed passive networks; a generalised and advanced viewpoint*, Electrical science, Academic Press, New York, 1969.

Wood, D. J., S. Lingireddy, and P. F. Boulos, *Pressure Wave Analysis of Transient Flow in Pipe Distribution Systems*, MWH Soft, Pasadena, California USA, 2005.

Woods, R. L., A first order square-root approximation for fluid transmission lines, in *Fluid transmission line dynamics: ASME Winter Annual Meeting*, edited by M. E. Franke and T. M. Drzewiecki, Boston, Massachusetts, 1983.

Wu, Q., and F. Fricke, Estimation of blockage dimensions in a duct using measured eigenfrequency shifts, *Journal of Sound and Vibration*, *133*(2), 289–310, 1989.

Wu, Q. L., Reconstruction of integrated crack function of beams from eigenvalue shifts, *Journal of Sound and Vibration*, *173*(2), 279–282, 1994.

Wu, Q. L., and F. Fricke, Determination of blocking locations and cross-sectional area in a duct by eigenfrequency shifts, *Journal of the Acoustical Society of America*, *87*(1), 67–75, 1990.

Wylie, E. B., Resonance in pressurized piping systems, *Journal of Basic Engineering, Transactions of the ASME*, (December), 960–966, 1965.

Wylie, E. B., and V. L. Streeter, *Fluid Transients in Systems*, Prentice-Hall Inc., Englewood Cliffs, New Jersey, USA, 1993.

Yang, J. C., and E. L. Hsu, Time-line interpolation for solution of the dispersion equation, *Journal of Hydraulic Research, IAHR*, *28*(4), 503–523, 1990.

Yang, W. C., and W. E. Tobler, Dissipative modal approximation of fluid transmission-lines using linear friction model, *Journal of Dynamic Systems Measurement and Control-Transactions of the ASME*, *113*(1), 152–162, 1991.

Zecchin, A. C., L. B. White, M. F. Lambert, and A. R. Simpson, Frequency-domain hypothesis testing approach to leak detection in a single fluid line, in *CCWI 2005,* *Water Management for the 21st Century*, vol. 2, edited by D. Savic, G. Walters, R. King, and S.-T. Khu, pp. 149–154, Exeter, UK, 2005.

Zecchin, A. C., M. F. Lambert, A. R. Simpson, and L. B. White, Laplace-domain comparison of linear models of a reservoir-pipe-valve system with a leak, in *8th Annual International Water Distribution Systems Analysis Symposium*, Cincinnati, Ohio, 2006.

Zecchin, A. C., A. R. Simpson, M. F. Lambert, L. B. White, and J. P. Vítkovský, Transient modeling of arbitrary pipe networks by a Laplace-domain admittance matrix, *Journal of Engineering Mechanics, ASCE*, *135*(6), 538–547, 2009.

Zhao, M., and M. S. Ghidaoui, Godunov-type solutions for water hammer flows, *Journal of Hydraulic Engineering, ASCE*, *130*(4), 341–348, 2004.

Zhong, M. Y., S. X. Ding, J. Lam, and H. B. Wang, An lmi approach to design robust fault detection filter for uncertain lti systems, *Automatica*, *39*(3), 543–550, 2003.

Zielke, W., Frequency-dependent friction in transient pipe flow, *Journal of Basic Engineering, ASME*, *90*(1), 109–115, 1968.

Zielke, W., E. B. Wylie, and R. B. Keller, Forced and self-excited oscillations in propellant lines, *Journal of Basic Engineering, Transactions of the ASME*, (December), 671–677, 1969.

Appendix A

Admittance Representation for Transfer Matrix

This appendix focuses on the most relevant form of the transfer matrix formulations of Section 2.4.2, the admittance formulation. For a fluid line of length l, the admittance form is given by

$$\begin{bmatrix} Q(0,s) \\ -Q(l,s) \end{bmatrix} = Z_c^{-1}(s) \begin{bmatrix} \coth\Gamma(s) & -\operatorname{csch}\Gamma(s) \\ -\operatorname{csch}\Gamma(s) & \coth\Gamma(s) \end{bmatrix} \begin{bmatrix} P(0,s) \\ P(l,s) \end{bmatrix}. \tag{A.1}$$

A novel analysis of this formulation is presented here, where the distribution of the poles of the Laplace-domain representation are used to discuss important physical characteristics. Section A.2 proposes an analytic inverse Laplace transform to the admittance representation, which holds analogies to the work of *Oldenburger and Goodson* [1964].

A.1 Some Physical Properties

The most important representation in this thesis is the admittance form (2.48). We now look at some of its properties. The stability aspects of the following lemma could be established from the passivity property of the admittance matrix, but the following proof gives insight.

Lemma A.1. *The admittance matrix form* (A.1) *is (1) reciprocal, (2) stable and (3) has a stable inverse.*

Proof. 1. The reciprocity (A.1) of is observed by its symmetry.

2. The stability of (A.1) is demonstrated by showing that the elemental functions of (A.1) are members of $\mathcal{H}_\infty$, that is $F(s) \in \mathcal{H}_\infty$ if

$$|F(s)| < \infty \quad \text{for all } s \in \mathbb{C}_+.$$

To demonstrate this, the elemental functions are first shown to be finite as $|s| \to \infty$, and secondly it demonstrated that the pole locations of the elemental functions lie in the open right hand plane. The finiteness of the elemental functions as $|s| \to \infty$ is observed by the fact that $\coth(s)$, and $\operatorname{csch}(s)$ are finite at $|s| = \infty$ [*Abramowitz and Stegun*, 1964], and given the form of Z_c in Corollary 2.3, it is seen that

$$\lim_{|s|\to\infty} Z_c(s) = \sqrt{\frac{R_0}{C_0}},$$

which is alcso clearly finite. To study the nature of the pole locations, it is insightful to express the transfer matrix as

$$\frac{1}{Z_c(s)\sinh\Gamma(s)}\begin{bmatrix}\cosh\Gamma(s) & -1 \\ -1 & \cosh\Gamma(s)\end{bmatrix} \tag{A.2}$$

Now as $\cosh x$ is bounded for finite x and $\Gamma(s)$ is finite for $|s| < \infty$, the poles of this transfer matrix occur at the points

$$\{s \in \mathbb{C} : Z_c(s)\sinh\Gamma(s) = 0\} \tag{A.3}$$

Expanding this out as an infinite product [*Abramowitz and Stegun*, 1964] yields

$$Z_c(s)\sinh\Gamma(s) = R_0[s + R(s)]\prod_{k=1}^{\infty}\left(1 + \frac{\Gamma^2(s)}{(k\pi)^2}\right) \tag{A.4}$$

(where the identity $Z_c(s)\Gamma(s) = R_0[s + R(s)]$ is used). Therefore the points in the set (A.3) correspond to the points

$$\{s \in \mathbb{C} : s + R(s) = 0\} \cup \{s \in \mathbb{C} : \Gamma(s) = \pm \mathrm{i}k\pi, k = 1, 2, \ldots\} \tag{A.5}$$

where the second set corresponds to the infinite product term in (A.4). Considering these two sets further, it is clear from (A.5) that the admittance matrix is a stable transfer function. It is noted that $s + R(s)$ is a positive real function (and strictly positive real for one of $r_0 > 0, r(t) \neq 0$), therefore the points $s + R(s) = 0$ must occur in closed (open) left hand plane. Similarly, in Theorem 2.3 it was shown that $\Gamma(s)$ is also a positive real (strictly positive real) function and hence points $\Gamma(s) = \pm \mathrm{i}k\pi$ at which the real part vanishes must also lie in the left half plane.

3. A Laplace-domain matrix function $\boldsymbol{A}(s)$ possesses a stable inverse as long as $|\det \boldsymbol{A}(s)| > 0$ for $s \in \mathbb{C}_+$ [*Desoer and Vidyasagar*, 1975]. The determinant of (A.1) is given by

$$\frac{\sinh \Gamma(s)}{Z_c(s)},$$

which can be expanded as

$$\frac{\sinh \Gamma(s)}{Z_c(s)} = C_0\left[s + C(s)\right] \prod_{k=1}^{\infty} \left(1 + \frac{\Gamma^2(s)}{(k\pi)^2}\right)$$

(where the identity $\Gamma(s)/Z_c(s) = C_0\left[s + C(s)\right]$ is used). Therefore the points at which the determinant becomes zero corresponds to the points

$$\{s \in \mathbb{C} : s + C(s) = 0\} \cup \{s \in \mathbb{C} : \Gamma(s) = \pm \mathrm{i}k\pi, k = 1, 2, \ldots\} \tag{A.6}$$

which is the same as (A.5) except the first set is associated with the capacitance C and not the resistance R. As with $s+R(s)$, $s+C(s)$ is a positive real (strictly positive real) function and only vanishes in the closed (open) left hand plane. Therefore, by appealing to the argument used in the preceding point of the proof, it is demonstrated that the determinant has a nonzero magnitude on $s \in \mathbb{C}_+$.

□

Remark: There is a very interesting structure to the positioning of the poles for a fluid line, namely that the poles are aligned on a contour parallel to the imaginary axis. It has been common knowledge for a long time [*Wylie and Streeter*, 1993] that the frequency response of a fluid line consisted of an infinite series of evenly spaced harmonics, this pole location structure was first realised in *Zecchin et al.* [2005] where is was used to study the movement of the poles for a single line system with varying leak properties.

A.2 Inverse Laplace Transform For The $\mathscr{L}_R$-Class

An important application of the Laplace-domain representation of fluid lines, that has received much in the literature, is the inversion Laplace-transform of the immitance forms (2.47)-(2.50). The inverse Laplace-transforms of these equations provides the impulse response functions that can be used in time-domain simulations.

Due to the presence of the transcendental functions, and the general structure of $\Gamma(s)$ and $Z_c(s)$, the inverses Laplace-transforms can not be determined directly, hence necessitating approximations to yield analytical inverses. A detailed overview of the different approaches of approximating these inverses was given in Chapter 5, where a general approach for inverting the Laplace representation of a general fluid network is presented. But below, a novel approach for the inversion of the admittance formulation (2.48) for the class of $\mathscr{L}_R$ fluid lines is presented. The approach is based on using the Mittag-Reffler expansions series expansions of the hyperbolic functions csch and coth, which has been studied in the context of electrical transmission lines by *Tanji and Ushida* [2004].

The Mittag-Leffler Expansions for coth and csch are

$$\coth x = \frac{1}{x} + \sum_{n=1}^{\infty} \frac{2x}{x^2 + (n\pi)^2}$$
$$\operatorname{csch} x = \frac{1}{x} + \sum_{n=1}^{\infty} \frac{2x(-1)^n}{x^2 + (n\pi)^2}$$

Based on the series expansion of the hyperbolic functions coth and csch, the admittance matrix can be expanded as

$$\boldsymbol{Y}(s) = \frac{1}{R_0\left[s + R(s)\right]} \begin{bmatrix} 1 & -1 \\ -1 & 1 \end{bmatrix} + \sum_{n=1}^{\infty} \frac{2C_0\left[s + C(s)\right]}{\Gamma^2(s) + (n\pi)^2} \begin{bmatrix} 1 & (-1)^{n+1} \\ (-1)^{n+1} & 1 \end{bmatrix} \tag{A.7}$$

where the pole set specified by (A.5) clearly holds for (A.7). The expression above is insightful as it demonstrates that the pipelines dynamics can be divided into a purely frictional term and a series of pipeline modes which posses their own resistive and capacitive behaviour. Employing the residue theorem [*Kreyszig*, 1999] to compute the Bromwich integral for the inverse Laplace transform, the inverse to (A.7) can be given by

$$\boldsymbol{\mathcal{Y}}(t) = \boldsymbol{\mathcal{Y}}_o(t) + \sum_{n=1}^{\infty} \boldsymbol{\mathcal{Y}}_n(t) \tag{A.8}$$

where $\boldsymbol{\mathcal{Y}}_o(t)$ is the purely resistive term and $\boldsymbol{\mathcal{Y}}_n(t)$ are the modal terms, which are given by

$$\boldsymbol{\mathcal{Y}}_o(t) = \frac{1}{R_0} \begin{bmatrix} 1 & -1 \\ -1 & 1 \end{bmatrix} \sum_{\zeta \in \Omega_o} \operatorname{Res}\left[\frac{1}{\left[s + R(s)\right]}, s = \zeta\right] e^{\zeta} \tag{A.9}$$

$$\boldsymbol{\mathcal{Y}}_n(t) = \begin{bmatrix} 1 & (-1)^{n+1} \\ (-1)^{n+1} & 1 \end{bmatrix} 2C_0 \sum_{\zeta \in \Omega_n} \operatorname{Res}\left[\frac{\left[s + C(s)\right]}{\Gamma^2(s) + (n\pi)^2}, s = \zeta\right] e^{\zeta}, n = 1, \ldots, \infty \tag{A.10}$$

where the sets Ω_o and $\Omega_n, n = 1, \ldots, \infty$ indicate the pole locations for each term, and are defined as

$$\Omega_o = \{s \in \mathbb{C} : s + R(s) = 0\} \tag{A.11}$$

$$\Omega_n = \left\{s \in \mathbb{C} : \Gamma^2(s) + (n\pi)^2 = 0\right\}, \quad n = 1, \ldots, \infty \tag{A.12}$$

where the existence $\boldsymbol{\mathcal{Y}}$ is conditional on the sums in (A.9)-(A.10) converging.

Although (A.9)-(A.12) yield insight as to the nature of the impulse response of the admittance matrix, then do not represent an easily computable system. For the general $\mathscr{L}$-class, the determination of the pole locations and the associated residues is a nontrivial task. To facilitate further analysis, the $\mathscr{L}_R$-class is considered from hereon. As discussed previously, this class encompasses most applied versions of the unsteady shear stress/inelastic pipe water-hammer equations, and so the consideration of this class does not represent an impractical restriction.

For the $\mathscr{L}_R$-class, the functions $r(s)$ and $c(s)$ can be expressed in the numerator/denominator form

$$r(s) = \frac{r_N(s)}{r_D(s)}, \quad c(s) = \frac{c_N(s)}{c_D(s)}$$

where $r_N(s)$, $r_D(s)$, $c_N(s)$ and, $c_D(s)$ are all polynomials in s with

$$r_D(s) = \prod_{k=1}^{N_r}(s + \nu_k), \quad c_D(s) = \prod_{k=1}^{N_c}(s + \mu_k)$$

where the orders of $r_N(s)$ and $c_N(s)$ are one less than $r_D(s)$ and $c_D(s)$, respectively. The advantage of working with the $\mathscr{L}_R$-class is that it guarantees that all the poles are simple, and hence analytic representations of the residues are straight forward. Expressing Γ with these polynomials gives

$$\Gamma^2(s) = R_0 \left[s + r_o + s\frac{r_N(s)}{r_D(s)}\right] C_0 \left[s + s\frac{c_N(s)}{c_D(s)}\right]$$

which leads to the rational expressions

$$\frac{1}{s + R(s)} = \frac{r_D(s)}{(s + r_o)\, r_D(s) + s r_N(s)} \tag{A.13}$$

$$\frac{s + C(s)}{\Gamma^2(s) + (n\pi)^2} = \frac{s r_D(s)\left[c_D(s) + c_N(s)\right]}{\left[(s + r_0) r_D(s) + s r_N(s)\right]\left[s c_D(s) + s c_N(s)\right] + r_D(s) c_D(s) (n\pi)^2}. \tag{A.14}$$

Considering the purely resistive term (A.13), the numerator it of order N_r and the denominator is of order N_r+1 leading to the expression

$$\frac{1}{s+R(s)}=\frac{1}{s-p_{o0}}\prod_{k=1}^{N_r}\frac{s-z_{ok}}{s-p_{ok}}. \tag{A.15}$$

where the z_{ok} and p_{ok} are the zeros and poles of (A.13). Considering (A.14), the numerator is of the order N_r+N_c+1 and the denominator is of the order N_r+N_c+2. As recognised in *Hullender and Healey* [1981]; *Hsue and Hullender* [1983], two of the poles are a complex conjugate pair corresponding to the mode frequency, and the remaining N_r+N_c poles are real poles corresponding to the dissipation associated with the mode, therefore (A.14) can be expressed as

$$\frac{s+C(s)}{\Gamma^2(s)+(n\pi)^2}=\frac{s-z_{n0}}{s^2-2\alpha_n s+\alpha_n^2+\omega_n^2}\prod_{k=1}^{N_r+N_c}\frac{s-z_{nk}}{s-p_{nk}}. \tag{A.16}$$

The zeros of complex conjugate term are given by $s=-\alpha_n+\mathrm{i}\omega_n,-\alpha_n-\mathrm{i}\omega_n$, and these values can be approximately given by

$$\alpha_n\approx\frac{r_0}{2},\quad \omega_n\approx\mathrm{i}\frac{n\pi}{\sqrt{R_0C_0}},$$

which demonstrates the approximate dynamics associated with the n-th mode, namely harmonic oscillatory term at radial frequency $n\pi/\sqrt{R_0C_0}$ exponentially decaying according to the linear shear term $r_0/2$.

Given this, the admittance impulse response functions can be expressed as

$$\boldsymbol{\mathcal{Y}}(t)=\boldsymbol{\mathcal{Y}}_o(t)+\sum_{n=1}^{\infty}\boldsymbol{\mathcal{Y}}_{Rn}(t)+\boldsymbol{\mathcal{Y}}_{Hn}(t)$$

where $\boldsymbol{\mathcal{Y}}_o(t)$ is the purely resistive term, $\boldsymbol{\mathcal{Y}}_{Rn}(t)$ is the resistive term associated with mode n and $\boldsymbol{\mathcal{Y}}_{Hn}(t)$ is harmonic term associated with mode n. This functions can be given as

$$\boldsymbol{\mathcal{Y}}_o(t)=\begin{bmatrix}1 & -1\\ -1 & 1\end{bmatrix}\sum_{k=0}^{N_r}a_{ok}e^{p_{ok}t} \tag{A.17}$$

$$\boldsymbol{\mathcal{Y}}_{Rn}(t)=2\begin{bmatrix}1 & (-1)^{n+1}\\ (-1)^{n+1} & 1\end{bmatrix}\sum_{k=1}^{N_r+N_c}a_{Rnk}e^{p_{nk}t} \tag{A.18}$$

$$\boldsymbol{\mathcal{Y}}_{Hn}(t)=2\begin{bmatrix}1 & (-1)^{n+1}\\ (-1)^{n+1} & 1\end{bmatrix}\left[a_{Hn}^R\cos(\omega_n t)-a_{Hn}^I\sin(\omega_n t)\right]e^{-\alpha_n t} \tag{A.19}$$

where the coefficients for the residues are

$$\left.\begin{aligned} a_{ok} &= \zeta_o(p_{ok}), && k = 0, \ldots, N_r \\ a_{Rnk} &= \zeta_n(p_{nk}), && k = 1, \ldots, N_r, n = 1, \ldots, \infty \\ a^R_{nk} &= 2\mathbb{R}\mathrm{e}\left\{\zeta_n(s_n)\right\}, && n = 1, \ldots, \infty \\ a^I_{nk} &= 2\mathbb{I}\mathrm{m}\left\{\zeta_n(s_n)\right\}, && n = 1, \ldots, \infty \end{aligned}\right\} \tag{A.20}$$

where $s_n = -\alpha_n + \mathrm{i}\omega_n$. As the poles are all simple, the functions to generate the residues can be given by taking the derivative of the denominator [*Kreyszig*, 1999], which yields

$$\begin{aligned} \zeta_o(s) &= \frac{r_D(s)}{\dfrac{\partial}{\partial s}\left[\text{denominator of (A.13)}\right]} \\ \zeta_n(s) &= \frac{s r_D(s)\left[c_D(s) + c_N(s)\right]}{\dfrac{\partial}{\partial s}\left[\text{denominator of (A.14)}\right]}, \quad n = 1, \ldots, \infty. \end{aligned}$$

The determination of the impulse response by this approach requires the solution to multiple polynomials of a high order, hence no futher analytic reduction can be achieved for the general case. The following example derives an analytic expression for the impulse response function for a simple case for which only a quadratic requires solution.

Example A.1. *Consider the linear friction elastic pipe case for which*

$$R(s) = R_0(s + r_0), \quad C(s) = C_0 s, \quad r_N(s), c_N(s) = 0, \quad r_D(s), c_D(s) = 0 \tag{A.21}$$

the poles of this system are given by the characteristic equations

$$R_0(s + r_0) = 0, \quad R_0 C_0 s(s + r_0) + (n\pi)^2 = 0, \quad n = 1, \ldots, \infty \tag{A.22}$$

which yields the solutions

$$s_0 = r_0, \quad s_n = -\frac{r_0}{2} \pm \mathrm{i}\sqrt{\frac{(n\pi)^2}{R_0 C_0} - \left(\frac{r_0}{2}\right)^2}, \quad n = 1, \ldots, \infty. \tag{A.23}$$

The residue functions are given by

$$\zeta_o(s) = \frac{1}{R_0}, \quad \zeta_n(s) = \frac{s}{R_0\left(2s + r_0\right)}, \quad n = 1, \ldots, \infty \tag{A.24}$$

As the unsteady shear stress and inelastic wall strain functions are zero ($r(s), c(s) = 0$), the modal functions $\boldsymbol{\mathcal{Y}}_{Rn} = \mathbf{0}, n = 1, \ldots, \infty$. The impulse response admittance *matrix is given by*

$$\boldsymbol{\mathcal{Y}}(t) = \boldsymbol{\mathcal{Y}}_o(t) + \sum_{n=1}^{\infty} \boldsymbol{\mathcal{Y}}_{Hn}(t) \tag{A.25}$$

where, given the pole locations (A.23) and the residue functions (A.24) and the general forms (A.17), (A.17), and (A.20), the matrix terms are given by

$$\boldsymbol{\mathcal{Y}}_o(t) = \begin{bmatrix} 1 & -1 \\ -1 & 1 \end{bmatrix} \frac{e^{-r_0 t}}{R_0} \tag{A.26}$$

$$\boldsymbol{\mathcal{Y}}_{Hn}(t) = 2 \begin{bmatrix} 1 & (-1)^{n+1} \\ (-1)^{n+1} & 1 \end{bmatrix} \left[\cos(\omega_n t) - \frac{r_0}{2} \frac{\sin(\omega_n t)}{\omega_n} \right] \frac{e^{-\frac{r_0}{2} t}}{R_0} \tag{A.27}$$

where $\omega_n = \mathbb{Im}\{s_n\}, n = 1, \ldots, \infty$.

Appendix B

The $\mathscr{M}$-Network

B.1 Introduction

This appendix introduces the $\mathscr{M}$-network which is essentially a generalisation of the compound node network $(\mathcal{G}(\mathcal{N},\Lambda),\mathcal{P},\mathcal{C})$ from Chapter 4. In contrast to considering the different elements of links and compound nodes, the $\mathscr{M}$-network is a network of interlinking $\mathscr{M}$-elements, where an $\mathscr{M}$-element is a general element type that encompasses both links with dynamics $\mathcal{P}$ and compound nodes with dynamics $\mathcal{C}$. The $\mathscr{M}$-network is introduced as it provides a convenient framework to prove the passivity properties used in Chapters 4 and 6, and it also provides a notationally simpler way of defining the numerical inverse Laplace transform (NILT) method in Chapter 5, and the detection and estimation problems in Chapter 6.

This Appendix is structured as follows. Section B.2 defines the $\mathscr{M}$-network and the associated mathematical objects. Section B.3 gives the important passivity theorems and some transformations of $\mathscr{M}$-networks. Section B.4 discusses the comparisons between $\mathscr{M}$-networks and Kirchoff networks, where the equivalent Kirchoff network of the specific case of a simple node network $(\mathcal{G}(\mathcal{N},\Lambda),\mathcal{P})$ is given.

B.2 Definitions

B.2.1 Network definitions

The primary building block for $\mathscr{M}$-networks are linear multinode elements, which are defined as follows.

Definition B.1. *A* linear multinode element *or* $\mathscr{M}$-element *is defined as an arbi-*

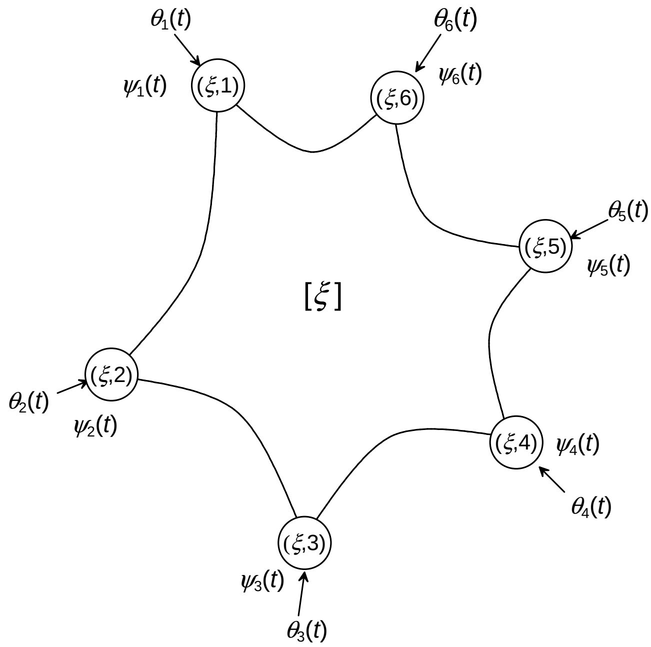

Figure B.1: Example of an $\mathscr{M}$-element.

trary hydraulic element interlinking n nodes with the admittance relationship

$$\begin{bmatrix} q_1(t) \\ \vdots \\ q_{n\lambda}(t) \end{bmatrix} = \int_0^t \begin{bmatrix} \mathcal{Y}_{11}(t-\tau) & \cdots & \mathcal{Y}_{1n}(t-\tau) \\ \vdots & \ddots & \vdots \\ \mathcal{Y}_{n1}(t-\tau) & \cdots & \mathcal{Y}_{nn}(t-\tau) \end{bmatrix} \begin{bmatrix} p_1(\tau) \\ \vdots \\ p_{n\lambda}(\tau) \end{bmatrix} d\tau \qquad \text{(B.1)}$$

where $\mathcal{Y}_{ij}(t)$ are the impulse response functions of the nodal flow at node i from the pressure at node j.

Remark: The $\mathscr{M}$-element presented here is akin to the multiport elements used in electrical networks [*Desoer and Kuh*, 1969] where the adopted terminology is purely for consistency. The advantage of considering multiport elements is that each element can be considered as an input output *black box*.

The general form of an $\mathscr{M}$-element is given in Figure B.1. Clearly a pipe, compound node or even a network can be considered as a $\mathscr{M}$-element, as demonstrated in the following examples.

Example B.1. *A $\mathscr{L}$-class link is a $\mathscr{M}$-element that interlinks two nodes where,* *with reference to (B.1),*

$$\begin{bmatrix} q_1(t) \\ q_2(t) \end{bmatrix} = \begin{bmatrix} q_u(t) \\ -q_d(t) \end{bmatrix}, \quad \begin{bmatrix} p_1(t) \\ p_2(t) \end{bmatrix} = \begin{bmatrix} p_u(t) \\ p_d(t) \end{bmatrix},$$
$$\begin{bmatrix} \mathcal{Y}_{11}(t) & \mathcal{Y}_{12}(t) \\ \mathcal{Y}_{21}(t) & \mathcal{Y}_{22}(t) \end{bmatrix} = \mathcal{L}^{-1}\left\{ \begin{bmatrix} \coth\Gamma(s) & -\operatorname{csch}\Gamma(s) \\ -\operatorname{csch}\Gamma(s) & \coth\Gamma(s) \end{bmatrix} \right\}(t)$$

Example B.2. *A simple node network $(\mathcal{G}(\mathcal{N},\Lambda),\mathcal{P})$ with node states $\boldsymbol{\psi}(t)$, $\boldsymbol{\theta}(t)$ and admittance matrix $\boldsymbol{Y}$ is a $\mathscr{M}$-element where*

$$\boldsymbol{q}(t) = \boldsymbol{\theta}(t), \quad \boldsymbol{p}(t) = \boldsymbol{\psi}(t), \quad \boldsymbol{\mathcal{Y}}(t) = \mathcal{L}^{-1}\left\{\boldsymbol{Y}(s)\right\}(t).$$

Example B.3. *A compound node i is a multinode element where*

$$\boldsymbol{q}(t) = \boldsymbol{\theta}_i(t), \quad \boldsymbol{p}(t) = \boldsymbol{\psi}_i(t), \quad \boldsymbol{\mathcal{Y}}(t) = \mathcal{L}^{-1}\left\{\boldsymbol{Y}_{\boldsymbol{c}i}(s)\right\}(t).$$

Example B.4. *A compound node network expanded into its simple node and simple connection representation is a $\mathscr{M}$-element with the multinode objects as defined in Example B.2.*

The topological connectivity of a $\mathscr{M}$-element is described by a $\mathscr{M}$-link can be organised into a network by using the following multi-link graph concepts.

Definition B.2.

1. *A $\mathscr{M}$-*link *ξ connected to n nodes is a n-tuple comprised of the nodes that it is connected to, that is $\xi = (i_1, \ldots i_n)$, and*
2. *A $\mathscr{M}$-*graph *$\mathcal{G}$ is given by $\mathcal{G}(\mathcal{N},\Xi)$, where $\mathcal{N}$ is the set of nodes and Ξ is the set of $\mathscr{M}$-links.*

Remark: This is not a conventional graph theory object, but it is adopted within this research to facilitate the mathematical description of hydraulic networks comprised of both pipes and hydraulic elements. An example of a $\mathscr{M}$-graph is given in Figure B.2 where $\xi_3 = (2,3,6,7)$ is a $\mathscr{M}$-link.

Definition B.3. *Consider the $\mathscr{M}$-graph $\mathcal{G}(\mathcal{N},\Xi)$ with $n_{\mathcal{N}}$ nodes and n_Ξ multi-links where $\mathscr{M}$-link k has $n_{\Xi k}$ connections. A* node-link *incidence matrix is given by the $[0,1]^{n_{\mathcal{N}}\times\sum_{k\in\Xi} n_{\Xi k}}$ matrix*

$$\boldsymbol{N} = \begin{bmatrix} \boldsymbol{N}_1 \cdots \boldsymbol{N}_{n_\Xi} \end{bmatrix} \tag{B.2}$$

where the $\boldsymbol{N}_k$ are $[0,1]^{n_{\mathcal{N}}\times n_{\Xi k}}$ matrices defined by

$$\{\boldsymbol{N}_k\}_{ij} = \begin{cases} 1 & \text{if the } j\text{-th connection of multi-link } k \text{ is incident to node } i. \\ 0 & \text{otherwise} \end{cases}$$

Remarks:

1. This definition is clearly a generalisation of the standard node-link incidence matrix.

2. Given that $\boldsymbol{N}$ has one and only one 1 in each column, it can be easily shown that rank $\boldsymbol{N}_k = n_{\Xi k}$ (full column rank) and, if $\mathcal{G}$ is a single component graph, that rank $\boldsymbol{N} = n_{\mathcal{N}}$ (full row rank).

The $\mathscr{M}$-network is now defined as follows.

Definition B.4. *A* multi-element network *or* $\mathscr{M}$-network *is a network consisting of the pair*

$$\left(\mathcal{G}\left(\mathcal{N}, \Xi\right), \mathcal{M}\right)$$

which is comprised of

1. *the $\mathscr{M}$-graph $\mathcal{G}\left(\mathcal{N}, \Xi\right)$ ($\mathcal{N}$ is the set of nodes, Ξ is the set of multi-links, each associated with a $\mathscr{M}$-element) combined with*

2. *the set of $\mathscr{M}$-element admittance impulse response functions $\mathcal{M} = \{\boldsymbol{\mathcal{Y}}_\xi : \xi \in \Xi\}$.*

The link end flow properties are related to the nodal flow injections ($\theta_i : \mathbb{R}_+ \mapsto \mathbb{R}, i \in \mathcal{N}$) and nodal pressures ($\psi_i : \mathbb{R}_+ \mapsto \mathbb{R}, i \in \mathcal{N}$) by the simple node relations

$$\sum_{(\xi,j)\in\Xi_i} q_{\xi j}(t) = \theta_i(t) \tag{B.3}$$

$$p_{\xi j}(t) = \psi_i(t) \quad (\xi, j) \in \Xi \tag{B.4}$$

for $i \in \mathcal{N}$ where (ξ, j) identifies the j-th connection of element ξ and Ξ_i is the set of all element connections incident to node i.

An example of an $\mathscr{M}$-network is given in Figure B.2.

B.2.2 General systems concepts

In the following, some important definitions for dynamic systems are outlined. Only linear time-invariant systems are considered here, however, more general systems are considered in other texts (*e.g. Desoer and Vidyasagar* [1975]; *Wohlers* [1969]). In the following, we consider input/output systems of the form $\boldsymbol{y} = \boldsymbol{\mathcal{G}} * \boldsymbol{x}$ with input $\boldsymbol{x} \in \mathbb{R}^n$, output $\boldsymbol{y} \in \mathbb{R}^m$, and the system impulse response $\boldsymbol{\mathcal{G}} \in \mathbb{R}^{n \times m}$.

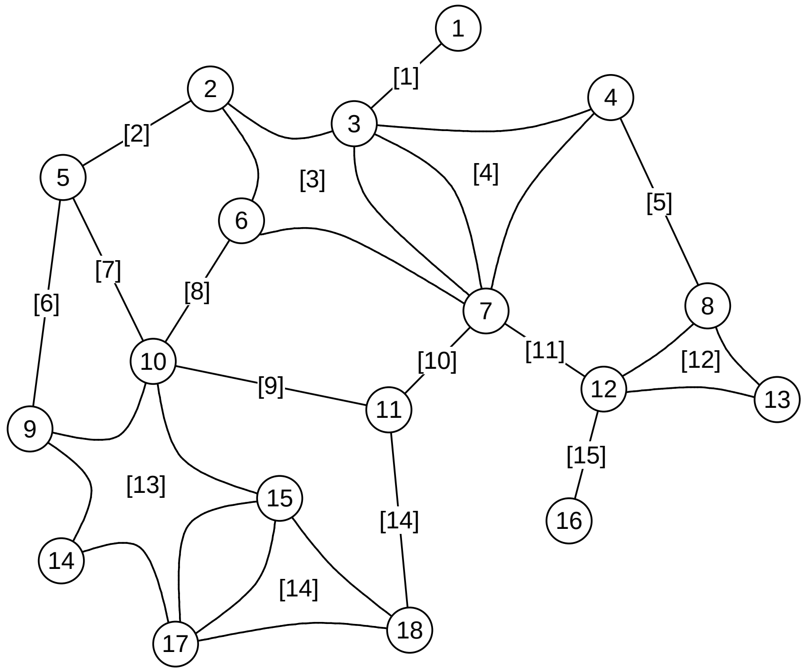

Figure B.2: Example of an $\mathscr{M}$-network.

Definition B.5. *The system* $\boldsymbol{y} = \boldsymbol{\mathcal{G}} * \boldsymbol{x}$ *is* bounded input/bounded output (BIBO) stable *if* $\boldsymbol{x} \in L^\infty$ *implies that* $\boldsymbol{y} \in L^\infty$*.*

Remarks:

1. Stability essentially means that $\boldsymbol{\mathcal{G}}$ is a bounded operator, which practically means that provided that the system input is bounded, then the output will be bounded also.
2. The definition can be rephrased as: there exists a constant K such that $||\boldsymbol{\mathcal{G}} * \boldsymbol{x}||_\infty \leq K||\boldsymbol{x}||_\infty, \boldsymbol{x} \in L^\infty$.
3. A necessary and sufficient condition for BIBO stability is that all the elements $\mathcal{G}_{ij} \in L^1$.
4. If $\boldsymbol{\mathcal{G}}$ is stable, then its Laplace transform $\boldsymbol{G}(s)$ has poles in the open left half plane.

Definition B.6. *The system* $\boldsymbol{y} = \boldsymbol{\mathcal{G}} * \boldsymbol{x}$ *is* causal *if for any two inputs* $\boldsymbol{x}_1$ *and* $\boldsymbol{x}_2$*, the condition*

$$\boldsymbol{x}_2(t) = \boldsymbol{x}_1(t), \quad t < t_0$$

implies the relationship

$$\boldsymbol{y}_2(t) = \boldsymbol{y}_1(t), \quad t < t_0$$

Remarks:

1. Causality essentially means that the output of the system is only a function of the historical inputs to the system.

2. In terms of the impulse response terms, causality implies $\mathcal{G}_{ij}(t) = 0$ for $t < 0$.

Definition B.7. *The system* $\boldsymbol{y} = \boldsymbol{\mathcal{G}} * \boldsymbol{x}$ *is* reciprocal *if for any two inputs* $\boldsymbol{x}_1$, $\boldsymbol{x}_2$ *and outputs* $\boldsymbol{y}_1$, $\boldsymbol{y}_2$

$$\left(\boldsymbol{x}_1^T * \boldsymbol{y}_2\right)(t) = \left(\boldsymbol{x}_2^T * \boldsymbol{y}_1\right)(t)$$

Remarks:

1. The significance of reciprocity is that the system outputs are, in some sense, symmetric to the inputs. That is y_k will respond to x_j in the same manner as y_j will to x_k.

2. Reciprocity implies that $\boldsymbol{G}$ is a symmetric operator, in the sense that $G_{k,j} \equiv G_{j,k}$.

Definition B.8. *The system* $\boldsymbol{y} = \boldsymbol{\mathcal{G}} * \boldsymbol{x}$ *is* strictly passive *if*

$$\int_0^t \left(\boldsymbol{x}^T \boldsymbol{y}\right)(\tau)\mathrm{d}\tau > 0 \quad \textit{for all } t \in \mathbb{R}_+ \tag{B.5}$$

for any $||\boldsymbol{x}|| \neq 0$. *The system is termed* passive *if the inequality is not strict.*

Remarks:

1. The physical significance of passivity is that energy cannot be produced within the system. The passivity constraint can also be expressed as the energy stored within the system is bounded by the energy input into the system.

2. Given the strictly passive system, $\boldsymbol{y} = \boldsymbol{\mathcal{G}} * \boldsymbol{x}$, it is a common result that the Laplace-transform of $\boldsymbol{\mathcal{G}}$ possesses the following properties [*Desoer and Vidyasagar*, 1975; *Triverio et al.*, 2007]

   (a) Each element of $\boldsymbol{G}$ is defined and analytic in $\mathbb{R}\mathrm{e}\{s\} > 0$

   (b) $\boldsymbol{G}(s) + \boldsymbol{G}^H(s)$ is nonnegative definite for all s such that $\mathbb{R}\mathrm{e}\{s\} > 0$, and

   (c) $\overline{\boldsymbol{G}(s)} = \boldsymbol{G}(\bar{s})$.

The following corollary to Definition B.8 demonstrates that strict passivity not only implies nonnegative definiteness of $\boldsymbol{G}(s) + \boldsymbol{G}^H(s)$ in the open right hand plane, but that it implies positive definiteness in the closed right hand plane. This result is important for the existence of the inverse of the admittance matrix block matrices performed within the thesis.

Corollary B.1. *Given the strictly passive system, $\boldsymbol{y} = \boldsymbol{\mathcal{G}} * \boldsymbol{x}$, the Laplace-transform $\boldsymbol{G}(s)$ of $\boldsymbol{\mathcal{G}}$ possesses the following property*

$$\boldsymbol{G}(s) + \boldsymbol{G}^H(s) \quad \textit{is positive definite for all } s \textit{ such that } \mathbb{R}\mathrm{e}\left\{s\right\} \geq 0$$

Proof. The proof takes two steps. Firstly Parseval's theorem is used to demonstrate positive definiteness on the domain $s = \mathrm{i}\omega$, and secondly, the second mean value theorem is used to extend this to the whole open right hand plane.

For the domain $\mathbb{R}\mathrm{e}\left\{s\right\} = 0$: Parseval's theorem can be used to yield the equalities

$$\begin{aligned} 0 &< \int_0^t \boldsymbol{x}^T(\tau)\left(\boldsymbol{\mathcal{G}} * \boldsymbol{x}\right)(\tau)\mathrm{d}\tau \\ &= \frac{1}{2\pi}\int_{-\infty}^{\infty} \boldsymbol{X}^H(\mathrm{i}\omega)\boldsymbol{G}(\mathrm{i}\omega)\boldsymbol{X}(\mathrm{i}\omega)\mathrm{d}\omega \\ &= \frac{1}{2\pi}\int_{-\infty}^{\infty} \boldsymbol{X}^H(\mathrm{i}\omega)\boldsymbol{G}^H(\mathrm{i}\omega)\boldsymbol{X}(\mathrm{i}\omega)\mathrm{d}\omega \end{aligned}$$

where $\boldsymbol{X}$ is the Laplace transform of $\boldsymbol{x}$, and the second equality arises from expressing the term in the time-domain integrand as $\left(\boldsymbol{\mathcal{G}} * \boldsymbol{x}\right)^T \boldsymbol{x}$. Given that $\overline{\boldsymbol{G}(s)} = \boldsymbol{G}(\bar{s})$, the imaginary component of the integrals disappears in the integration. As $\boldsymbol{x}$ is an arbitrary function, the term in the integrand must be positive for all ω, this means that

$$\mathbb{R}\mathrm{e}\left\{\boldsymbol{X}^H(\mathrm{i}\omega)\boldsymbol{G}^H(\mathrm{i}\omega)\boldsymbol{X}(\mathrm{i}\omega)\right\}, \mathbb{R}\mathrm{e}\left\{\boldsymbol{X}^H(\mathrm{i}\omega)\boldsymbol{G}(\mathrm{i}\omega)\boldsymbol{X}(\mathrm{i}\omega)\right\} > 0 \text{ for all } \omega \in \mathbb{R}.$$

A necessary condition that arises from the inequalities above is that the real part of $\boldsymbol{G}$ is positive definite [*Johnson*, 1975], that is

$$\boldsymbol{G}^H(\mathrm{i}\omega) + \boldsymbol{G}(\mathrm{i}\omega) \text{ is positive definite for all } \omega \in \mathbb{R}.$$

For the domain $\mathbb{R}\mathrm{e}\left\{s\right\} \geq 0$: Consider the system $\widetilde{\boldsymbol{G}}_a(s) = \boldsymbol{G}(a+s)$, where $a \geq 0$, with the time-domain impulse response function $\widetilde{\boldsymbol{\mathcal{G}}}_a$. For this system, the following identities hold for nonzero $\boldsymbol{x}$:

$$\begin{aligned} \int_0^t \boldsymbol{x}^T(\tau)\left(\widetilde{\boldsymbol{\mathcal{G}}}_a * \boldsymbol{x}\right)(\tau)\mathrm{d}\tau &\overset{(1)}{=} \int_0^t \boldsymbol{x}^T(\tau)\int_0^\tau e^{-(\tau-u)a}\boldsymbol{\mathcal{G}}(\tau-u)\boldsymbol{x}(u)\mathrm{d}u\mathrm{d}\tau \\ &= \int_0^t e^{-2\tau a}\boldsymbol{z}^T(\tau)\left(\boldsymbol{\mathcal{G}} * \boldsymbol{z}\right)(\tau)\mathrm{d}\tau, \text{ where } \boldsymbol{z}(t) = e^{ta}\boldsymbol{x}(t) \\ &\overset{(2)}{=} \int_0^{\tilde{t}} \boldsymbol{z}^T(\tau) \text{ where } 0 < \tilde{t} < t\left(\boldsymbol{\mathcal{G}} * \boldsymbol{z}\right)(\tau)\mathrm{d}\tau \\ &\overset{(3)}{>} 0 \end{aligned} \tag{B.6}$$

where (1) holds as $\widetilde{\boldsymbol{\mathcal{G}}}_a = e^{-at}\boldsymbol{\mathcal{G}}(t)$, (2) is a result of the second mean value theorem for integration [*Tong*, 2002], and (3) holds as $\boldsymbol{\mathcal{G}}$ is strictly passive and $\boldsymbol{z}$ is a nonzero function. The interpretation of (B.6) is that $\widetilde{\boldsymbol{\mathcal{G}}}_a$ is a strictly passive system. Therefore, given the first part of this proof, it holds that

$$\widetilde{\boldsymbol{G}}_a(\mathrm{i}\omega) + \widetilde{\boldsymbol{G}}_a^H(\mathrm{i}\omega)$$

is positive definite on $\omega \in \mathbb{R}$, which in turn implies that

$$\boldsymbol{G}(a + \mathrm{i}\omega) + \boldsymbol{G}^H(a + \mathrm{i}\omega)$$

is positive definite on $\omega \in \mathbb{R}$ and $a > 0$, which means that $\boldsymbol{G}(s) + \boldsymbol{G}^H(s)$ is positive definite for $\mathbb{R}\mathrm{e}\{s\} \geq 0$. □

B.3 Network Theorems

The following theorem is a generalisation of the network admittance matrix models model presented in Chapters 3 and 4.

Theorem B.1. *For a $\mathscr{M}$-network $(\mathcal{G}(\mathcal{N}, \Xi), \{\boldsymbol{\mathcal{Y}}_\xi : \xi \in \Xi\})$, the nodal flow injections $\boldsymbol{\theta} = [\theta_1 \cdots \theta_{n_n}]^T$ are related to the nodal pressures $\boldsymbol{\psi} = [\psi_1 \cdots \psi_{n_n}]^T$ by the network admittance relationship*

$$\boldsymbol{\theta}(t) = \int_0^t \boldsymbol{\mathcal{Y}}(t-\tau)\boldsymbol{\psi}(\tau)d\tau \tag{B.7}$$

where the network admittance function is built from the element admittance functions $\{\boldsymbol{\mathcal{Y}}_\xi : \xi \in \Xi\}$ by

$$\{\boldsymbol{\mathcal{Y}}(t)\}_{i,j} = \begin{cases} \displaystyle\sum_{\{(\xi,k)\in\Xi_i\}} \mathcal{Y}_{\xi kk}(t) & \textit{for } j = i \\ \displaystyle\sum_{(\xi,k,m)\in\Xi_{ij}} \mathcal{Y}_{\xi km}(t) & \textit{otherwise} \end{cases} \tag{B.8}$$

where $\Xi_{ij} = \{(\xi, k, m) : (\xi, k) \in \Xi_i, (\xi, m) \in \Xi_j\}$ identifies the connections of elements connected to both node i and node j.

Proof. As this is a generalisation of the network model derived in Chapters 3 and 4, the proof is kept brief. Organising the element connection flows and pressures, and admittance impulse response functions as follows

$$\boldsymbol{q}(t) = \begin{bmatrix} \boldsymbol{q}_1(t) \\ \vdots \\ \boldsymbol{q}_{n_\Xi}(t) \end{bmatrix}, \quad \boldsymbol{p}(t) = \begin{bmatrix} \boldsymbol{p}_1(t) \\ \vdots \\ \boldsymbol{p}_{n_\Xi}(t) \end{bmatrix}, \quad \boldsymbol{\mathcal{Y}}_\Xi(t) = \begin{bmatrix} \boldsymbol{\mathcal{Y}}_1(t) & & \\ & \ddots & \\ & & \boldsymbol{\mathcal{Y}}_{n_\Xi}(t) \end{bmatrix} \tag{B.9}$$

a matrix representation of (6.1) is given by

$$\boldsymbol{q}(t) = \int_0^t \boldsymbol{\mathcal{Y}}_\Xi(t-\tau)\boldsymbol{p}(\tau)d\tau. \tag{B.10}$$

As in Chapter 3, the nodal pressure and flow relationships (B.3)-(B.4) can be given in a matrix form as

$$\begin{bmatrix} \boldsymbol{N}_1 & \cdots & \boldsymbol{N}_{n_\Xi} \end{bmatrix} \begin{bmatrix} \boldsymbol{q}_1(t) \\ \vdots \\ \boldsymbol{q}_{n_\Xi}(t) \end{bmatrix} = \boldsymbol{\theta}(t) \tag{B.11}$$

$$\begin{bmatrix} \boldsymbol{q}_1(t) \\ \vdots \\ \boldsymbol{q}_{n_\Xi}(t) \end{bmatrix} = \begin{bmatrix} \boldsymbol{N}_1^T \\ \vdots \\ \boldsymbol{N}_{n_\Xi}^T \end{bmatrix} \boldsymbol{\psi}(t) \tag{B.12}$$

where the $\boldsymbol{N}_i$ are node-element incidence matrices. Combining (B.10)-(B.12) yields

$$\boldsymbol{\theta}(t) = \int_0^t \begin{bmatrix} \boldsymbol{N}_1 & \cdots & \boldsymbol{N}_{n_\Xi} \end{bmatrix} \boldsymbol{\mathcal{Y}}_\Xi(t-\tau) \begin{bmatrix} \boldsymbol{N}_1^T \\ \vdots \\ \boldsymbol{N}_{n_\Xi}^T \end{bmatrix} \boldsymbol{\psi}(t)d\tau$$

where, in comparison to (B.7), shows

$$\boldsymbol{\mathcal{Y}}(t) = \begin{bmatrix} \boldsymbol{N}_1 & \cdots & \boldsymbol{N}_{n_\Xi} \end{bmatrix} \begin{bmatrix} \boldsymbol{\mathcal{Y}}_1(t) & & \\ & \ddots & \\ & & \boldsymbol{\mathcal{Y}}_{n_\Xi}(t) \end{bmatrix} \begin{bmatrix} \boldsymbol{N}_1 & \cdots & \boldsymbol{N}_{n_\Xi} \end{bmatrix}^T \tag{B.13}$$

for which the incidence matrix identities used in Chapter 3 can be used to show that (B.13) is equal to (B.8). □

A fundamental theorem for this class of networks is as follows.

Theorem B.2. *Given a $\mathscr{M}$-network $(\mathcal{G}(\mathcal{N},\Xi), \{\boldsymbol{\mathcal{Y}}_\xi : \xi \in \Xi\})$ where $\mathcal{G}$ is a single component graph with a network admittance matrix $\boldsymbol{\mathcal{Y}}$. If all the $\mathscr{M}$-elements $\xi \in \Xi$ are (1) causal, (2) stable, (3) reciprocal, (4) passive, (5) strictly passive, then the network admittance matrix inherits these properties respectively.*

Proof. Causality, stability and reciprocity are trivially shown (but included for completeness). Passivity and strict passivity are slightly more difficult and treated together. The passivity proof follows a similar line to that used in *Desoer and Kuh* [1969] for passivity of lumped electrical networks.

1. *Causality* is dependent only on the elemental functions independently, so it is clearly inherited.

2. The network admittance matrix is *stable* if the elemental functions are in the function space L^1. As the elemental functions are simply additions of the $\mathscr{M}$-elements elemental functions, they are clearly within L^1 when the $\mathscr{M}$-element functions are in L^1.

3. As the system is linear, the network is *reciprocal* if $\{\boldsymbol{\mathcal{Y}}\}_{ij} \equiv \{\boldsymbol{\mathcal{Y}}\}_{ij}$ *Wohlers* [1969]. Given the form of $\boldsymbol{\mathcal{Y}}$ in (B.13), this clearly holds if $\boldsymbol{\mathcal{Y}}_\xi \in \Xi$ are symmetric (reciprocal).

4. Given the definitions in Chapter 2, the network is *passive* if

$$\int_0^t \left(\boldsymbol{x}^T \cdot \boldsymbol{\mathcal{Y}} * \boldsymbol{x}\right)(\tau) d\tau \geq 0$$

for all $\boldsymbol{x} : \mathbb{R}_+ \mapsto \mathbb{R}^{n_\mathcal{N}}$, where the strict equality for $||\boldsymbol{x}|| > 0$ implies strict passivity. Consider the following expansion

$$\boldsymbol{\mathcal{Y}}(t) = \sum_{\xi \in \Xi} \boldsymbol{N}_\xi \boldsymbol{\mathcal{Y}}_\xi(t) \boldsymbol{N}_\xi^T$$

which implies that $\left(\boldsymbol{x}^T \cdot \boldsymbol{\mathcal{Y}} * \boldsymbol{x}\right)$ can be expressed as

$$\sum_{\xi \in \Xi} \left[\boldsymbol{N}_\xi^T \boldsymbol{x}(t)\right]^T \int_0^t \boldsymbol{\mathcal{Y}}_\xi(t-\tau) \left[\boldsymbol{N}_\xi^T \boldsymbol{x}(\tau)\right]^T d\tau. \tag{B.14}$$

defining $\boldsymbol{y}_\xi = \boldsymbol{N}_\xi^T \boldsymbol{x}$, the integral in (B.14) can be expressed as

$$\sum_{\xi \in \Xi} \int_0^t \left(\boldsymbol{y}_\xi^T \cdot \boldsymbol{\mathcal{Y}}_\xi * \boldsymbol{y}_\xi\right) d\tau. \tag{B.15}$$

Due to the passivity of each element $\xi \in \Xi$, each term in the summation is nonnegative, hence the inheritance of passivity by the network from the elements is demonstrated.

5. The system is strictly passive if the inequality in (B.14) is strict for all nonzero functions $\boldsymbol{x} : \mathbb{R}_+ \mapsto \mathbb{R}^{n_\mathcal{N}}$. If each element $\xi \in \Xi$ is strictly passive, then each

term in the summation (B.15) is a positive number. Therefore (B.15) will be a positive number for any $\boldsymbol{x} : \mathbb{R}_+ \mapsto \mathbb{R}^{n_\mathcal{N}}$ only if each term in $\boldsymbol{x}$ appears in at least one of the $\boldsymbol{y}_\xi$. This criteria holds for the multi-graph $\mathcal{G}$ as no node in $\mathcal{N}$ is disconnected. Therefore the inheritance of strict passivity by the network from the elements is demonstrated.

□

Remark: These conditions are sufficient but not necessary. One could concoct a scenario where individual $\mathscr{M}$-elements do not possess the stated properties of causality, stability, reciprocity, and passivity, but the aggregated effect of the elements on the network matrix could be such that the overall network still does possess these properties.

This then leads onto the following theorem

Theorem B.3. *Given a $\mathscr{M}$-network $(\mathcal{G}(\mathcal{N}, \Xi), \{\boldsymbol{\mathcal{Y}}_\xi : \xi \in \Xi\})$ where $\mathcal{G}$ is a single component graph. If the network admittance matrix $\boldsymbol{\mathcal{Y}}$ is strictly passive, then the network impedance matrix $\boldsymbol{\mathcal{Z}} = \boldsymbol{\mathcal{Y}}^{-1}$ is well defined for all s within the right hand plane, and is strictly passive.*

Proof. Within the proof, we deal primarily with the properties of the Laplace transform $\boldsymbol{Z}$ of $\boldsymbol{\mathcal{Z}}$.

1. *Existence.* Firstly, note that for $\boldsymbol{A} \in \mathbb{C}^{n \times n}$ with $\mathbb{R}\mathrm{e}\{\boldsymbol{A}\}$ positive definite, then $\boldsymbol{A}$ is nonsingular [*Johnson*, 1975]. For a strictly passive system, $\boldsymbol{Y}(s) + \boldsymbol{Y}^H(s)$ is positive definite on $\mathbb{R}\mathrm{e}\{s\} \geq 0$, and hence $\boldsymbol{Z}(s) = \boldsymbol{Y}^{-1}(s)$ exists on $\mathbb{R}\mathrm{e}\{s\} \geq 0$.

2. *Passivity.* For the criteria (1), recognising the cofactor expansion of $\boldsymbol{Z}(s) = \boldsymbol{Y}^{-1}(s)$, the elemental functions of $\boldsymbol{Z}(s)$ are comprised of additions and multiplications of the elemental functions of $\boldsymbol{Y}(s)$ divided by $\det \boldsymbol{Y}(s)$. Therefore, as $Y_{ij}(s)$ has poles only in the left open plane, and $\det \boldsymbol{Y}(s) > 0$ on the left open plane, then the elemental functions of $\boldsymbol{Z}(s)$ are in H^∞, that is, they are analytic in the left open plane. For the criteria (2), from *Johnson* [1975], for $\boldsymbol{A} \in \mathbb{C}^{n \times n}$ with $\mathbb{R}\mathrm{e}\{\boldsymbol{A}\}$ positive definite, then $\mathbb{R}\mathrm{e}\left\{\boldsymbol{A}^{-1}\right\}$ is also positive definite, hence $\boldsymbol{Z}(s) + \boldsymbol{Z}^H(s)$ is positive definite on $\mathbb{R}\mathrm{e}\{s\} > 0$. Criteria (3) follows from the cofactor expansion of the elemental terms.

□

Remarks:

1. Here we still have the problem that $\boldsymbol{Y}^{-1}(s)$ does not necessarily exist on $s = \mathrm{i}\omega$.

We have the following simple corollary.

Corollary B.2. *If a strictly passive network admittance matrix $\boldsymbol{\mathcal{Y}}$ is causal, stable and reciprocal then the network impedance matrix $\boldsymbol{\mathcal{Z}} = \boldsymbol{\mathcal{Y}}^{-1}$ is causal, stable, and reciprocal.*

Proof. 1. *Causality* is implied by passivity [*Triverio et al.*, 2007].

2. *Stability.* From the passivity proof above, it was shown that the elemental functions of $Z_{ij}(s) \in H^{\infty}$, implying that $\mathcal{Z}_{ij} \in L^{\infty}$, which means that the system is L^p stable for $1 \geq p < \infty$, that is $\boldsymbol{x} \in L^p \Rightarrow \boldsymbol{\mathcal{Z}} * \boldsymbol{x} \in L^p$.

3. *Reciprocity.* The inverse of a symmetric matrix is symmetric, hence $\boldsymbol{Z}(s)$ is reciprocal.

□

Lemma B.1. *Given a $\mathscr{M}$-network $(\mathcal{G}(\mathcal{N}, \Xi), \{\boldsymbol{\mathcal{Y}}_{\xi} : \xi \in \Xi\})$ with a strictly passive admittance impulse response matrix $\boldsymbol{\mathcal{Y}}$. Then any principal minor of $\boldsymbol{\mathcal{Y}}$ represents the impulse response matrix for a strictly passive system.*

Proof. The requirement for strict passivity $\int_0^t (\boldsymbol{x}^T \boldsymbol{\mathcal{Y}} * \boldsymbol{x})(\tau) d\tau \geq 0$ for all $||x|| > 0$ is only satisfied if all the principal minors of $\boldsymbol{\mathcal{Y}}$ are themselves strictly passive. □

Remark: The physical interpretation of this lemma is that if a subnetwork is removed or considered in isolation, then, despite the additional pressure dependent outflow terms along the diagonal, then this subnetwork is itself strictly passive.

The useful aspect of this lemma is in the following corollary

Corollary B.3. *Given a $\mathscr{M}$-network $(\mathcal{G}(\mathcal{N}, \Xi), \{\boldsymbol{\mathcal{Y}}_{\xi} : \xi \in \Xi\})$ with a strictly passive admittance impulse response matrix $\boldsymbol{\mathcal{Y}}$. Any principal minor of its transform $\boldsymbol{Y}(s)$ has a nonsingular strictly passive stable inverse.*

Proof. This follows simply from the lemma above, but could also be shown from the property that $\boldsymbol{Y}(s) + \boldsymbol{Y}^H(s)$ is strictly positive definite. □

The following network reduction theorem presents an application of the theory developed within this section. This theorem holds analogies with the development of the computational models in Sections 3.5 and 4.6.

Theorem B.4. *Consider the $\mathscr{M}$-network $(\mathcal{G}(\mathcal{N},\Xi),\{\boldsymbol{\mathcal{Y}}_\xi : \xi \in \Xi\})$ with a strictly passive admittance impulse response matrix $\boldsymbol{\mathcal{Y}}$. Say that the nodes are partitioned into three sets (*i.e. *$\mathcal{N} = \mathcal{N}_A \cup \mathcal{N}_B \cup \mathcal{N}_C$ each consisting of n_A, n_B and n_C nodes) such that no node $i \in \mathcal{N}_A$ is connected to any node $j \in \mathcal{N}_C$, that is $\Xi_{ij} = \emptyset$ for all $i \in \mathcal{N}_A, j \in \mathcal{N}_C$. (In this instance the impulse response matrix can be partitioned as*

$$\boldsymbol{\mathcal{Y}}(t) = \left[\begin{array}{c:c:c} \boldsymbol{\mathcal{Y}}_{AA}(t) & \boldsymbol{\mathcal{Y}}_{AB}(t) & \mathbf{0} \\ \hdashline \boldsymbol{\mathcal{Y}}_{BA}(t) & \boldsymbol{\mathcal{Y}}_{BB}(t) & \boldsymbol{\mathcal{Y}}_{BC}(t) \\ \hdashline \mathbf{0} & \boldsymbol{\mathcal{Y}}_{CB}(t) & \boldsymbol{\mathcal{Y}}_{CC}(t) \end{array}\right]$$

where $\boldsymbol{\mathcal{Y}}_{XY}$ is a $n_X \times n_Y$ matrix, $X, Y = A, B, C$.) Say that the nodal injections $\theta_i, i \in \mathcal{N}_C$ are all controlled at zero, then a dynamically equivalent network is given by the $\mathscr{M}$-network

$$\left(\mathcal{G}\left(\mathcal{N}_A \cup \mathcal{N}_B, \{\xi_o\} \cup \Xi/\Xi_C\right), \{\boldsymbol{\mathcal{Y}}_{\xi_o}\} \cup \{\boldsymbol{\mathcal{Y}}_\xi : \xi \in \Xi/\Xi_C\}\right) \tag{B.16}$$

*where Ξ_C is the set of elements connected to any node in $\mathcal{N}_C$, $\xi_o = (i_{B1}, \ldots, i_{Bn_B})$ is an $\mathscr{M}$-element connected to all the nodes in $\mathcal{N}_B$ (*i.e. *$\{i_{B1}, \ldots, i_{Bn_B}\} = \mathcal{N}_B$) with the element admittance matrix*

$$\boldsymbol{\mathcal{Y}}_{\xi_o}(t) = \boldsymbol{\mathcal{Y}}_{BB_{+C}}(t) - \left(\boldsymbol{\mathcal{Y}}_{BC} * \boldsymbol{\mathcal{Z}}_{CC} * \boldsymbol{\mathcal{Y}}_{CB}\right)(t)$$

where $\boldsymbol{\mathcal{Y}}_{BB_{+C}}$ is the contribution to $\boldsymbol{\mathcal{Y}}_{BB}$ resulting from the elements in Ξ_C, and $\boldsymbol{\mathcal{Z}}_{CC} = \boldsymbol{\mathcal{Y}}_{CC}^{-1}$ is an impedance matrix where the inverse is in the sense of a convolution. The impulse response matrix for the network (B.16) is given by

$$\left[\begin{array}{c:c} \boldsymbol{\mathcal{Y}}_{AA}(t) & \boldsymbol{\mathcal{Y}}_{AB}(t) \\ \hdashline \boldsymbol{\mathcal{Y}}_{BA}(t) & \boldsymbol{\mathcal{Y}}_{BB}(t) - \left(\boldsymbol{\mathcal{Y}}_{BC} * \boldsymbol{\mathcal{Z}}_{CC} * \boldsymbol{\mathcal{Y}}_{CB}\right)(t) \end{array}\right] \tag{B.17}$$

which is strictly passive.

Proof. To undertake the proof, firstly it will be demonstrated how (B.16) is constructed from (B.17) under the assumption that $\theta_i(t) = 0, t \in \mathbb{R}, i \in \mathcal{N}_C$, secondly it will be shown how this relates to the $\mathscr{M}$-network (B.16) and finally is will shown that the $\mathscr{M}$-network (B.16) is strictly passive.

1. Given $\theta_i(t) = 0, t \in \mathbb{R}, i \in \mathcal{N}_B$, the admittance expression for the $\mathscr{M}$-network $(\mathcal{G}(\mathcal{N},\Xi),\{\boldsymbol{\mathcal{Y}}_\xi : \xi \in \Xi\})$ is

$$\left[\begin{array}{c} \boldsymbol{\theta}_A(t) \\ \hdashline \boldsymbol{\theta}_B(t) \\ \hdashline \mathbf{0} \end{array}\right] = \int_0^t \left[\begin{array}{c:c:c} \boldsymbol{\mathcal{Y}}_{AA}(t-\tau) & \boldsymbol{\mathcal{Y}}_{AB}(-\tau) & \mathbf{0} \\ \hdashline \boldsymbol{\mathcal{Y}}_{BA}(t-\tau) & \boldsymbol{\mathcal{Y}}_{BB}(t-\tau) & \boldsymbol{\mathcal{Y}}_{BC}(t-\tau) \\ \hdashline \mathbf{0} & \boldsymbol{\mathcal{Y}}_{CB}(t-\tau) & \boldsymbol{\mathcal{Y}}_{CC}(t-\tau) \end{array}\right] \left[\begin{array}{c} \boldsymbol{\psi}_A(\tau) \\ \hdashline \boldsymbol{\psi}_B(\tau) \\ \hdashline \boldsymbol{\psi}_C(\tau) \end{array}\right] \mathrm{d}\tau$$

From Lemma B.1, it is known that, for a strictly passive network, all principal minors of $\boldsymbol{\mathcal{Y}}$ are themselves impulse response matrices for strictly passive systems and hence have well defined inverses. Therefore $\boldsymbol{\mathcal{Z}}_{CC} = \boldsymbol{\mathcal{Y}}_{CC}^{-1}$ exists and hence, the nodal pressures $\boldsymbol{\psi}_C$ can be expressed as

$$\boldsymbol{\psi}_C(t) = -\left(\boldsymbol{\mathcal{Z}}_{CC} * \boldsymbol{\mathcal{Y}}_{CB} * \boldsymbol{\psi}_B\right)(t) \tag{B.18}$$

from which (B.17) is easily derived.

2. The matrix $\boldsymbol{\mathcal{Y}}_{BB}$ can be expressed as $\boldsymbol{\mathcal{Y}}_{BB} = \boldsymbol{\mathcal{Y}}_{BB_C} + \boldsymbol{\mathcal{Y}}_{BB_{+C}}$ where $\boldsymbol{\mathcal{Y}}_{BB_{-C}}$ is constructed from elements not within the set Ξ_C and $\boldsymbol{\mathcal{Y}}_{BB_{+C}}$ is constructed from elements within the set Ξ_C, that is

$$\boldsymbol{\mathcal{Y}}_{BB_{-C}}(t) = \sum_{\xi \in \Xi/\Xi_C} \boldsymbol{N}_{\xi B} \boldsymbol{\mathcal{Y}}_\xi(t) \boldsymbol{N}_{\xi B}^T$$
$$\boldsymbol{\mathcal{Y}}_{BB_{+C}}(t) = \sum_{\xi \in \Xi_C} \boldsymbol{N}_{\xi B} \boldsymbol{\mathcal{Y}}_\xi(t) \boldsymbol{N}_{\xi B}^T.$$

Given this, (B.17) can be expressed as

$$\underbrace{\left[\begin{array}{c:c} \boldsymbol{\mathcal{Y}}_{AA}(t) & \boldsymbol{\mathcal{Y}}_{AB}(t) \\ \hdashline \boldsymbol{\mathcal{Y}}_{BA}(t) & \boldsymbol{\mathcal{Y}}_{BB_{-C}}(t) \end{array}\right]}_{\text{term I}} + \underbrace{\left[\begin{array}{c:c} \boldsymbol{0} & \boldsymbol{0} \\ \hdashline \boldsymbol{0} & \boldsymbol{\mathcal{Y}}_{BB_{+C}}(t) - \left(\boldsymbol{\mathcal{Y}}_{BC} * \boldsymbol{\mathcal{Z}}_{CC} * \boldsymbol{\mathcal{Y}}_{CB}\right)(t) \end{array}\right]}_{\text{term II}}. \tag{B.19}$$

Term I in (B.19) is recognised as the admittance matrix for the $\mathscr{M}$-network

$$\left(\mathcal{G}\left(\mathcal{N}_A \cup \mathcal{N}_B, \Xi/\Xi_C\right), \{\boldsymbol{\mathcal{Y}}_\xi : \xi \in \Xi/\Xi_C\}\right), \tag{B.20}$$

and term II can be expressed as

$$\left[\begin{array}{c} \boldsymbol{0} \\ \hdashline \boldsymbol{I} \end{array}\right] \left[\boldsymbol{\mathcal{Y}}_{BB_{+C}}(t) - \left(\boldsymbol{\mathcal{Y}}_{BC} * \boldsymbol{\mathcal{Z}}_{CC} * \boldsymbol{\mathcal{Y}}_{CB}\right)(t)\right] \left[\begin{array}{c:c} \boldsymbol{0} & \boldsymbol{I} \end{array}\right]$$

which, from the proof to Theorem B.2, can be recognised as the expression for an $\mathscr{M}$-element included in a $\mathscr{M}$-network with a node element incidence matrix $[\boldsymbol{0}\,\boldsymbol{I}]^T$ and an element admittance matrix $\boldsymbol{\mathcal{Y}}_{\xi_o}$ (B.18). As recognised by the form of the incidence matrix, this element is connected to all nodes in $\mathcal{N}_B$. Calling this additional element ξ_o leads to the form of the $\mathscr{M}$-network in (B.16).

3. By Theorem B.2, the $\mathscr{M}$-network (B.16) is strictly passive if the $\mathscr{M}$-network (B.20) and the element ξ_o are both strictly passive. The network (B.20) is strictly passive as, by assumption, all its elements are strictly passive (Theorem

B.2). The passivity of the element ξ_o can be demonstrated as follows. Consider the Laplace transform of $\boldsymbol{\mathcal{Y}}_{\xi_o}$

$$\boldsymbol{Y}_{\xi_o}(s) = \boldsymbol{Y}_{BB_{+C}}(s) - \boldsymbol{Y}_{BC}(s)\boldsymbol{Y}_{CC}^{-1}(s)\boldsymbol{Y}_{CB}(s) \tag{B.21}$$

this is recognised as being the Schur complement of the matrix

$$\left[\begin{array}{c:c} \boldsymbol{Y}_{BB_{+C}}(s) & \boldsymbol{Y}_{BC}(s) \\ \hdashline \boldsymbol{Y}_{CB}(s) & \boldsymbol{Y}_{CC}(s) \end{array}\right] \tag{B.22}$$

which in turn is the Laplace transform of the admittance matrix for the $\mathscr{M}$-network $(\mathcal{G}(\mathcal{N}_B \cup \mathcal{N}_C, \Xi_C), \{\boldsymbol{\mathcal{Y}}_\xi : \xi \in \Xi_C\})$. By Theorem B.2, the matrix (B.22) is strictly positive definite for s in the closed right hand plane, therefore, its Schur complement $\boldsymbol{Y}_{\xi_o}(s)$ is also strictly positive definite for s in the closed right hand plane [*Horn and Zhang*, 2005]. The other passivity criteria (in the remarks to Definition B.8) for $\boldsymbol{Y}_{\xi_o}(s)$ are easily demonstrated, and hence $\boldsymbol{Y}_{\xi_o}(s)$ is strictly passive.

□

B.4 Kirchoff Network Equivalents

Within this section, the connection between Kirchoff networks networks and $\mathcal{M}$-networks is further explored. This is undertaken by deriving a Kirchoff type representation of the simple node network structure $(\mathcal{G}(\mathcal{N}, \Lambda), \mathcal{P})$ from Chapter 3, which is a special case of a $\mathcal{M}$-network. To facilitate the discussion, the one dimensional (1-D) system terminology of *Brown* [1967] is adopted here. That is, a 1-D system possesses two different types of variables that are

- *Symmetric variables*, which refer to variables that have the same sense when viewed from either direction. Examples of such variables are voltage and pressure.
- *Asymmetric variables*, which refer to variables that have the opposite sense when viewed from different directions. Examples of such variables are flows and currents.

Brown [1967] highlights that the product of associated symmetric and asymmetric variables yields a power term.

The primary difference between Kirchoff networks, as defined in Section B.4.1, and the networks considered within this thesis is that Kirchoff networks deal with links that possess a constant asymmetric variable state, whereas the networks considered in this thesis deal with links with distributed parameter states for both the symmetric and asymmetric states. How this difference manifests itself is that Kirchoff network links can be represented by two states (*e.g.* current and voltage drop) that are related by a single function. However for the hyperbolic partial differential equation (PDE) links considered within this thesis, the spatial distribution is governed by the boundary conditions, yielding a link representation of four states (*i.e.* upstream and downstream flow and pressure), which are related by a 2×2 transfer matrix relationship. Despite these differences in the link types, the nodal constraints are essentially the same. This section explores the relationship between the two network types.

B.4.1 Kirchoff networks

Before a Kirchoff network (K-network) can be defined, a few definitions are required first.

Definition B.9. *For a directed graph $\mathcal{G}(\mathcal{N}, \Lambda)$ comprised of $n_n + 1$ nodes and n_λ links, the complete nodal incidence matrix is defined as the $n_n \times n_\lambda$ matrix*

$$\left\{\acute{\boldsymbol{A}}\right\}_{i,j} = \begin{cases} 1 & \textit{if node } i \textit{ is upstream of link } j \\ -1 & \textit{if node } i \textit{ is downstream of link } j \\ 0 & \textit{if link } j \textit{ is not incident to node } i \end{cases}$$

Definition B.10. *For a directed graph $\mathcal{G}(\mathcal{N}, \Lambda)$ comprised of $n_n + 1$ nodes and n_λ links and $n_m + 1$ loops, the complete loop incidence matrix is defined as the $n_n \times n_\lambda$ matrix*

$$\left\{\acute{\boldsymbol{M}}\right\}_{i,j} = \begin{cases} 1 & \textit{if link } j \textit{ has a positive orientation in loop } i \\ -1 & \textit{if link } j \textit{ has a negative orientation in loop } i \\ 0 & \textit{if link } j \textit{ is not within loop } i \end{cases}$$

An important result for the above matrices is given in the following lemma.

Lemma B.2. *[Desoer and Kuh, 1969] Given the graph matrices as defined above, then the following identities hold*

1. $\operatorname{rank} \acute{\boldsymbol{N}} = n_n$,

2. *there are $n_m = n_l - n_n + 1$ independent loops and* $\operatorname{rank} \acute{\boldsymbol{M}} = n_m$.

In many applications, only full rank equivalents of the node and loop incidence matrices are used *Chen* [1983], that is the $n_n \times n_\lambda$ node incidence matrix $\boldsymbol{N}$ and the $n_m \times n_\lambda$ loop incidence matrix $\boldsymbol{M}$. These matrices are constructed from the original complete matrices by the removal of a single row. This operation is equivalent to defining a reference node or outer loop that is not required within the calculations.

A K-network is defined below.

Definition B.11. *The pair* $(\mathcal{G}(\mathcal{N}, \Lambda), \mathcal{K})$ *comprised of the graph* $\mathcal{G}(\mathcal{N}, \Lambda)$*, and the link function set* $\mathcal{K} = \{y_1, \ldots, y_{n_\Lambda}\}$*, whose links posses the asymmetric states* v_j *and symmetric states* u_j *(*$\lambda_j \in \Lambda$*) with the admittance relationship* $v_j(t) = y_j(u_j)(t)$ *(*y_j^{-1} *exists) is termed a Kirchoff-network (*K*-network) if the following network properties hold*

1. $\acute{\boldsymbol{N}}\boldsymbol{v} = \boldsymbol{0}$ *(Kirchoff's current law)*

2. $\acute{\boldsymbol{M}}\boldsymbol{u} = \boldsymbol{0}$ *(Kirchoff's voltage law)*

where $\boldsymbol{v} = [v_1 \cdots v_{n_\Lambda}]^T$ *and* $\boldsymbol{u} = [u_1 \cdots u_{n_\Lambda}]^T$.

The two primary examples of K-networks are steady-state water distribution system (WDS)s and temporarily varying lumped parameter electrical circuits. For the WDS (electrical circuit) network types, the asymmetric variable is the pipeline flow rate (current) and the symmetric variable is the pressure (or voltage) drop along the pipe (line). Kirchoff's current law is interpreted as a nodal continuity expression for either mass (summation of inflows is equal to the summation of outflows) for WDSs, or current (summation of incoming currents is equal to the summation of outgoing currents) for electrical circuits. Kirchoff's voltage law is interpreted as an energy conservation expression in either pressure (the cumulative change in pressure about a loop is zero) for WDSs, or voltage (the cumulative change in voltage about a loop is zero) for electrical circuits. The discussion here is simplified, somewhat as there are important technicalities associated with incorporating different source types [*Chen*, 1983].

To compute the network state $(\boldsymbol{u}, \boldsymbol{v})$, the above identities admit two popular types of network equation formulations. The first approach, termed the nodal equations [*Desoer and Kuh*, 1969] involves resolving the network equations into a series of n_n equations in terms of a set of n_n unknowns $\boldsymbol{U}$ called the nodal variables which are defined by $\boldsymbol{u} = \boldsymbol{N}^T\boldsymbol{U}$. The second approach involves resolving the network equations into a series of n_m equations in terms of n_m unknowns $\boldsymbol{V}$ called the loop variables, which are defined by $\boldsymbol{v} = \boldsymbol{M}^T\boldsymbol{V}$.

B.4.2 Equivalent Kirchoff networks

Given the apparent difference and similarities between K-networks and the distributed parameter networks considered within this thesis an interesting question is whether there is an equivalent K-network representation of a distributed parameter network of the type $(\mathcal{G}(\mathcal{N},\Lambda),\mathcal{P})$ from Chapter 3. It turns out that there is quite a natural representation.

Generalising the admittance mapping (2.48) for fluid lines, here reciprocal lines are considered, that is, each link admittance function is of the form

$$\begin{bmatrix} Q_u(s) \\ -Q_d(s) \end{bmatrix}_\lambda = \begin{bmatrix} Y_1(s) & Y_2(s) \\ Y_2(s) & Y_1(s) \end{bmatrix}_\lambda \begin{bmatrix} P_u(s) \\ P_d(s) \end{bmatrix}_\lambda \tag{B.23}$$

where $Y_1 = Z_c^{-1}\coth\Gamma$ and $Y_1 = Z_c^{-1}\,\mathrm{csch}\,\Gamma$ for $\mathscr{L}$-lines. Networks comprised of such links are termed reciprocal networks, and are symbolised also by $(\mathcal{G}(\mathcal{N},\Lambda),\mathcal{P})$ where $\mathcal{P}$ is the set of Y_1 and Y_2 functions for each link. For such networks, the upstream and downstream flows can be expressed as

$$\begin{bmatrix} Q_u(s) \\ Q_d(s) \end{bmatrix}_\lambda = \begin{bmatrix} Q_{uu}(s) \\ Q_{du}(s) \end{bmatrix}_\lambda + \begin{bmatrix} Q_{ud}(s) \\ Q_{dd}(s) \end{bmatrix}_\lambda \tag{B.24}$$

where the vectors on the right correspond to the contributions to the upstream and downstream flow driven by the upstream and downstream pressure respectively. The following definition outlines a form of a constant link state network (of the form required for K-networks) for a reciprocal distributed parameter network. This network representation will later be shown to a K-network.

Definition B.12. *Given a reciprocal distributed parameter network $(\mathcal{G}(\mathcal{N},\Lambda),\mathcal{P})$, with node states $\boldsymbol{\Psi}$, and $\boldsymbol{\Theta}$, and link upstream and downstream states $\boldsymbol{P_u}$, $\boldsymbol{P_d}$, $\boldsymbol{Q_u}$, and $\boldsymbol{Q_d}$, the* equivalent constant link state network *is given by the graph $\mathcal{G}_e(\mathcal{N}_e,\Lambda_e)$ with link admittances $Y_{e\lambda}, \lambda\in\Lambda_e$ and link states $\boldsymbol{P_e}$, and $\boldsymbol{Q_e}$ where*

1. *The node and link sets for the graph $\mathcal{G}_e$ are given by*

$$\begin{aligned} \mathcal{N}_e &= \{0\}\cup\mathcal{N} \\ \Lambda_e &= \Lambda\cup\{(1,0),\ldots,(n_n,0)\} \end{aligned}$$

2. *The link pressure and flow states are given by*

$$\boldsymbol{P_e}(s) = \begin{bmatrix} \boldsymbol{P_{eo}}(s) \\ \hdashline \boldsymbol{P_{ea}}(s) \end{bmatrix}, \quad \boldsymbol{Q_e}(s) = \begin{bmatrix} \boldsymbol{Q_{eo}}(s) \\ \hdashline \boldsymbol{Q_{ea}}(s) \end{bmatrix}$$

where $\boldsymbol{P_e}$ and $\boldsymbol{Q_e}$ are length $(n_\lambda + n_n) \times 1$, $\boldsymbol{P_{eo}}$ and $\boldsymbol{Q_{eo}}$ are the partitions corresponding to the n_λ original links and $\boldsymbol{P_{ea}}$ and $\boldsymbol{Q_{ea}}$ are the partitions corresponding to the n_n artificial links. These are defined as

$$\begin{aligned}
\boldsymbol{P_{eo}}(s) &= \boldsymbol{P_u}(s) - \boldsymbol{P_d}(s) \\
\boldsymbol{Q_{eo}}(s) &= \boldsymbol{Q_{ud}}(s) + \boldsymbol{Q_{du}}(s) \\
\boldsymbol{P_{ea}}(s) &= \boldsymbol{\Psi}(s) - P_0(s)\mathbf{1} \\
\boldsymbol{Q_{ea}}(s) &= \boldsymbol{N_u}\left(\boldsymbol{Q_{uu}} - \boldsymbol{Q_{du}}\right) - \boldsymbol{N_d}\left(\boldsymbol{Q_{dd}} - \boldsymbol{Q_{ud}}\right) - \boldsymbol{\Theta}(s)
\end{aligned}$$

3. The admittance functions are defined as

$$Y_{e\lambda}(s) = \begin{cases} -Y_{2\lambda}(s) & \text{if } \lambda \in \Lambda \\ \sum_{l \in \Lambda_i} Y_{1l}(s) + Y_{2l}(s) & \text{if } \lambda \in \{(1,0), \ldots, (n_n, 0)\} \end{cases}$$

for $\lambda \in \Lambda_e$.

Remarks:

1. $\mathcal{G}_e$ has the same topology as $\mathcal{G}$ except that it has an additional node 0 and there are n_n additional links connecting each node in $\mathcal{N}$ to node 0.

2. Ordering the nodes with node 0 first, and the links with the additional n_n links last, the incidence matrix for graph $\mathcal{G}_e$ is given by

$$\boldsymbol{\acute{N}_e} = \left[\begin{array}{c|c} \mathbf{0}_{(1\times n_\lambda)} & -\mathbf{1}_{(1\times n_n)} \\ \hline \boldsymbol{N_u} - \boldsymbol{N_d} & \boldsymbol{I} \end{array}\right]$$

   but in most applications, only a full rank submatrix of $\boldsymbol{\acute{N}_e}$ is of interest, this is achieved by removing the first row to yield

$$\boldsymbol{N_e} = \left[\begin{array}{c|c} \boldsymbol{N_u} - \boldsymbol{N_d} & \boldsymbol{I} \end{array}\right]$$

3. Diagonally aligning the admittance functions leads to the matrix representation

$$\boldsymbol{Y_e}(s) = \left[\begin{array}{c:c} \boldsymbol{Y_{eo}}(s) & \mathbf{0} \\ \hdashline \mathbf{0} & \boldsymbol{Y_{ea}}(s) \end{array}\right]$$

   where $\boldsymbol{Y_{eo}} = \text{diag}\left\{Y_{e1}, \ldots, Y_{en_\lambda}\right\}$ and $\boldsymbol{Y_{ea}} = \text{diag}\left\{Y_{e(1,0)}, \ldots, Y_{e(n_n,0)}\right\}$, which, in matrix representation is expressed by

$$\begin{aligned}
\boldsymbol{Y_{eo}}(s) &= -\boldsymbol{Y_2}(s) \\
\boldsymbol{Y_{ea}}(s) &= \boldsymbol{N_u}\left[\boldsymbol{Y_1}(s) + \boldsymbol{Y_2}(s)\right]\boldsymbol{N_u}^T + \boldsymbol{N_d}\left[\boldsymbol{Y_1}(s) + \boldsymbol{Y_2}(s)\right]\boldsymbol{N_d}^T
\end{aligned}$$

4. Noting that

$$\boldsymbol{Y_{ea}}(s)\boldsymbol{P_{ea}}(s) = \boldsymbol{N_u}\left[\boldsymbol{Q_{uu}}(s) - \boldsymbol{Q_{du}}(s)\right] - \boldsymbol{N_d}\left[\boldsymbol{Q_{dd}}(s) - \boldsymbol{Q_{ud}}(s)\right]$$

   it can be demonstrated that the flow variable in the artificial links is expressed as the addition of two terms

$$\boldsymbol{Q_{ea}}(s) = \underbrace{\boldsymbol{Y_{ea}}(s)\boldsymbol{P_{ea}}(s)}_{\text{term I}} - \underbrace{\boldsymbol{\Theta}(s)}_{\text{term II}} \tag{B.25}$$

   where $\boldsymbol{Y_{ea}}$ is the link admittance relationship for the artificial links. The interpretation of (B.25) can be made by analogy with electrical circuits [*Desoer and Kuh*, 1969]. The current from a general link within an electrical circuit contains two terms, a passive term and an active term. The passive term is purely a function of the voltage difference across the link and the active term arises from the presence of a current source located on the link. Hence, by analogy, term I in (B.25) is the pressure dependent passive term and term II is the controlled active term. Therefore, within the constant link state framework, the controlled nodal outflows for the network $\mathcal{G}$ become the controlled flow sources on the artificial links for the network $\mathcal{G}_e$.

5. The flow variable for the original links $\boldsymbol{Q_{eo}}$ considers the influence of the pressure at the upstream point to the flow at the downstream point $\boldsymbol{Q_{du}}$ and the influence of the pressure at the downstream point to the flow at the upstream point $\boldsymbol{Q_{ud}}$. As such, $\boldsymbol{Q_{eo}}$ neglects local influences. These local influences (as described by $\boldsymbol{Q_{uu}}$ and $\boldsymbol{Q_{dd}}$) are captured in the artificial link flow variables $\boldsymbol{Q_{ea}}$.

The equivalent constant link state network is now shown to be a K-network.

Theorem B.5. *Given the equivalent constant link state network $\mathcal{G}_e(\mathcal{N}_e, \Lambda_e)$ with admittance functions $\mathcal{P}_e = \{Y_{e\lambda} : \lambda \in \Lambda_e\}$ based on the reciprocal distributed parameter network $(\mathcal{G}(\mathcal{N}, \Lambda), \mathcal{P})$, then the network described by $(\mathcal{G}_e(\mathcal{N}_e, \Lambda_e), \mathcal{P}_e)$ is a K-network*

Proof. This proof involves showing that the two criteria of the definition of a K-network hold for the constant link state network. Firstly, consider Kirchoff's current law

$$\begin{aligned}
\boldsymbol{N_e Q_e}(s) &= \left[\begin{array}{c:c} \boldsymbol{N_u} - \boldsymbol{N_d} & \boldsymbol{I} \end{array}\right] \left[\begin{array}{c} \boldsymbol{Q_{eo}}(s) \\ \hdashline \boldsymbol{Q_{ea}}(s) \end{array}\right] \\
&= \left[\begin{array}{c:c} \boldsymbol{N_u} - \boldsymbol{N_d} & \boldsymbol{I} \end{array}\right] \\
&\quad \times \left[\begin{array}{c} \boldsymbol{Q_{ud}}(s) + \boldsymbol{Q_{du}}(s) \\ \hdashline \boldsymbol{N_u}\left[\boldsymbol{Q_{uu}}(s) - \boldsymbol{Q_{du}}(s)\right] - \boldsymbol{N_d}\left[\boldsymbol{Q_{dd}}(s) - \boldsymbol{Q_{ud}}(s)\right] - \boldsymbol{\Theta}(s) \end{array}\right] \\
&= \boldsymbol{N_u}\left(\boldsymbol{Q_{uu}}(s) + \boldsymbol{Q_{ud}}(s)\right) - \boldsymbol{N_d}\left(\boldsymbol{Q_{dd}}(s) + \boldsymbol{Q_{du}}(s)\right) - \boldsymbol{\Theta}(s) \\
&= \boldsymbol{0}
\end{aligned}$$

where the last step arises purely from the properties of the original reciprocal network. Considering now the second criteria, Kirchoff's voltage law. Considering any loop through the graph $\mathcal{G}_e$ whose positively oriented links are given by the set $\mathcal{A}^+$ and negatively oriented links are in the set $\mathcal{A}^-$. Summating the pressure changes about the loop gives the expression

$$\sum_{\lambda \in \mathcal{A}^+} P_{e\lambda}(s) - \sum_{\lambda \in \mathcal{A}^-} P_{e\lambda}(s)$$

which can be expanded in terms of the upstream and downstream pressures from the original reciprocal network to yield

$$\sum_{\lambda \in \mathcal{A}^+} \left(P_{u\lambda}(s) - P_{d\lambda}(s)\right) - \sum_{\lambda \in \mathcal{A}^-} \left(P_{u\lambda}(s) - P_{d\lambda}(s)\right). \tag{B.26}$$

Now, the loop traverses a set of nodes $\mathcal{A}_n$ where each node is visited only once. This means that exactly two pressure terms in (B.26) correspond to the pressure Ψ_i for each $i \in \mathcal{A}_n$ as these pressures are equal to the upstream or downstream pressures in the links. If one of these pressures has a positive sign, then it is either the upstream node in a positively oriented link or the downstream node in a negatively oriented link. A negative sign corresponds to a downstream node in a positively oriented link or an upstream node in a negatively oriented link. Enumerating the combinations of the pairs of scenarios that can occur (*e.g.* node i is downstream of a positively oriented link (negative term) then it must either be upstream of a positively oriented link (positive term) or downstream of a negatively oriented link (positive term)) reveals that the terms always appear in opposite sign. Hence (B.26) is equal to zero. □

The equivalent constant link state network is now shown to yield an equivalent nodal admittance map to the original reciprocal network.

Theorem B.6. *The equivalent constant link state network* $(\mathcal{G}_e(\mathcal{N}_e, \Lambda_e), \mathcal{P}_e)$ *derived from the reciprocal network* $(\mathcal{G}(\mathcal{N}, \Lambda), \mathcal{P})$*, yields the same admittance map from the nodal pressures to the nodal flows* $\boldsymbol{\Psi} \mapsto \boldsymbol{\Theta}$ *as the original reciprocal network.*

Proof. The link relationship for the network $\mathcal{G}_e$ is

$$\boldsymbol{Q_e}(s) = \boldsymbol{Y_e}(s)\boldsymbol{P_e}(s) - \left[\begin{array}{c} \mathbf{0} \\ \hdashline \boldsymbol{\Theta}(s) \end{array}\right] \tag{B.27}$$

Noting that $\boldsymbol{N_e}\boldsymbol{Q_e} = \mathbf{0}$ and $\boldsymbol{P_e} = \boldsymbol{N_e}^T\boldsymbol{\Psi}$, (B.27) can be rearranged to yield

$$\boldsymbol{\Theta}(s) = \boldsymbol{N_e}\boldsymbol{Y_e}(s)\boldsymbol{N_e}^T\boldsymbol{\Psi}.$$

Expanding out the matrix expression yields

$$\begin{aligned}
\boldsymbol{N_e}\boldsymbol{Y_e}(s)\boldsymbol{N_e}^T =& - [\boldsymbol{N_u} - \boldsymbol{N_d}]\,\boldsymbol{Y_2}(s)\,[\boldsymbol{N_u} - \boldsymbol{N_d}]^T \\
&+ \boldsymbol{N_u}[\boldsymbol{Y_1}(s) + \boldsymbol{Y_2}(s)]\,\boldsymbol{N_u}^T + \boldsymbol{N_d}[\boldsymbol{Y_1}(s) + \boldsymbol{Y_2}(s)]\,\boldsymbol{N_d}^T \\
=& \boldsymbol{N_u}\boldsymbol{Y_1}(s)\boldsymbol{N_u}^T + \boldsymbol{N_u}\boldsymbol{Y_2}(s)\boldsymbol{N_d}^T + \boldsymbol{N_d}\boldsymbol{Y_1}(s)\boldsymbol{N_d}^T + \boldsymbol{N_d}\boldsymbol{Y_2}(s)\boldsymbol{N_u}^T \\
=& \left[\begin{array}{c:c} \boldsymbol{N_u} & \boldsymbol{N_d} \end{array}\right] \left[\begin{array}{c:c} \boldsymbol{Y_1}(s) & \boldsymbol{Y_2}(s) \\ \hdashline \boldsymbol{Y_2}(s) & \boldsymbol{Y_1}(s) \end{array}\right] \left[\begin{array}{c:c} \boldsymbol{N_u} & \boldsymbol{N_d} \end{array}\right]^T
\end{aligned}$$

which is the exact admittance matrix expression for the original reciprocal network. Thus the dynamics of the equivalent K-network network are equivalent to the original reciprocal network. □

These theorems lead onto the following important corollary

Corollary B.4. *Any reciprocal distributed parameter network* $(\mathcal{G}(\mathcal{N}, \Lambda), \mathcal{P})$*, can be transformed into a dynamically equivalent* K*-network given by* $(\mathcal{G}_e(\mathcal{N}_e, \Lambda_e), \mathcal{P}_e)$*.*

Proof. This is a direct result from Theorems B.5 and B.6. □

The significance of this proposition is that any reciprocal distributed parameter network can be described by an equivalent K-network of an equivalent topology, with an additional reference node and n_n additional artificial links connecting this node to each of the original nodes. What this means is that any theorems relating to K-networks can be applied to reciprocal distributed parameter networks through this transformation. The next section discusses an important application.

B.5 Loop equations of a $\mathscr{M}$-Network

In the previous section, it was demonstrated that for any reciprocal distributed parameter network, there exists an equivalent K-network. The benefit of this is that work that applies to K-networks can be applied to the K-network representation of the reciprocal distributed parameter network. Possibly the most fundamental of these theories is the loop equation representation of the network.

The two common representations of lumped parameter electrical networks are the node equations or the loop equations [*Desoer and Kuh*, 1969; *Chen*, 1983]. The node equations arise from the application of Kirchoff's current law, and the loop equations arise from the application of Kirchoff's voltage law. The admittance matrix formulation from Chapter 3 is essentially a node formulation of the equations, and it arises naturally from the application of the nodal continuity equations to couple the pipeline end states. Dealing directly with the distributed links has meant that no construction of the loop equations has been possible, as there is no clear representation of the distributed link states as a function of loop based variables. However, working with the K-network equivalent of a reciprocal distributed parameter network means that standard approaches for deriving the loop equations (*e.g. Chen* [1983]) can be followed.

The link impedance relationships for the equivalent K-network can be expressed as

$$\boldsymbol{P_e}(s) = \boldsymbol{Z_e}(s)\left(\boldsymbol{Q_e}(s) + \begin{bmatrix} \mathbf{0} \\ \hdashline \boldsymbol{\Theta}(s) \end{bmatrix}\right) \tag{B.28}$$

where the link impedances are given by $\boldsymbol{Z_e} = \boldsymbol{Y_e}^{-1}$. The loop method, involves applying Kirchoff's voltage law to reduce (B.28) into a system of $n_m = n_\lambda$ equations in n_m unknowns termed the loop variables. These are defined as

$$\boldsymbol{Q_e}(s) = \boldsymbol{M}^T\boldsymbol{\Phi}(s) \tag{B.29}$$

where, as per prior notation, $\boldsymbol{M}$ is the loop incidence matrix, and $\boldsymbol{\Phi}(s)$ is the $n_m \times 1$ loop variable, which in this instance is interpreted as loop flows. Employing Kirchoff's second law ($\boldsymbol{MP_e} = \mathbf{0}$) and (B.29) yields the loop equations

$$\boldsymbol{MZ_e}(s)\begin{bmatrix} \mathbf{0} \\ \hdashline \boldsymbol{\Theta}(s) \end{bmatrix} = -\boldsymbol{MZ_e}(s)\boldsymbol{M}^T\boldsymbol{\Phi}(s) \tag{B.30}$$

where $\boldsymbol{MZ_eM}^T$ is known as the loop impedance matrix [*Desoer and Kuh*, 1969]. Equation (B.30) holds for a completely arbitrary loop incidence matrix. The construction of a loop matrix for any graph is not unique [*Chen*, 1983], as it requires only linear independence of the loops that it is constructed from. The following sections identify two alternative constructions and discuss their properties.

B.5.1 Loop construction 1

Equation (B.28) can be expanded as

$$\left[\begin{array}{c} \boldsymbol{P_{eo}}(s) \\ \hdashline \boldsymbol{P_{ea}}(s) \end{array}\right] = \left[\begin{array}{c:c} \boldsymbol{Z_{eo}}(s) & \mathbf{0} \\ \hdashline \mathbf{0} & \boldsymbol{Z_{ea}}(s) \end{array}\right] \left(\left[\begin{array}{c} \boldsymbol{Q_{eo}}(s) \\ \hdashline \boldsymbol{Q_{ea}}(s) \end{array}\right] + \left[\begin{array}{c} \mathbf{0} \\ \hdashline \boldsymbol{\Theta}(s) \end{array}\right] \right) \tag{B.31}$$

where $\boldsymbol{Z_{eo}} = \boldsymbol{Y_{eo}}^{-1}$ and $\boldsymbol{Z_{ea}} = \boldsymbol{Y_{ea}}^{-1}$.

A feasible loop matrix is

$$\boldsymbol{M} = \left[\begin{array}{c:c} \boldsymbol{M}_{11} & \mathbf{0} \\ \hdashline \boldsymbol{M}_{21} & \boldsymbol{M}_{22} \end{array}\right]$$

where $\boldsymbol{M}_{11}$ is a $(n_\lambda - n_n + 1) \times n_\lambda$ loop incidence matrix corresponding to the original graph $\mathcal{G}$ and $\left[\begin{array}{c:c} \boldsymbol{M}_{21} & \boldsymbol{M}_{22} \end{array}\right]$ is a $(n_n - 1) \times (n_\lambda + n_n)$ loop incidence matrix corresponding to the $n_n - 1$ loops in graph $\mathcal{G}_e$ that are independent from the $(n_\lambda - n_n + 1)$ loops described by $\boldsymbol{M}_{11}$, where the partition corresponds to the incidence matrix sections for the original and artificial links. The feature of this formulation is that it utilises a maximum set of independent loops that do not involve the artificial links. The loop flow set is likewise partitioned as

$$\boldsymbol{\Phi}(s) = \left[\begin{array}{c} \boldsymbol{\Phi_o}(s) \\ \hdashline \boldsymbol{\Phi_a}(s) \end{array}\right]$$

where $\boldsymbol{\Phi_o}$ corresponds to the $n_\lambda - n_n + 1$ loops involving only the original links, and $\boldsymbol{\Phi_a}$ corresponds to the $n_n - 1$ loops involving the artificial links. Given (B.29), the link flows are expressed as

$$\left[\begin{array}{c} \boldsymbol{Q_{eo}}(s) \\ \hdashline \boldsymbol{Q_{ea}}(s) \end{array}\right] = \left[\begin{array}{c:c} \boldsymbol{M}_{11}^T & \boldsymbol{M}_{21}^T \\ \hdashline \mathbf{0} & \boldsymbol{M}_{22}^T \end{array}\right] \left[\begin{array}{c} \boldsymbol{\Phi_o}(s) \\ \hdashline \boldsymbol{\Phi_a}(s) \end{array}\right]$$

Applying these realisations of $\boldsymbol{M}$ and $\boldsymbol{\Phi}$ to (B.30) yields

$$\left[\begin{array}{c} \mathbf{0} \\ \hdashline \boldsymbol{M}_{22}\boldsymbol{Z_{ea}}(s)\boldsymbol{\Theta}(s) \end{array}\right] = \\ - \left[\begin{array}{c:c} \boldsymbol{M}_{11}\boldsymbol{Z_{eo}}(s)\boldsymbol{M}_{11}^T & \boldsymbol{M}_{11}\boldsymbol{Z_{eo}}(s)\boldsymbol{M}_{21}^T \\ \hdashline \boldsymbol{M}_{21}\boldsymbol{Z_{eo}}(s)\boldsymbol{M}_{11}^T & \boldsymbol{M}_{21}\boldsymbol{Z_{eo}}(s)\boldsymbol{M}_{21}^T + \boldsymbol{M}_{22}\boldsymbol{Z_{ea}}(s)\boldsymbol{M}_{22}^T \end{array}\right] \left[\begin{array}{c} \boldsymbol{\Phi_o}(s) \\ \hdashline \boldsymbol{\Phi_a}(s) \end{array}\right]$$

from which it can be deduced that the original loop flows are uniquely identified from the artificial loop flows as

$$\boldsymbol{\Phi_o}(s) = -\left[\boldsymbol{M}_{11}\boldsymbol{Z_{eo}}(s)\boldsymbol{M}_{11}^T\right]^{-1}\boldsymbol{M}_{11}\boldsymbol{Z_{eo}}(s)\boldsymbol{M}_{21}^T\boldsymbol{\Phi_a}(s)$$

where $\boldsymbol{M}_{11}\boldsymbol{Z_{eo}}\boldsymbol{M}_{11}^T$ can be interpreted as a loop impedance matrix for the original graph. We then get the relationship between $\boldsymbol{\Theta}$ and $\boldsymbol{\Phi_a}$ as

$$\begin{aligned}&\boldsymbol{M}_{22}\boldsymbol{Z_{ea}}(s)\boldsymbol{\Theta}(s) = \\ &\quad\left[\begin{array}{c}\boldsymbol{M}_{21}\boldsymbol{Z_{eo}}(s)\boldsymbol{M}_{11}^T\left[\boldsymbol{M}_{11}\boldsymbol{Z_{eo}}(s)\boldsymbol{M}_{11}^T\right]^{-1}\boldsymbol{M}_{11}\boldsymbol{Z_{eo}}(s)\boldsymbol{M}_{21}^T \\ -\left(\boldsymbol{M}_{21}\boldsymbol{Z_{eo}}(s)\boldsymbol{M}_{21}^T + \boldsymbol{M}_{22}\boldsymbol{Z_{ea}}(s)\boldsymbol{M}_{22}^T\right)\end{array}\right]\boldsymbol{\Phi_a}(s)\end{aligned}.$$

B.5.2 Loop construction 2

An alternative construction of the loop incidence matrix is

$$\boldsymbol{M} = \left[\begin{array}{c:c}\boldsymbol{I} & -\boldsymbol{N}^T\end{array}\right] \tag{B.32}$$

where $\boldsymbol{I}$ is clearly $n_\lambda \times n_\lambda$ and $\boldsymbol{N}$ is the node incidence matrix. Equation (B.32) has the interpretation of involving one and only one original link in each defined loop where each loop is completed by two artificial links corresponding to the upstream and downstream nodes of the original link. That is, the path of every loop involves the artificial reference node 0. With this construction, loop flows are given by the actual link flows, that is

$$\left[\begin{array}{c}\boldsymbol{Q_{eo}}(s) \\ \boldsymbol{Q_{ea}}(s)\end{array}\right] = \left[\begin{array}{c}\boldsymbol{I} \\ \hdashline -\boldsymbol{N}\end{array}\right]\boldsymbol{\Phi}(s) \tag{B.33}$$

which implies the relationships $\boldsymbol{Q_{eo}} = \boldsymbol{\Phi}$ and $\boldsymbol{Q_{ea}} = -\boldsymbol{N}\boldsymbol{\Phi}$ (which reflects the continuity relationship $\boldsymbol{N_e}\boldsymbol{Q_e} = \boldsymbol{0}$). Premultiplying (B.31) by (B.32) yields the expression for the loop flow variable as a function of the nodal outflows

$$\boldsymbol{\Phi}(s) = \left[\boldsymbol{Z_{eo}}(s) + \boldsymbol{N}^T\boldsymbol{Z_{ea}}(s)\boldsymbol{N}\right]^{-1}\boldsymbol{N}^T\boldsymbol{Z_{ea}}(s)\boldsymbol{\Theta}(s). \tag{B.34}$$

A corresponding relationship can be derived between the nodal properties of $\boldsymbol{\Psi}$ and $\boldsymbol{\Theta}$. Noting from (B.31) and (B.33) that

$$\boldsymbol{\Psi}(s) = \boldsymbol{Z_{ea}}(s)\left[\boldsymbol{N}\boldsymbol{\Phi}(s) + \boldsymbol{\Theta}(s)\right]. \tag{B.35}$$

which substituting in (B.34) yields

$$\boldsymbol{\Psi}(s) = \Big[\boldsymbol{Z_{ea}}(s) - \boldsymbol{Z_{ea}}(s)\boldsymbol{N}\left[\boldsymbol{Z_{eo}}(s) + \boldsymbol{N}^T\boldsymbol{Z_{ea}}(s)\boldsymbol{N}\right]^{-1}\boldsymbol{N}^T\boldsymbol{Z_{ea}}(s)\Big]\,\boldsymbol{\Theta}(s). \quad \text{(B.36)}$$

It can be observed that as (B.36) maps from the nodal flows to the nodal pressures, it is an impedance mapping, and in fact the matrix in (B.36) is actually the inverse of the network admittance matrix (3.13) derived in Chapter 3. An interesting connection between the impedance matrix in (B.36) and the network admittance matrix (3.13) is that (B.36) is a form of the Woodbury-Sherman-Morrison formula [*Golub and Van Loan*, 1983] for the inverse of (3.13).

Appendix C

Extended Review of the Hydraulic Network Identification Literature

From the large body of literature on hydraulic network identification methods, five key differentiating properties of the surveyed methods have been identified. These properties are (i) the class of the methodology in terms of the system characteristics that are identified, (ii) the system configuration that the methods are designed to deal with, (iii) the information required by the methodology, (iv) the application of the methodology to the hydraulic system, and (v) the data processing involved in the methodology. The different classes of the methodologies was discussed in Chapter 6, and the remaining properties (ii)-(v) are discussed within this appendix.

The literature review presented here is organised as a discussion of the forms these properties take within the methods surveyed. It is important to note that the review is heavily biased toward leak detection. The reason for this is that the practical importance of this problem has meant that it has been a major focus in hydraulic system identification research. Additionally, the review is mainly concerned with transient methods, however steady-state methods are discussed where relevant.

C.1 System Configuration

Within the hydraulic network identification literature, different methods are designed to be applied to systems of different configurations, where a systems configuration is defined by the type of hydraulic network, the boundary conditions to this network, and the nature and complexity of the components to be identified. Methods designed for more general system types are more powerful in terms of breadth of application, but methods designed for simpler system types have the advantage of exploiting particular properties of their system type.

C.1.1 Hydraulic system type

Hydraulic network systems are categorised as either (in order of simplicity), (i) a simple line, which is a continuous line of uniform cross-sectional properties, (ii) a compound line, which is a line comprised of pipes in parallel, pipes in series, branches, valves and any other configuration that does involve second order looping [*Fox*, 1977], or (iii) a network, which is any generalised nodal layout with interlinked fluid lines. Due to the inherent complexities in modelling transient state fluid networks, and the subtleties associated with anomaly detection in such networks, the vast majority of methods have dealt only with simple or compound lines.

The class 1 analytic methods and most of the class 2 and 3 techniques deal only with uniform lines, despite the fact that, in some cases, their formulation could be generalised to deal with networks[1] (*e.g.* [*Digernes*, 1980; *Benkherouf and Allidina*, 1988; *Zecchin et al.*, 2006; *Chen et al.*, 2006]). Extensions to the single line are considered in *Emara-Shabaik et al.* [2002] and *Kiuchi* [1993], where a distribution of demands is assumed. Further complications are considered in *Mpesha et al.* [2001, 2002] where pipes in series, loops and branches are incorporated into the system under study. The only transient hydraulic network identification methods that have been applied to generalised networks are the class 1 numerical methods (*e.g.* the inverse transient method (ITM) [*Liggett and Chen*, 1994; *Vítkovský et al.*, 2000; *Covas et al.*, 2001; *Wang et al.*, 2002a]).

Despite their limited system type, the methods designed for single lines are more robust to the uncertainties of real world systems (particularly classes 2 and 3), owing to their simplicity (*e.g.* [*Isermann*, 1984]) or utilisation of particular system attributes (*i.e.* *Verde* [2001]). The general network methods are known to be extremely sensitive to modelling errors [*Vítkovský et al.*, 2007].

C.1.2 Boundary conditions

There are two main types of required boundary conditions adopted within the hydraulic parameter identification literature, namely modellable hydraulic boundary conditions, and measurement stations that bound the system section of interest. A vast majority of the methodologies that have arisen from the civil engineering field (class 1) deal with the simplified system of a reservoir-pipe-valve (R-P-V) configuration [*Lee*, 2001; *Lee et al.*, 2003a, 2002, 2003b, 2004, 2005a; *Covas and Ramos*,

[1]The analytic methods (*i.e.* reflectometry methods [*Silva et al.*, 1996], transient damping [*Wang et al.*, 2002b], the patterned frequency response methods [*Lee*, 2001; *Lee et al.*, 2003a,b, 2004, 2005a], and the steady state methods of *Baghdadi and Mansy* [1988]; *Dinis et al.* [1999]) do not possess this potential as the physics of the single line are tightly intertwined in the diagnostic process.

1999; *Covas et al.*, 1999; *Wang et al.*, 2002b], where the valve has been the source of generation of the transient conditions. The majority of the methods from the control literature (classes 2 and 3) deal with measurement stations as boundary conditions, of either just pressure [*Billmann and Isermann*, 1987; *Wang et al.*, 1993], just flow [*Thompson and Skogman*, 1983; *Isermann*, 1984] or combinations of either [*Digernes*, 1980; *Verde*, 2001]. An additional method of dealing with unknown boundary conditions is to time gate the data trace [*Silva et al.*, 1996; *Brunone*, 1999]. This allows for the consideration of a partition of the data that corresponds to sections of the network that are under investigation.

The advantage of modelling the boundary conditions is that a reduced number of measurement stations are required [*Zecchin et al.*, 2005], and the entire system is considered, rather than just the section between the measurement stations. However, the use of measurement stations as a boundary condition eliminates the need to model the boundary, and hence removes the modelling error associated with the boundary model and simplifies the modelling. This attribute is extremely beneficial when dealing with complex boundaries or sub-networks of larger networks. For example, if, for operational reasons or otherwise, the sub-network of interest cannot be isolated with valves, and the wider network is not desired, or able, to be modelled, the utilisation of measurement stations as boundaries would be required. Some criticism of the use of measurement stations as boundary conditions exists. *Vítkovský* [2001] found that the use of a measurement station as a boundary condition disguised important physical phenomena (*i.e.* unsteady frictional effects, and leak induced effects). This was attributed to the fact that the boundary condition was not independent of the system's dynamic behaviour.

C.1.3 Anomaly configuration

Anomaly configuration refers to the number and types of anomalies that a methodology can deal with. Some methodologies can only deal with systems with a single leak, others are designed to deal with multiple faults. The methodologies are discussed with reference to the anomaly configurations they are designed to deal with and their ability to be extended to deal with arbitrary anomaly configurations.

Most of the leak detection methods surveyed have been applied to systems with only one leak. Some methods are specifically designed to detect only the influence of a single leak, and rely only on the existence of only one leak for their diagnosis to operate correctly [*Wang et al.*, 2002a; *Benkherouf and Allidina*, 1988].

Some methods are designed to deal with multiple leaks, for example: the inverse transient method can (in theory) deal with an arbitrary number of leaks [*Liggett* *and Chen*, 1994]; under the linearity assumptions of the adopted base model, *Lee et al.* [2005a]; *Mpesha et al.* [2001] extended their frequency domain techniques to identify the influence of two leaks on the frequency response. The difficulty in differentiating between single and multiple leaks is noted in the literature for single lines [*Benkherouf and Allidina*, 1988], and networks [*Liggett and Chen*, 1994; *Wang et al.*, 2002a]. Only one paper has addressed the issue of identifiability of simultaneous leaks [*Verde*, 2001] by the use of specialised observers [*Hou and Muller*, 1994] that are are able to isolate the influence of individual leaks. This methodology was designed for a single line only.

No methodology has been designed to deal specifically with different types of fluid line anomalies. The closest, is the work of *Digernes* [1980] where the adopted methodology was designed to differentiate between sensor failure and the onset of leaks. As this methodology can deal with multiple failures of different types, it could clearly be extended to deal with blockages or other anomalies. Similarly, all methods that use a generic hydraulic model as the basis of their signal processing (*i.e.* inverse methods, and fault detection methods of Section C.4) could be easily adapted to deal with different anomalies with the use of specific anomaly models. With regard to this, a concern would be that the continuous monitoring methods may not be as able to detect a blockage as it may have a too subtle influence on the mildly transient nominal conditions.

The fault signature methods of Section C.4, rely exclusively on the physical characteristics of a leak for their detection diagnosis (*i.e.* frequency response characteristics, [*Lee et al.*, 2005a; *Mpesha et al.*, 2001], influence on damping rates [*Wang et al.*, 2002b], wave reflection behaviour *Brunone* [1999] *etc.*), and as such are designed only for leaks. The advancement of these methods to deal with anomalies of different types requires a similar analysis as that used for leaks in terms of determining the signature of the influence of the anomaly. Such work had been shown in *Wang et al.* [2002a] where a block was modelled as an impulse function in the momentum equation as opposed to the continuity equation for a leak, and in *Lee et al.* [2005a] where the the anomaly transfer function of a block was used instead of a leak.

C.2 System Information

System information refers to the nature of the information required by the methodology in terms of (i) data acquisition (the number and types of sensors, and noise within measurements), and (ii) *a priori* system knowledge (system configuration and parametric uncertainties).

C.2.1 Sensor types and identifiability

There is a close relationship between the type of required boundary conditions and the sensor layout design. Many of the methodologies that deal with known boundary conditions utilise only single pressure sensors [*Lee et al.*, 2005a; *Covas and Ramos*, 1999; *Wang et al.*, 2002a] (*Mpesha et al.* [2001, 2002] uses flow measurements also). Many of the methods that use measurement stations as boundary conditions use measurements of pressure [*Billmann and Isermann*, 1987; *Wang et al.*, 1993], flow [*Thompson and Skogman*, 1983; *Isermann*, 1984] or both [*Digernes*, 1980; *Verde*, 2001], at the boundaries combined with one or more measurement stations of pressure [*Billmann and Isermann*, 1987; *Wang et al.*, 1993], flow [*Thompson and Skogman*, 1983; *Isermann*, 1984] or both [*Digernes*, 1980; *Verde*, 2001] throughout the length of the fluid line.

There are important practical and theoretical concerns associated with the sensor layout design. The practical constraints are the points at which measurement stations can be set up within a system, and the accuracy and cost associated with the number and type of each sensor. The theoretical concerns are primarily to do with the observability and identifiability of a system [*Ljung*, 1999]. For the success of any inverse or system identification method, it is fundamental that the system is identifiable. A system is identifiable if there exists a unique solution to the inverse or system identification problem (*i.e.* a one to one mapping exists from the data sets to the parameter space). Observability is closely related to identifiability, however, with reference to distributed parameter systems, *Goodson and Polis* [1974] state that the constraint of identifiability is less severe than that of observability, and further that

> *A measurement location could be chosen where the data would not contain all the information necessary to determine the dependent variable [state] but would contain sufficient information to determine the parameters.*

Goodson and Polis [1974] cites three available techniques to aid in the placement of measurement locations, namely sensors should be placed in locations which (i) avoid zeros of eigenfunctions of processes that can be expressed as series expansions of such functions, (ii) intersect the full manifold of characteristic lines for hyperbolic systems (*i.e.* long enough measurement time so as to account for the longest delays), and (iii) maximise the sensitivity with respect to the parameter variations.

Largely, the leak detection methods do not formally consider the issues of observability or identifiability, except for *Verde* [2001]; *Ashton and Shields* [1999]. The issues encountered within the literature associated with identifiability are (i) the inability to differentiate between single and multiple leaks [*Benkherouf and Allidina*, 1988; *Wang et al.*, 2002a; *Verde*, 2001], (ii) insufficient information to ensure a unique solution to the inverse problem [*Liggett and Chen*, 1994; *Wang et al.*, 2002a], (iii) the sensitivity of sensors to leak locations [*Ferrante et al.*, 2001; *Ferrante and Brunone*, 2003a; *Lee et al.*, 2005a; *Wang et al.*, 2001], and (iv) the effect of parameter uncertainty [*Verde*, 2001; *Emara-Shabaik et al.*, 2002].

In agreement with the recommendations of *Goodson and Polis* [1974] and in keeping with traditional inverse theory, *Liggett and Chen* [1994] argued that the measurement stations should be placed at those locations that are most sensitive to parameter variations[2]. The consideration of these issues was studied further in *Vítkovský et al.* [2003b]. Drawing on a number of formulations of measurement point sensitivities to parameters, *Vítkovský et al.* [2003b] formulated a heuristic approach to optimising the informational value of the data collected for a given number of measurement stations.

The issue of sensitivity of sensors to leak location was mainly noted in the frequency based methods [*Ferrante et al.*, 2001; *Ferrante and Brunone*, 2003a; *Lee et al.*, 2005a; *Covas et al.*, 2005a] for single line problems. *Ferrante et al.* [2001]; *Ferrante and Brunone* [2003a] identified *shadow zones* where the leak influence was hidden. *Lee et al.* [2002] commented that the influence the leak location has on the harmonics of the frequency response is due to the harmonic mode shapes. By use of a standing wave methodology [*Covas et al.*, 2005a] observed that the leak influence was unnoticeable when the leak was located near or at an anti-node of the harmonic modes. This problem can be related to the guidelines set out by *Goodson and Polis* [1974] in that the shadow zones correspond to the zeros of the eigenfunctions (which in this case are sinusoids) of the linearised equations.

C.2.2 Parameter uncertainty

Most methods assume that the base parameters are known or can be identified off-line. For all process based leak detection methodology surveyed within this section, sufficiently accurate knowledge of the system parameters is essential. The reason for this is that the methods depend on a sufficient description of the behaviour of the system so as to provide meaningful processing of the data in the diagnosis phase. As an indication of the sensitivity of methods to parameter uncertainty, *Lee et al.* [2005a] reported that lack of robustness to parameter uncertainty is a serious lim-

[2]Sensitivity is measured by the gradient of the pressure at each node with respect to each parameter.

itation to the ITM, and *Emara-Shabaik et al.* [2002] reported a degradation in the performance of their methodology for even a 1 % error in the (real as opposed to model) friction factor and wave speed. Within the literature, the system uncertainties are related to limited properties of the conduit material, namely the resistance coefficients (or friction factors, dependent on the internal roughness of the line) and the wavespeed (dependent on the material properties of the pipeline).

It has been noted by many authors [*Billmann and Isermann*, 1987; *Verde*, 2001; *Vítkovský*, 2001; *Covas and Ramos*, 2001; *Wang et al.*, 2002a] that an accurate knowledge of the resistance coefficient is paramount to leak detection. The reason for this is that leaks and friction both act as energy loss mechanisms and, despite the difference in the nature of the energy loss (*i.e.* lumped as opposed to distributed), their impact on pressure transients is similar [*Dinis et al.*, 1999; *Wang et al.*, 2001]. Based on limited experiments with errors in friction factor values, *Emara-Shabaik et al.* [2002] recommended that leak detection techniques would need to involve online parameter identification methods. In an attempt to combat the uncertainty associated with unknown friction factors, various authors have adopted different measures: *Billmann and Isermann* [1987] used a least squares updating estimation of the friction factor; the ITM [*Liggett and Chen*, 1994] treats friction factors as parameters to be calibrated.

Accurate knowledge of the transient wavespeeds is important for many methods in determining locations of anomalies. *Covas et al.* [2001] reported that experimental determination is straight of wavespeeds for single lines is straight forward, but for networks their determination is a lot more difficult as wavespeeds can change from line to line and there are typically links within the network that are not bounded by sensors. Variations in wavespeeds arise from conduits of different material strength properties, and diameter. An additional complication with determining the wavespeed is the impact of dissolved oxygen [*Wang et al.*, 2002a] and entrapped air within the system.

C.2.3 Model uncertainty

Modelling error is identified by many authors as a problem for the practical implementation of identification within hydraulic networks, particularly leak detection methods.

In terms of generalised fault detection and isolation, many different formulations are proposed that deal with system uncertainties in the form of unmodelled physical processes [*Zhong et al.*, 2003; *Han et al.*, 2005]. *Frank and Ding* [1994] highlights three approaches to modelling uncertainty, namely additive perturbations, input multiplicative, and output multiplicative perturbations. *Han et al.* [2005] deals with process uncertainties by considering errors in the system matrices.

C.2.4 Measurement uncertainty

Measurements of any real dynamical system involve noise of some description. The sources of noise within measurements from a fluid network are (i) random changes in boundary conditions to the fluid network lines (*e.g.* noise from pumps or random domestic use), (ii) noise from the containing environment of conduits (*e.g.* ground vibrations from traffic), (iii) random state perturbations from turbulence, and (iv) measurement noise.

Few methodologies give a formal recognition of noise in the development of their diagnostic methods [*Candy and Rosza*, 1980; *Digernes*, 1980; *Benkherouf and Allidina*, 1988; *Wang et al.*, 1993; *Emara-Shabaik et al.*, 2002]. There have been, however, many *ad hoc* approaches to robustifying methods to the presence of noise: the use of a matched filter approach to estimate the spectral densities [*Lee et al.*, 2005a]; quadratic error minimisation for parameter calibration [*Liggett and Chen*, 1994]; wavelet filtering methods [*Ferrante and Brunone*, 2003b]; flow correlation techniques [*Billmann and Isermann*, 1987];

Methods based on state estimation approaches typically involve the assumption of additive white Gaussian measurement noise, in conjunction with Gaussian input (or system) noise. No leak detection methodologies have considered the issue of noise entering the system from random boundary effects, which effectively serve as unknown inputs [*Zhong et al.*, 2003].

C.3 Mode of Application

The mode of application refers to the manner in which the hydraulic network identification methodologies are applied to the networks in terms of online or offline application, active or passive approaches and the nature of the required transient state.

C.3.1 Continuous monitoring versus batch application

An important descriptor of a hydraulic network identification method is whether it is designed for continuous monitoring, or for batch applications. Continuous monitoring methods are those that track and diagnose the systems behaviour continuously whilst the system is *online*, whereas batch methods are designed to be employed for finite length testing periods and essentially analyse a frozen time-invariant *snapshot* of the system. Clearly, batch methods could be applied in a continuous fashion (*i.e.* repeat the testing with a high frequency), but there are basic differences, namely that batch methods are designed to deal with time-invariant systems.

A fundamental difference between the methods is the time scales at which the dynamic system is observed and hence the physical processes of the system that the diagnostic process is based on. Continuous monitoring methods have sample rates of the order of seconds [*Isermann*, 1984; *Baghdadi and Mansy*, 1988; *Dinis et al.*, 1999; *Venkatasubramanian et al.*, 2003] to minutes [*Isermann*, 1984; *Baghdadi and Mansy*, 1988; *Dinis et al.*, 1999; *Venkatasubramanian et al.*, 2003], whereas the batch methods have sampling rates of the order of 10^{-3} to 10^{-2} seconds. Due to the different time scale considerations, different phenomena are being observed. The continuous monitoring methods typically monitor continuity in mass and momentum between a series of two or more measurement stations. Conversely, batch methods focus on the detailed pressure history response of a line or network from an induced transient (*e.g.* [*Liggett and Chen*, 1994]). As pressure waves travel at speeds of 300 m/s (in gas) to 1,400 m/s (in liquids), a high sampling rate is needed to accurately resolve the detail of reflections and transmissions within the wave passage. In these methods, it is primarily the anomalies influence on the passage of an induced wave front that is considered, not the longer time scale influence of the anomaly on mass or momentum continuity.

Due to the different time scales of consideration, different levels of model complexity are required. As the continuous monitoring methods do not consider the finer details of the pressure response, the standard 1-D waterhammer equations [*Wylie and Streeter*, 1993] are used to model essentially, the fluid line inventory (*i.e.* time varying accumulation of mass within the reach, similar to the direct inventory techniques [*Thompson and Skogman*, 1983; *Kiuchi*, 1993]). For the batch methods, as the diagnosis is based on the details in the pressure response, more complex models are required to capture and mimic the details.

Despite the apparent appeal of continuous monitoring methods, there are advantages and disadvantages to each approach. Continuous methods generally require the development of some state of normality to calibrate the system parameters [*Emara-Shabaik et al.*, 2002; *Billmann and Isermann*, 1987] (or remove the influence of the initial Kalman filter covariance matrix) and the diagnostic process involves tracking the system response to identify deviations from the nominal behaviour [*Loparo et al.*, 1991]. The presupposition of this application is that the system is initially operating in a fault free state. With new or highly regulated systems, this is not a problem. However, the prime system of interest within much research, water distribution system (WDS)s, are typically old and not highly regulated or maintained. Therefore, continuous monitoring methods generally will only detect the onset of new anomalies and not those already in existence. Additionally, since the continuous monitoring techniques involve the tracking of some performance statistic, they usually require a period of time to detect a fault after its onset, *e.g.* seconds [*Wang et al.*, 1993] to minutes [*Billmann and Isermann*, 1987; *Digernes*, 1980] to hours [*Isermann*, 1984], depending on the sampling rate, fluid type and flow regime.

C.3.2 Flow regime and input type

The flow regimes that hydraulic network identification methods operate in are either steady state, oscillatory, mildly transient, or transient. For the unsteady methods, to estimate the state or identify the parameters of the fluid network, some form of input is needed to excite a response from the system. The type of input dictates the assumed flow regime for the identification method. Four categories of input types are observed here, three active input methods, and a passive method.

In all cases, the batch methods use an active input. The reason for this is to stimulate and excite the system so that more detail of its structure can be seen and the output made more information rich. For linear systems, only the frequencies in the input are seen in the output, therefore there is benefit in inputting a broader range of frequencies into the system [*Lynn*, 1982]. Active methodologies typically start with the system in steady state [*Liggett and Chen*, 1994; *Lee et al.*, 2005a; *Covas et al.*, 2000], and inject some signal into the system (usually via a valve perturbation). The three types of inputs are step inputs [*Silva et al.*, 1996], oscillatory inputs [*Covas et al.*, 2005a] and arbitrary inputs [*Liggett and Chen*, 1994].

The step input methods are typically based on detecting the reflections after the passage of the first wave, and as such, they require the simple input to allow for the detection of these reflections. Examples of step inputs are found in *Silva et al.* [1996] and *Brunone* [1999]. Oscillatory inputs have either been pseudo-random binary signals [*Liou*, 1998] or pure sinusoids [*Mpesha et al.*, 2001]. The oscillatory input methods aim excite the system over a long enough period to achieve a steady oscillatory state. The oscillatory nature of the system aids in determining the systems impulse response [*Liou*, 1998], frequency response [*Mpesha et al.*, 2001] or standing wave behaviour [*Covas et al.*, 2005a], all of which can be used to detect the presence of leaks. Due to the ease of generation, most acoustic methods use sinusoidal inputs (*e.g.* [*Sharp*, 1996; *de Salis et al.*, 2002]).

The arbitrary input methods require measurement (or modelling) of the input so as to enable correct modelling of the system. Typically the arbitrary inputs are step changes in discharge (as this is the most convenient type of signal generated), but are considered as arbitrary input methodologies, as the methodologies can deal with inputs of arbitrary form (*e.g.* [*Liggett and Chen*, 1994]). Other common input types used are discharge pulses [*Lee et al.*, 2005a].

Passive methods do not involve the inducement of any signals into the system, but use the existing natural fluctuations in the systems boundaries, that exist in nominal operation, as the source of excitation for the system [*Verde*, 2001; *Billmann and Isermann*, 1987]. All the continuous monitoring methods are passive. Even though the passive methodologies do not excite the system across an as broad range of frequencies as the active methods do, longer time traces are used to gain sufficient information for the diagnosis.

C.4 Data Processing

The data processing of a hydraulic network identification refers to the way that the system measurements are processed, how the base model is used to interpret the data, and the transformation or preprocessing of the data.

C.4.1 Base model

As discussed, for the diagnostic process to relate artifacts in the data series to system anomalies, some form of model of the physical system is required (both fluid line models, and anomaly models). The two main types of models used to filter the data are process based models, and empirical models. To extract a greater degree of information from the data as to the location, type and size of the anomaly, process based models are generally required. However, to simply detect the onset of an anomaly, empirical models calibrated to the nominal system behaviour can be used. For process based models there exists no analytical solution to the system equations, thus approximation techniques must be employed. The only two approximation methods are time-domain discretisation schemes, and linearised frequency-domain methods. These models are discussed below.

Time-domain approximate models

Benkherouf and Allidina [1988] outlined two typical approaches to discretising a distributed parameter system to make it numerically solvable, (i) a continuous-time/discrete-space approach where the $\partial/\partial x$ operator is approximated by an appropriate finite difference scheme, or (ii) a discrete-time/discrete-space where both the $\partial/\partial x$ and $\partial/\partial t$ operators are replaced with appropriate discretisation schemes. Examples of these approaches include the continuous-time/discrete-space approach of *Loparo et al.* [1991] who formulated the problem in a stochastic differential framework (maintaining the time derivative) and used a backward difference to approximate the space derivative. For the discrete-time/discrete-space, two alternatives adopted in leak detection are the backward-time/centred-space [*Emara-Shabaik et al.*, 2002] or the method of characteristics (MOC) [*Benkherouf and Allidina*, 1988; *Liggett and Chen*, 1994; *Vítkovský et al.*, 2000].

For the solution of transient flow in fluid lines, the MOC is generally the preferred method as it solves the hyperbolic system almost exactly[3] along the systems characteristic lines. Other discretisation schemes have been shown to induce numerical dissipation into the solution [*Ghidaoui and Karney*, 1994]. However, for systems whose nodal points do not exactly coincide with the intersection points of the characteristic lines, interpolation methods are required for the application of MOC to such systems [*Goldberg and Wylie*, 1983; *Sibetheros et al.*, 1991; *Verwey and Yu*, 1993; *Wiggert and Sundquist*, 1977; *Karney and Ghidaoui*, 1997; *Chaudhry and Husssini*, 1985]. In these situations, these methods suffer similar numerical artifacts as other discretisation schemes [*Ghidaoui et al.*, 1998].

Time-domain models of differing complexity have been used for the detection of leaks. The processed based continuous monitoring methods use only the simplest 1-D water hammer equations where quasi-steady friction is assumed [*Benkherouf and Allidina*, 1988; *Emara-Shabaik et al.*, 2002; *Verde*, 2001]. For the batch applications, due to the induced transient state, the $\partial q/\partial t$ term is more significant, hence unsteady frictional effects required consideration [*Zielke*, 1968]. In addition to unsteady friction, viscoelasticity has been cited as an important model component when using inverse methods on some case studies [*Covas et al.*, 2004a,b, 2005b].

Frequency-domain approximate models

In the pioneering work of *Brown* [1962], an analytic Laplace-domain transfer function relating the pressure and flow at two points in a reflectionless non-turbulent line was derived. Exploiting the linearity assumption, this has since been generalised to fluid lines of arbitrary boundary conditions [*Goodson and Leonard*, 1972]. This framework provides a basis for which a number of transmission line operators, derived from different fundamental fluid dynamic assumptions (*i.e.* frictionless line, friction linear

[3] Approximation methods are still involved to solve the integration of the quadratic flow term $\int_C q|q|dt$ along the characteristic C.

with flow, compressible fluid, isothermal conditions *etc.*, see *Goodson and Leonard* [1972] and *Stecki and Davis* [1986] for an overview).

Despite, its exact nature for laminar flow, a source of error in using Laplace-domain models when dealing with transitional and turbulent flow is the requirement of the linearisation of the resistance term (*i.e.* for turbulent flow, the resistance is quadratic in flow). The hyperbolic system is usually linearised about the steady-state variables [*Wylie and Streeter*, 1993; *Chaudhry*, 1987]. Many authors have successfully used the linear frequency domain model [*Wylie and Streeter*, 1993; *Chaudhry*, 1987; *Lee et al.*, 2005a; *Mpesha et al.*, 2002], however, no general guidelines or thorough error analysis exists to determine the range of flow regimes appropriate for linearised modelling. The only guide is the qualitative requirement that the disturbance about the steady-state not too large.

The Laplace-domain models have three underlying axioms [*Stecki and Davis*, 1986]: (i) upstream and downstream variables of pressure and flow in a reflectionless line are related to one another via a complex exponential transfer function; (ii) in a reflectionless line, the pressure and flow at a single point are related to one another via the characteristic impedance; (iii) the net pressure and net flow are dependent on the addition and difference, respectively, of their counterpart quantities in the positive and negative travelling waves (essentially, the principal of superposition applies here). For hydraulic modelling, these axioms are organised into three different frameworks, namely, the impedance method [*Wylie*, 1965; *Wylie and Streeter*, 1993], the transfer matrix method [*Chaudhry*, 1970, 1987], and a block diagram approach [*Johnson and Wandling*, 1967]. For application to leak detection, the transfer matrix method has been used by *Mpesha et al.* [2001]; *Lee et al.* [2005a] the impedance method used by *Ferrante et al.* [2001] and *Ferrante and Brunone* [2003a], and a developed form of the block diagram approach used by *Zecchin et al.* [2005].

A significant advantage of the Laplace-domain models is that, as direct expressions for the transformed pressure and flow are achieved, they are computationally insignificant in comparison to their time-domain counterparts. Additionally, as the Laplace-domain methods do not require any spatial or temporal discretisation, the true distributed nature of the system is retained [*Schoukens and Pintelon*, 1991]. The main advantages of time-domain over Laplace-domain modelling is that the non-linearities in the system equations can be included in the model (most importantly the friction term, but to a lesser extent, the convective velocity terms). This is clearly only required for transitional and turbulent flow models.

Empirical models

Empirical models provide no insight into the physics of the system, but they can be used online to detect abrupt changes in the system behaviour. Examples of empirical models applied to leak detection is the end flow correlation method of *Isermann* [1984] and *Billmann and Isermann* [1987], the auto-regressive method of *Wang et al.* [1993], and the artificial neural network method of *Stoianov et al.* [2002b]. Empirical models are a lot simpler to use than process based models, however, they require a sufficient amount of data of the nominal behaviour to calibrate their parameters [*Wang et al.*, 1993], and learn the structure of fault patterns [*Stoianov et al.*, 2002b].

C.4.2 Domain of diagnosis

Methodologies either consider the system in its time-domain form or perform some transformation to consider the behaviour in either the frequency-domain [*Lee*, 2001; *Lee et al.*, 2003a, 2002, 2003b, 2004, 2005a; *Covas and Ramos*, 1999; *Ferrante et al.*, 2001; *Ferrante and Brunone*, 2003a; *Mpesha et al.*, 2001, 2002] or in some discrete wavelet-domain [*Stoianov et al.*, 2002a,b; *Ferrante and Brunone*, 2001, 2003b; *Ferrante et al.*, 2005]. The issues associated with the differing domains of diagnosis are, firstly, the ability to model the system in the different domains, and secondly, the ability to see the impact of an anomaly in each domain and estimate its parameters.

Aside from the long time scale influences of anomalies on the continuity of mass and momentum, two main phenomena are observed, on shorter time scales, that indicate the presence of a leak. First, is the high frequency artifacts in the transient response due to the reflections created by the presence of the leak [*Lee et al.*, 2005a]. Second is the increase in the damping rate of the energy within the system [*Wang et al.*, 2002b]. As the leak acts as an additional loss mechanism, it causes the energy of any signal within the system to decay at a faster rate.

All of the continuous monitoring techniques operate on time-domain data as this is a more natural domain to consider the time evolution of system statistics or testing for uncharacteristic system changes that are indicative of sudden faults [*Willsky*, 1976]. Similarly, reflectometry methods [*Silva et al.*, 1996] based on the arrival times of reflections require time-domain information. Also, due to the existence of time-domain models for generalised networks, the parameter calibration of the inverse methods has typically been done using time domain data and models [*Liggett and Chen*, 1994; *Vítkovský et al.*, 2002].

A well known approach to modelling the resonant behaviour of fluid lines is the use of transfer function methods (*i.e.* the transfer matrix method, or the impedance method [*Chaudhry*, 1987; *Wylie and Streeter*, 1993]) to relate the frequency response of pressure and flow at two sections. These methods have been utilised by numerous authors [*Jönsson and Larson*, 1992; *Covas and Ramos*, 2001; *Mpesha et al.*, 2001, 2002; *Ferrante and Brunone*, 2003a; *Lee et al.*, 2003a, 2004, 2005a] in an attempt to develop leak detection measures based on anomalous behaviour in the frequency response. Two major, yet different opinions exist in the literature as to the influence of a leak on a fluid line frequency response, namely that the presence of the leak (i) creates a new harmonic sub-system that in turn creates the appearance of a new resonant frequency in the frequency response [*Jönsson and Larson*, 1992; *Mpesha et al.*, 2001, 2002], or (ii) induces a pattern in the magnitudes of the harmonics of the nominal frequency response [*Covas and Ramos*, 2001; *Ferrante et al.*, 2001; *Ferrante and Brunone*, 2003a; *Lee et al.*, 2003a, 2004, 2005a]. Limitations of the existing frequency domain methods are that (i) they have only been applied to compound R-P-V systems where relatively large leaks are assumed, and (ii) the detection of the leakage is dependent of the leak location, as, due to the harmonics of the system, there are zones where the leak influence is undetectable [*Covas and Ramos*, 2001; *Ferrante et al.*, 2001; *Ferrante and Brunone*, 2003a].

An emerging methodology for leak detection within pipelines is the use of wavelets [*Ferrante and Brunone*, 2003a; *Stoianov et al.*, 2001; *Ivetic and Savic*, 2002], the advantage of wavelets is their ability to localise the frequency spectrum in time. This is important in leak detection as it is noted that a leak induces a frequency dependent damping in time [*Ivetic and Savic*, 2002] that is overlooked in the time averaging approach of the traditional Fourier methods.

The uses of the wavelet transform for the detection of leaks in fluid lines is varied. *Ferrante and Brunone* [2003a] used the ability of the wavelet transform to clearly highlight discontinuities in the pressure trace due to the reflected wave, and then used standard wave reflection techniques to estimate the leak location. In a novel application, *Stoianov et al.* [2001] used the wavelet transform to extract the mid-level frequency characteristics of a pressure trace, and used a pre-trained artificial neural network as a pattern recognition tool to estimate the leak size and location. *Ivetic and Savic* [2002] presented a more illustrative approach showing the more obvious impact of the leak in the wavelet coefficient space as opposed to the frequency response. The wavelet approach is an interesting area that has a lot of potential, but it is still in the early stages of development.

Appendix D

Numerical Example Details

The parameteric details for the numerical examples are given in this Appendix. For all numerical examples, the physical parameters of water were taken as density $\rho = 999.1$ m^3/kg, gravity $g = 9.81$m/s^2, and kinematic viscosity $\nu = 1 \times 10^{-6}$ m^2/s. All computational procedures were undertaken as outlined in Appendix E.

The network data tables are contained in the following. Unless otherwise stated, the wavespeed was taken as 1000 m/s, the friction factor[1] as 0.02 (for the turbulent-steady-friction (TSF) pipes), and the relative roughness as 0.001 (for the turbulent-unsteady-friction (TUF) pipes).

The *11-pipe network*, given in Figure 5.9, is based on the 11-pipe network used by [*Pudar and Liggett*, 1992]. The adopted nodal and link properties are given in Tables D.1 and D.2.

The *35-pipe network*, given in Figure 5.10, is based on the 35-pipe network used by [*Pudar and Liggett*, 1992]. The adopted nodal and link properties are given in Tables D.3 and D.4.

The *51-pipe network*, given in Figure 3.6, is based on the 51-pipe network used by [*Vítkovský*, 2001]. The adopted nodal and link properties are given in Tables D.5 and D.6.

The *94-pipe network*, given in Figure 3.9, is based on the 94-pipe network used by [*Datta and Sridharan*, 1994]. The adopted nodal and link properties are given in Tables D.7 and D.8.

[1]The term *friction factor* refers to the Darcy-Weisbach friction factor [*Streeter et al.*, 1997].

Table D.1: Nodal properties for the 11-pipe network.

node	base demand (L/s)	elevation (m)
1	*reservoir*	30
2	0.00	0
3	0.00	0
4	126.18	0
5	0.00	0
6	0.00	0
7	0.00	0

Table D.2: Link properties for the 11-pipe network.

link	start node	end node	length (m)	diameter (mm)
1	1	2	1371	254
2	1	3	762	254
3	2	3	609	254
4	2	5	1066	254
5	2	4	457	254
6	4	5	762	254
7	5	6	762	254
8	6	7	914	254
9	5	7	1219	254
10	3	7	762	254
11	3	5	609	254

Table D.3: Nodal properties for the 35-pipe network.

node	base demand (L/s)	elevation (m)
1	*reservoir*	182.88
2	22.65	0
3	116.67	0
4	70.79	0
5	102.51	0
6	16.99	0
7	50.12	0
9	0.85	0
10	2.83	0
11	6.80	0
12	16.99	0
13	20.67	0
14	16.99	0
15	66.54	0
16	25.49	0
17	11.33	0
18	5.38	0
19	14.16	0
20	22.09	0

Table D.4: Link properties for the 35-pipe network.

link	start node	end node	length (m)	diameter (mm)
1	1	2	1554	1524
2	1	13	1798	1524
3	2	3	1143	762
4	2	14	1706	762
5	2	13	914	508
6	3	4	2286	1016
7	3	5	914	762
8	3	15	1219	1067
9	4	5	1676	1219
10	5	6	1524	762
11	5	16	1219	762
12	6	7	1981	762
13	6	17	914	508
14	6	16	1219	610
15	7	8	1219	610
16	7	18	1371	508
17	8	9	914	508
18	8	19	1752	914
19	8	18	1524	508
20	9	10	914	508
21	10	11	3108	762
22	10	20	1097	762
23	11	12	1493	762
24	11	14	914	508
25	12	13	944	762
26	13	14	1493	762
27	14	15	883	508
28	14	19	2072	254
29	14	20	1889	762
30	15	16	914	610
31	15	17	1219	508
32	15	19	1828	762
33	17	18	1036	508
34	18	19	914	508
35	19	20	914	508

Table D.5: Nodal properties for the 51-pipe network.

node	base demand (L/s)	elevation (m)
1	*reservoir*	132.4
2	113.26	0
3	169.90	0
4	141.58	0
5	226.54	0
6	84.96	0
7	113.26	0
9	226.54	0
10	226.54	0
11	226.54	0
12	113.26	0
13	113.26	0
14	169.90	0
15	226.54	0
16	0.00	0
17	226.54	0
18	0.00	0
19	169.90	0
20	0.00	0
21	*reservoir*	121.92
22	113.26	0
23	169.90	0
24	113.26	0
25	169.90	0
26	113.26	0
27	283.18	0
28	56.64	0
29	113.26	0
30	169.90	0
31	0.00	0
32	113.26	0
33	169.90	0
34	169.90	0
35	*reservoir*	121.4

Table D.6: Link properties for the 51-pipe network.

link	start node	end node	length (m)	diameter (mm)	friction factor
1	1	2	870	1524.0	0.0247
2	2	3	450	609.6	0.0248
3	3	4	460	457.2	0.0274
4	4	5	895	304.8	0.0289
5	5	6	457	304.8	0.0338
6	6	7	467	304.8	0.0400
7	2	8	457	609.6	0.0243
8	3	9	457	457.2	0.0276
9	4	10	467	304.8	0.0356
10	5	11	450	304.8	0.0400
11	6	12	450	304.8	0.0198
12	7	13	460	457.2	0.0392
13	8	9	450	457.2	0.0298
14	9	10	450	457.2	0.0340
15	8	14	467	609.6	0.0262
16	9	15	457	609.6	0.0289
17	10	16	457	304.8	0.0341
18	11	18	934	304.8	0.0357
19	12	19	914	304.8	0.0400
20	13	20	914	609.6	0.0362
21	14	15	467	457.2	0.0162
22	15	16	457	457.2	0.0298
23	16	17	914	304.8	0.0340
24	17	18	934	304.8	0.0322
25	18	19	457	304.8	0.0320
26	19	20	457	304.8	0.0400
27	20	21	934	914.4	0.0400
28	14	22	885	609.6	0.0268
29	16	24	885	457.2	0.0298
30	17	25	905	609.6	0.0355
31	18	26	885	609.6	0.0400
32	19	27	885	304.8	0.0393
33	20	28	905	609.6	0.0337
34	22	23	457	304.8	0.0345
35	23	24	457	304.8	0.0400

continued on the next page

link	start node	end node	length (m)	diameter (mm)	friction factor
36	24	25	905	304.8	0.0357
37	25	26	885	304.8	0.0308
38	26	27	450	304.8	0.0314
39	27	28	460	304.8	0.0352
40	22	29	895	609.6	0.0286
41	24	30	885	457.2	0.0385
42	25	31	905	609.6	0.0298
43	26	32	885	304.8	0.0320
44	27	33	457	304.8	0.0313
45	28	34	905	304.8	0.0319
46	29	30	450	609.6	0.0296
47	30	31	885	609.6	0.0298
48	31	32	905	609.6	0.0261
49	32	33	450	457.2	0.0269
50	33	34	450	457.2	0.0315
51	31	35	994	914.4	0.0279

Table D.7: Node properties for the 94-pipe network.

node	base demand (L/s)	elevation (m)
1	*reservoir*	940
2	*reservoir*	940
3	*reservoir*	940
4	0	0
5	0	0
6	106	0
7	0	0
9	0	0
10	0	0
11	126	0
12	0	0
13	0	0
14	0	0
15	84	0
16	0	0
17	84	0
18	126	0
19	0	0
20	0	0
21	0	0
22	126	0
23	0	0
24	0	0
25	0	0
26	0	0
27	0	0
28	0	0
29	378	0
30	126	0
31	104	0
32	62	0
33	0	0
34	358	0
35	0	0
36	0	0

continued on the next page

node	base demand (L/s)	elevation (m)
37	0	0
38	0	0
39	0	0
40	0	0
41	0	0
42	126	0
43	0	0
44	0	0
45	400	0
46	0	0
47	0	0
48	0	0
49	0	0
50	0	0
51	0	0
52	0	0
53	0	0
54	0	0
55	420	0
56	42	0
57	0	0
58	0	0
59	0	0
60	0	0
61	148	0
62	126	0
63	316	0
64	126	0
65	0	0
66	0	0
67	0	0
68	0	0
69	42	0
70	42	0
71	42	0
72	0	0

continued on the next page

node	base demand (L/s)	elevation (m)
73	*reservoir*	900
74	*reservoir*	900
75	*reservoir*	900
76	*reservoir*	900
77	*reservoir*	900
78	*reservoir*	900
79	*reservoir*	900
80	*reservoir*	900
81	*reservoir*	900
82	*reservoir*	900
83	*reservoir*	900
84	*reservoir*	900
85	*reservoir*	900
86	*reservoir*	900
87	0	0

Table D.8: Link properties for the 94-pipe network.

link	start node	end node	length (m)	diameter (mm)
1	1	4	3660	1200
2	4	5	50	582
3	5	82	120	300
4	5	6	1000	300
5	6	67	30	300
6	7	83	30	600
7	4	8	2600	1200
8	8	9	500	400
9	9	10	10	500
10	8	11	700	1200
11	11	12	1000	900
12	12	81	50	600
13	12	13	1800	900
14	13	14	100	600
15	14	15	400	600
16	15	16	500	600
17	16	17	1500	600
18	12	18	3200	900
19	18	80	50	600
20	18	19	1800	675
21	19	20	10	500
22	20	21	40	300
23	20	40	6000	300
24	11	22	30	750
25	22	23	570	750
26	23	24	400	600
27	24	86	600	600
28	22	25	30	600
29	25	26	1800	600
30	26	27	2100	600
31	27	28	800	400
32	28	29	800	300
33	27	30	1000	300
34	30	31	30	300
35	27	32	2500	600

continued on the next page

link	start node	end node	length (m)	diameter (mm)
36	32	33	10	500
37	2	34	3660	1200
38	7	34	1000	600
39	34	35	1100	1200
40	35	36	2200	1200
41	36	37	6600	1750
42	37	38	4000	675
43	38	79	4000	675
44	79	39	1500	250
45	39	40	10	500
46	40	41	1500	250
47	37	42	1500	675
48	42	43	1600	675
49	43	71	500	600
50	42	44	1350	450
51	44	75	1900	600
52	75	45	800	600
53	45	74	3000	600
54	45	46	200	675
55	46	77	100	300
56	46	47	1600	675
57	37	47	10	500
58	37	78	15	375
59	36	48	600	600
60	48	49	5	450
61	49	84	440	450
62	48	50	450	600
63	24	50	5	600
64	50	51	170	600
65	51	52	270	600
66	86	52	840	600
67	52	53	1000	600
68	53	54	10	500
69	54	55	1000	600
70	55	56	3200	600
71	56	85	30	600

continued on the next page

link	start node	end node	length (m)	diameter (mm)
72	3	57	3140	1129
73	57	58	150	600
74	58	7	800	600
75	58	59	200	600
76	59	60	2200	600
77	77	61	30	300
78	60	33	1400	400
79	33	62	800	400
80	62	63	800	400
81	57	64	1300	1129
82	64	73	100	586
83	72	65	500	600
84	65	66	460	600
85	66	67	10	500
86	67	68	30	225
87	67	69	1000	400
88	69	70	200	400
89	64	74	1700	1129
90	74	71	5200	600
91	71	76	2200	600
92	37	87	10	500
93	87	74	4800	900
94	37	85	750	600

Appendix E

Computational Procedures

The computational procedures for every numerical example given in this thesis were performed by software created by the author. The source code for the software was written in Fortran 90/95, and consists of over 60 files and over 15,000 lines of code. The software was designed as a multi-purpose hydraulic network solver, aimed at computing the steady-state, transient-state, and Laplace-domain behaviour of an arbitrarily configured network comprised of over 13 different hydraulic element types. These primary operations of the software were designed to be implemented in different ways so as to be able to perform the following procedures: steady-state simulation, transient-state simulation, steady-oscillatory-state simulation (both sinesweeps and multisine simulations), frequency-response simulations, time-domain simulation by the numerical inverse Laplace transform (NILT), and parameter estimation procedures by both the decoupled maximum likelihood estimation (MLE) and expectation-maximisation (EM) methods of Chapter 6.

This appendix outlines the computational details of the hydraulic elements, the three different types of hydraulic network solvers and the resulting computational procedures adopted within this thesis.

E.1 Hydraulic Elements

The software was designed to deal with networks of an arbitrary structure comprised of 13 different element types. Given the three different hydraulic solver types, each element possessed steady-state routines, transient-state routines and Laplace-domain routines. The elements are detailed below.

1. *Reservoir*. The steady-state, transient-state and Laplace-domain routines were based directly on those used in *Wylie and Streeter* [1993].

2. *Junction.* As with the reservoir, the steady-state, transient-state and Laplace-domain routines for the junction type were based directly on those used in [*Wylie and Streeter*, 1993]. The junctions served as the transient generators through the adoption of controlled time dependent flow injections, namely:

   (a) step perturbations, including sharp steps, linear ramps and sinusoidal ramps;

   (b) pulse perturbations, including rectangular, triangular, and windowed sinusoidal pulses;

   (c) oscillatory inputs, including pure sinusoids and multisine signals, where the phase distribution for the multisines was computed according to the Schroeder algorithm [*Schroeder*, 1970].

   For each of the different outflow types, both the discrete-time and analytic Laplace-domain representations were incorporated.

3. *Laminar steady-state friction (LSF) pipe.* The steady-state, transient-state and Laplace-domain routines were based directly on those used in *Wylie and Streeter* [1993].

4. *Turbulent steady-state (TSF) friction pipe.* For this pipe type, the Darcy-Weisbach friction factor was taken as a constant. The standard steady-state headloss model was used *Streeter et al.* [1997], the transient-state routines were based on the linear-implicit approximation *Arfaie et al.* [1993], and the Laplace-domain routines were based on those used in [*Wylie and Streeter*, 1993].

5. *Viscoelastic (VE) pipe.* An extension of the laminar-steady-friction (LSF), this pipe type uses the standard steady-state routines *Streeter et al.* [1997], the transient-state routines are taken from [*Covas et al.*, 2005b], and the Laplace-domain routines were derived by this author and are given in Section 2.4. The following viscoelastic (VE) material types are incorporated into the software:

   (a) PVC [*Gally et al.*, 1979];

   (b) different PE functions from [*Ghilardi and Paoletti*, 1986; *Covas et al.*, 2005b];

   (c) mild-steel-mortar-lined field pipes [*Stephens*, 2008].

   For the PVC and PE materials, the wavespeed function was taken from [*Gally et al.*, 1979].

6. *Laminar unsteady-friction (LUF) pipe.* An extension of the LSF, this pipe type used the standard headloss routines from *Streeter et al.* [1997], the transient-state model was based on the [*Vítkovský et al.*, 2002] approximation (the 5 and 10 term models), and the Laplace-domain model was taken as the Laplace-transform of the [*Vítkovský et al.*, 2002] approximation (see Section 2.4). Despite the fact that exact analytic forms for the Laplace-domain model exist *Goodson* [1970], the transform of the [*Vítkovský et al.*, 2002] approximation was used for the purpose of comparison between the time- and frequency-domain models.

7. *Turbulent unsteady-friction (TUF) pipe.* An extension of the turbulent-steady-friction (TSF) pipe, this model used the *Streeter et al.* [1997] steady-state routines but where the friction factor was computed by the explicit *Romeo et al.* [2002] approximation, the transient state-routines were as for the TSF but where the unsteady-friction term was modelled according the *Vardy and Brown* [2007] model (the 7, 10 and 13 term models), and the Laplace-domain routines were taken as the Laplace-transform of this model. As with the laminar-unsteady-friction (LUF), analytic forms of the unsteady term exist [*Vardy and Brown*, 2007], but for the sake of comparison, the transform of the *Vardy and Brown* [2007] model was used.

8. *Emitter.* The emitter was modelled as an orifice exhausting to the atmosphere. Standard steady-state routines were used *Streeter et al.* [1997], a custom derived, case based analytic model was used for the transient-state model (basically a junction with a pressure dependent outflow, where the direction of flow invoked different model equations), and the standard Laplace-domain model was used *Chaudhry* [1987].

9. *Inline valve.* Standard steady-state orifice routines were used *Streeter et al.* [1997], as with the emitter, a custom derived, case based analytic model was used for the transient-state model, and the standard Laplace-domain model was used *Chaudhry* [1987].

10. *Capacitor* (or *dead end*). This element type did not impact the steady-state behaviour, standard time-domain and Laplace-domain routines were used [*Chaudhry*, 1987].

11. *Accumulator* (or *air chamber*). This element type did not impact the steady-state behaviour, the transient state-model was a custom developed Newton solver based on the original three equation model [*Wylie and Streeter*, 1993], and standard Laplace-domain routines were used [*Wylie and Streeter*, 1993].

12. *Linear compound node.* This is an introduced compound node model consisting of an arbitrary number of links connected to a node through linear loss elements (linearised orifice equations), where the node has a pressure dependent outflow involving a linear term (linearised emitter equations) and a capacitive term. Custom derived analytic time-domain and Laplace-domain routines were implemented.

13. *Compound node.* A nonlinear version of the linear compound node where the pipes are connected by the nonlinear orifices, and the node has a nonlinear emmitter-based pressure dependent outflow. The transient-state routines involved the use of a Newtons solver, and the Laplace-domain model was similar to that used for the linear compound node.

E.2 Hydraulic Network Solvers

The details of the three different solver types are outlined below.

Steady-state solver. For the steady-state solver, an extension to the Todini-Pilati algorithm was used *Todini and Pilati* [1988]. This extension involved the implementation of custom derived terms for the nodal elements involving pressure dependent outflow terms. Custom derived analytic derivatives were implemented for all element types. The matrix inversion routine was sourced from `http://www.algarcia.org/nummeth/Fortran/`.

Transient-state solver. The transient state solver routines were based on the method of characteristics (MOC) [*Wylie and Streeter*, 1993], where a diamond computational grid was adopted. The elemental routines were as outlined above, but the interaction between the link types (those hydraulic elements that are distributed or involve temporal delays) and the node types was designed such that a common time grid existed for all nodal computations. This necessitated that the discretisation of the distributed elements was an even number of reaches of a temporal step half that of the temporal step experienced at the nodes. That is to say that at each time-step, the characteristic information from the previous time point (both from the discrete points along the link and from the nodes at the link boundaries) was used to, (i) solve the state values at the interior points of the link, and then (ii) solve for the characteristic information propagating to the next time step and out to the nodes at the link boundaries. The characteristic information propagating from the line boundaries was then used to solve for the state values at the nodal points, from which the characteristic information propagating to the next time step was determined.

Laplace-domain solver. The Laplace-domain solver was based on the computable models derived in Sections 3.5 and 4.6. The admittance block matrices were constructed as complex variable matrices, where the analytic form of these block matrices, from Chapters 3 and 4, were used to set pointers from the network elements to the appropriate positions in the network matrices (the diagonal terms were computed separately). At each desired point $s \in \mathbb{C}$, the complex admittance function values for each network element was computed, followed by the network matrix operations. The complex matrix inversion routine was sourced from `http://www.algarcia.org/nummeth/Fortran/`.

As the three hydraulic network solvers are entirely independent in their computational routines, they were able to be conveniently used for validation and verification of each other, and of the different element types. That is, the steady-state solver was compared to the transient solver, where the steady-state was used as the initial condition for the transient-solver and the boundary conditions were kept constant. The transient-solver was compared to the Laplace-domain solver in the frequency-domain, where the frequency-response was calculated from the transient-solver via the discrete Fourier transform (DFT) and from the Laplace-domain solver by restricting s to the imaginary axis (see Section 3.6 for further details).

E.3 Simulation Types

The hydraulic solvers were organised to perform different types of simulations as outlined below.

The three basic simulation types(*steady-state simulation*, *transient-state simulation* and *frequency-domain simulation*) are based on direct applications of the three different hydraulic solvers (The Laplace-domain solver with $s = \mathrm{i}\omega_i, i = 1, \ldots, N$ performing the frequency-domain simulation) to specific networks and hydraulic scenarios. The steady-state solver was implemented as a first step for both the transient-state and Laplace-domain solvers as it provided the initial conditions for the transient-state solver, and the operating point about which the Laplace-domain solver was linearised.

Steady-oscillatory simulation. The steady-oscillatory simulations involved the use of junctions with either sinusoudal (single frequency) or multisine (multiple frequencies) flow perturbations, with the intention of exciting the network into a steady-oscillatory state. This process involved a lead in simulation time with the transient-state network solver, after which window lengths of the time-domain data were periodically tested for convergence in their DFTs (phase adjustments were made to allow for the different delays of the data windows). The window length of the time-domain data was specially designed so that the Fourier frequencies of the DFT of the window of data corresponded to the frequencies of the oscillatory excitations. An overlap of 50% was used for consecutive windows. The network was considered to be in an oscillatory state once the DFTs were consistent within a specified tollerance for a number of consecutive windows.

The NILT time-domain simulation. The mathematical expressions for the NILT, upon which the software development was based, are given in Chapter 5, and the computational procedures are as follows. Firstly the Laplace-domain network solver was computed at the points $s = a + in\Delta\omega, n = 1, \ldots, N$ for given a, $\Delta\omega$ and N. Given these fixed complex valued function points, the Fourier-Crump algorithm [*Crump*, 1976] was used to compute the time-domain value at the set of desired time points.

Parameter estimation simulations. Numerical routines for the two types of network parameter estimation methods (decoupled MLE method from Section 6.4 and the EM method from Section 6.5). The routines for both these methods were organised similarly and are outlined in the following. The first step involved the creation of the time-domain network data from the steady-oscillatory simulator. For each trial, a different independent Gaussian sequence was added to the time-domain data to create the noisy measured data (where the Gaussian variates were generated by the AS 111 algorithm [*Beasley and Springer*, 1977]), of which the DFT was used to compute the noisy frequency-domain data (the DFT was computed by the Cooley-Tukey radix-2 fast Fourier transform [*Sorensen et al.*, 1987]).

The second step involved the computation of the parameter estimates by solving of the minimisation problems in Sections 6.4 and 6.5 for the MLE and EM methods respectively. This was done using the evolutionary computational framework of particle swarm optimisation (PSO) [*Kennedy and Eberhart*, 1995]. The form of the PSO implemented within the software is a single objective, velocity constrained algorithm that implements the inertial weight method [*del Valle et al.*, 2008]. The neighbourhood structures incorporated within the software are the global best, the von Neumann toroidal grid, and the unself von Neumann toroidal grid [*del Valle et al.*, 2008]. The unself von Neumann toroidal grid was found to be the best structure for the applications within this thesis. Additionally, the PSO also contained a custom developed feature that was implemented to improve its performance. This feature is essentially a random perturbation method (an analogue to real mutation in real valued genetic algorithms [*Herrera et al.*, 1998]) introduced at late stage in the search aimed at increasing the algorithms explorative ability within the near optimal regions found in these mature stages of the search.